



January 2018

Glacial Lake Reflectance As A Proxy For Changing Glacial Conditions And Impacts On Streamflow

Lance Diangelis

Follow this and additional works at: <https://commons.und.edu/theses>

Recommended Citation

Diangelis, Lance, "Glacial Lake Reflectance As A Proxy For Changing Glacial Conditions And Impacts On Streamflow" (2018). *Theses and Dissertations*. 2400.

<https://commons.und.edu/theses/2400>

This Thesis is brought to you for free and open access by the Theses, Dissertations, and Senior Projects at UND Scholarly Commons. It has been accepted for inclusion in Theses and Dissertations by an authorized administrator of UND Scholarly Commons. For more information, please contact zeinebyousif@library.und.edu.

GLACIAL LAKE REFLECTANCE AS A PROXY FOR CHANGING GLACIAL
CONDITIONS AND IMPACTS ON STREAMFLOW

by

Lance Vincent DiAngelis
Bachelor of Arts, University of Phoenix, 2011
Master of Science, University of Saint Francis, 2013

A Thesis

Submitted to the Graduate Faculty

Of the

University of North Dakota

In partial fulfillment of the requirements

For the degree of

Master of Science


Grand Forks, North Dakota

December
2018


This thesis, submitted by Lance DiAngelis in partial fulfillment of the requirements for the Degree of Master of Science from the University of North Dakota, has been read by the Faculty Advisory Committee under whom the work has been done and is hereby approved.



Jeffrey A. VanLooy, Ph.D., Chair

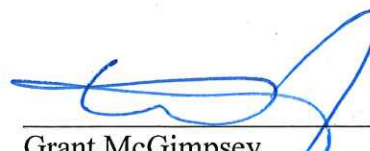


Xiaodong Zhang, Ph.D.



Gregory S. Vandeberg, Ph.D.

This thesis is being submitted by the appointed advisory committee as having met all of the requirements of the School of Graduate Studies at the University of North Dakota and is hereby approved.



Grant McGimpsey
Dean of the School of Graduate Studies

November 28, 2018
Date

PERMISSION

Title Glacial Lake Reflectance as a Proxy for Changing Glacial Conditions and Impacts on Streamflow

Department Earth System Science and Policy

Degree Master of Science

In presenting this thesis in partial fulfillment of the requirements for a graduate degree from the University of North Dakota, I agree that the library of this University shall make it freely available for inspection. I further agree that permission for extensive copying for scholarly purposes may be granted by the professor who supervised my thesis work or, in his absence, by the Chairperson of the department or dean of the School of Graduate studies. It is understood that any financial gain shall not be allowed without my written permission. It is also understood that due recognition shall be given to me and to the University of North Dakota in any scholarly use which may be made of any material in my thesis.

Lance DiAngelis
10/5/2018

ACKNOWLEDGMENTS

I wish to express my appreciation to the Earth System Science and Policy department for funding my master's thesis as well as field research. In addition, I would also like to extend my appreciation to my advisors who have helped shape my research with meaningful suggestions. I would also like to thank Jacki Klancher for allowing me to collaborate with the students and faculty participating in the ICCE field research trip in the summer of 2016. Finally, I would like to express my sincere gratitude to my advisor Jeff VanLooy. I couldn't have completed this research without the countless hours of meetings and editing we had during this project.

For my daughter Scarlett

ABSTRACT

Climate change continues to manifest itself through increased temperatures across the Western United States. Subsequently glaciers in the Wind River Range of Wyoming have been in decline since the end of the Little Ice Age and continue to lose mass during the annual ablation season. Understanding these changes is of paramount importance for water resource managers. This study uses data from Landsat 5, 7 and 8 over a 33-year period from 1984-2017 to determine the long-term change in water color for lakes in the range related to glacial flour discharge. Water color can be used to indicate changes in the discharge of glacial flour which in turn may indicate changes in glacial activity. Further, the long-term trend indicates years of higher and lower reflectance. The high values can occur in single years or in groups of years and indicates significant glacial ablation. The long-term water color changes were also compared to changes in streamflow in Dinwoody Creek, Bull Lake Creek and Pine Creek to identify how glacier contributions are changing in these basins. This data was then paired with glacier area measurements to identify how changes in mass are affecting glacier contributions to streamflow.

TABLE OF CONTENTS

CHAPTER I.....	1
INTRODUCTION	1
Site of research.....	4
The problem.....	5
The Purpose and Significance of the Study	8
Study Objectives	8
CHAPTER II.....	9
LITERATURE REVIEW	9
Studying Glacial Changes.....	9
Measurement of Mass Balance	11
Glaciological Method.....	11
Geodetic Method.....	13
Accumulation Area Ratio Method	15
Imagery for Glacial Analysis	17
Delineation of Glacier Characteristics using Remote Sensing	18
Hydraulically and Non-Hydraulically Connected Lakes	21
Glacier Lake Classification and Measurements.....	22
Studies in the Wind River Range.....	24
CHAPTER III	34
METHODOLOGY	34
Data Sets	35
Image Correction	39
Ratios and Indices for Analysis	40
Analytical Process.....	41
Defining Glacial Areas	41
Defining Lake Area and Extracting Reflectance Values	42
Statistical and Descriptive Analysis.....	42
Uncertainty.....	44
CHAPTER IV	45
RESULTS	45
Glacial lakes with increased reflectance	45
Glacial lakes with no change in reflectance.....	52

Glacial lakes with a decrease in reflectance.....	56
Mean reflectance of all glacial lakes over time.....	58
Area Change Analysis.....	60
CHAPTER V	63
DISCUSSION.....	63
Climatic factors controlling glacial lake reflectance.....	64
Other factors controlling glacial lake reflectance	67
Analysis of Upper Dinwoody Lake	69
Basin-wide Lake Reflectance Changes Compared to Stream Flow, SWE, and Glacier Area	76
Key Melt Years	83
CHAPTER VI.....	85
CONCLUSION.....	85
Limitations of the Study.....	88
Future Work	89
Application of Results.....	90
REFERENCES	92

TABLE OF CONTENTS - FIGURES

Figure 1. Wind River Range Study Area.	4
Figure 2. Landsat 8 image (9-12-2015) representing the three lake color classes of glacially fed lakes in the Wind River Range, Wyoming; (a) Upper and Lower Titcomb Lakes (blue), (b) Upper and Lower Dinwoody Lakes (turquoise), and (c) Scott Lake (gray).....	24
Figure 3. Torrey Creek watershed to the east of the Continental Divide. See Figure 1 for location in the greater Wind River Range area.	25
Figure 4. Dinwoody Creek watershed to the east of the Continental Divide. See Figure 1 for location in the greater Wind River Range area.	26
Figure 5. Bull Lake Creek watershed to the east of the Continental Divide. See Figure 1 for location in the greater Wind River Range area.	27
Figure 6. Green River watershed to the west of the Continental Divide. See Figure 1 for location in the greater Wind River Range area.	27
Figure 7. Pine Creek watershed to the west of the Continental Divide. See Figure 1 for location in the greater Wind River Range area.	28
Figure 8. Flow diagram of analytical process.	35
Figure 9. Glacial lake reflectance values (R_w) for the Blue, Green, Red, and NIR wavelengths (top), and summed glacial lake reflectance values ($R_{w(VIS-NIR)}$) indicating color classes (bottom) for Lower Titcomb, Upper Titcomb, Lower Dinwoody, Upper Dinwoody, and Scott Lakes in the Wind River Range, Wyoming.....	43
Figure 10. Scatter plot of mean late summer glacial lake reflectance (R_w) for Scott Lake. Blue dotted line indicates trend line with equation and R^2 value.	46
Figure 11. Scatter plot of mean late summer glacial lake reflectance (R_w) for Upper Green River Lake. Blue dotted line indicates trend line with equation and R^2 value.	47
Figure 12. True color images showing Upper Green River Lake color variation with corresponding R_w values for August (a) 1993 (R_w value of 0.01), (b) 2002 (R_w value of 0.09) and (c) 2010 (R_w value of 0.05).	47
Figure 13. Scatter plot of mean late summer glacial lake reflectance (R_w) for Lower Green River Lake. Blue dotted line indicates trend line with equation and R^2 value.	48
Figure 14. Scatter plot of mean late summer glacial lake reflectance (R_w) for Upper Dinwoody Lake. Blue dotted line indicates trend line with equation and R^2 value.	49
Figure 15. Scatter plot of mean late summer glacial lake reflectance (R_w) for Lower Dinwoody Lake. Blue dotted line indicates trend line with equation and R^2 value.	50
Figure 16. Scatter plot of mean late summer glacial lake reflectance (R_w) for Mile Long Lake. Blue dotted line indicates trend line with equation and R^2 value.	51
Figure 17. Scatter plot of mean late summer glacial lake reflectance (R_w) for Unnamed Lake 1. Blue dotted line indicates trend line with equation and R^2 value.	52

Figure 18. Scatter plot of mean late summer glacial lake reflectance (R_w) for Little Milky Lake. Blue dotted line indicates trend line with equation and R^2 value.	53
Figure 19. Scatter plot of mean late summer glacial lake reflectance (R_w) for Big Milky Lake. Blue dotted line indicates trend line with equation and R^2 value.	53
Figure 20. Scatter plot of mean late summer glacial lake reflectance (R_w) for Upper Titcomb Lake. Blue dotted line indicates trend line with equation and R^2 value.	55
Figure 21. Scatter plot of mean late summer glacial lake reflectance (R_w) for Lower Titcomb Lake. Blue dotted line indicates trend line with equation and R^2 value.	55
Figure 22. Scatter plot of mean late summer glacial lake reflectance (R_w) for Bomber Lake. Blue dotted line indicates trend line with equation and R^2 value.	56
Figure 23. Scatter plot of mean late summer glacial lake reflectance (R_w) for Baby Lake. Blue dotted line indicates trend line with equation and R^2 value.	57
Figure 24. Scatter plot of mean late summer glacial lake reflectance (R_w) for Baker Lake. Blue dotted line indicates trend line with equation and R^2 value.	58
Figure 25. Scatter plot of mean late summer glacial lake reflectance (R_w) for all lakes in the Wind River Range. Blue dotted line indicates trend line with equation and R^2 value.	60
Figure 26. Scatter plot of maximum annual SWE (cm) for the Elkhart Park SNOTEL station over time. Blue dotted line indicates trend line with equation and R^2 value.	66
Figure 27. Scatter plot of mean summer maximum temperatures ($^{\circ}\text{C}$) for Dinwoody Glacier from PRISM data set over time. Blue dotted line indicates trend line with equation and R^2 value.	66
Figure 28. Scatter plot of mean summer temperature ($^{\circ}\text{C}$) and max annual SWE (cm) for the Elkhart Park SNOTEL station. Blue dotted line indicates trend line with equation and R^2 value.	67
Figure 29. Scatter plot of mean summer lake reflectance (R_w) for Upper Dinwoody Lake compared with SWE (cm) for Elkhart Park SNOTEL station. Blue dotted line indicates trend line with equation and R^2 value.	70
Figure 30. Scatter plot of mean summer lake reflectance (R_w) for Upper Dinwoody Lake compared with mean temperature ($^{\circ}\text{C}$) for Dinwoody Glacier. Blue dotted line indicates trend line with equation and R^2 value.	71
Figure 31. Scatter plot of mean summer lake area (km^2) for Upper Dinwoody Lake over time. Blue dotted line indicates trend line with equation and R^2 value.	72
Figure 32. Scatter plot of mean summer lake reflectance (R_w) compared to mean summer lake area (km^2) for Upper Dinwoody Lake. Blue dotted line indicates trend line with equation and R^2 value.	72
Figure 33. Scatter plot of mean summer lake reflectance (R_w) with predicted mean summer lake reflectance ($\text{Pred}(R_w)$) for Upper Dinwoody Lake. The multi-linear regression compares mean summer lake reflectance to SWE (cm), lake area (km^2) and T_{mean} ($^{\circ}\text{C}$). Blue dotted line indicates trend line with equation and R^2 value.	74
Figure 34. Scatter plot of mean summer lake size (km^2) and mean summer streamflow ($\text{m}^3 \text{s}^{-1}$). Blue dotted line indicates trend line with equation and R^2 value.	76
Figure 35. Scatter plot of mean summer streamflow ($\text{m}^3 \text{s}^{-1}$) and max annual SWE (cm) in Pine Creek. Blue dotted line indicates trend line with equation and R^2 value.	78

Figure 36. Scatter plot of mean summer streamflow ($\text{m}^3 \text{s}^{-1}$) over time at the Pine Creek USGS Gage Station. Blue dotted line indicates trend line with equation and R^2 value. 78

Figure 37. Scatter plot of mean summer streamflow ($\text{m}^3 \text{s}^{-1}$) and max annual SWE (cm) in Bull Lake Creek. Blue dotted line indicates trend line with equation and R^2 value. 79

Figure 38. Scatter plot of mean summer streamflow (cms) and time at the Bull Lake Creek USGS Gage Station. Blue dotted line indicates trend line with equation and R^2 value. 80

Figure 39. Scatter plot of mean summer streamflow ($\text{m}^3 \text{s}^{-1}$) and max annual SWE (cm) in Dinwoody Creek. Blue dotted line indicates trend line with equation and R^2 value. 82

Figure 40. Scatter plot of mean summer streamflow ($\text{m}^3 \text{s}^{-1}$) and over time at the Dinwoody Creek USGS Gage Station. Blue dotted line indicates trend line with equation and R^2 value. 82

Figure 41. Anomalies of Mean Summer Lake Reflectance (R_w) of the Wind River Range between 1984 – 2017. Blue bars indicate anomaly value. 84

TABLE OF CONTENTS – TABLES

Table 1. Landsat sensor characteristics.....	37
Table 2. SRTM Characteristics ¹	38
Table 3. Change in glacial lake reflectance for the 14 analyzed lakes between 1984 and 2017(R^2 , significance (p) values, and trend of reflectance change for each lake over the study period).....	59
Table 4. Total glacial area (km^2) and the percent change between observation dates for the Wind River Range glaciers.....	61
Table 5. Total glacier area (A) (km^2) and change in area (%) from the previous year by basin for the observation dates.....	62
Table 6. Descriptive statistics of the SWE (cm) at the Elkhart Park SNOTL Station, lake area (km^2) of Upper Dinwoody Lake, and T_{mean} ($^{\circ}\text{C}$) from the PRISM data over Dinwoody Glacier.....	73
Table 7. Coefficients and significance (p-values) of the variables of SWE (cm), T_{mean} ($^{\circ}\text{C}$) and lake area (km^2) in the predictive model for glacial lake reflectance of Upper Dinwoody Lake.....	74

CHAPTER I

INTRODUCTION

Climate change continues to manifest itself through increased temperatures and changes in precipitation cycles across the planet (IPCC 2014). Subsequently, glaciers across the globe have experienced trends of mass gain and loss based on these changing climatic conditions. Some glaciers gained mass in the Northern Cascades (Meier and Post 1962) during the 1950s and the Andes (Soruco et al. 2009) during the 1970s and 1980s, however, these trends have reversed due to enhanced temperatures and alterations to the precipitation cycle. This is evident particularly in the Pacific Northwest (Pelto 2008) and Inter-mountain West and occur as a result of current Pacific and Atlantic Ocean Oscillation Phases (Wise 2010). Currently, temperate alpine glaciers are steadily losing mass in the Western United States (Rasmussen and Conway 2001; Pelto 2008; Rasmussen 2009; Reidel and Larrabee 2011), Alaska and western Canada (Meier and Post 1962; Arendt et al. 2002; Shea et al. 2009; Benn and Evans, 2010; Pelto et al. 2013), Europe (Haug et al. 2009; Carturan et al. 2013) and the Himalayas (Berthier et al. 2007; Wagnon et al. 2007). These changes are not heterogeneous within glacial regions highlighting the complexity of glacial response to climate change (Furbish and Andrews 1984; VanLooy et al. 2014). Complementing these findings is the IPCC (2014) report indicating, “The atmosphere and ocean have warmed, the amounts of snow and ice have diminished, and sea level has risen.” The report indicates this is due to a 0.85°C temperature increase across the globe from the period

of 1880 to 2012. Although variation exists, the overall trend indicates that glaciers are losing mass annually (Benn and Evans 2010).

Mountain glacier contribution to sea level rise is one of the many problems associated with anthropogenic climate change. Sea level rise has the potential to displace thousands of people from low-lying island nations and other coastal areas. Mountain glaciers have the potential to add 0.65 ± 0.16 m (Dyurgerov and Meier 2005) to sea level rise if all glaciers were to melt away. While this is vastly smaller than the potential total contribution of the Greenland and Antarctic Ice Sheets, the rate at which mountain glaciers are contributing is 0.77 mm/yr between 1993-2003 while Greenland and Antarctica only contributed 0.42 mm/yr during this same period (Bindoff et al. 2007; Benn and Evans 2010). The Patagonia region is contributing 0.105 mm/yr (Rignot et al. 2003) which is five times higher than the Alaska region when comparing size of the ice fields (Arendt et al. 2002).

Glacial runoff is the lifeblood of many regions of the globe and changing glacial conditions will stress local watersheds dependent on summer runoff from glaciers. Variations of glacier runoff contribution occur across the globe with temperate regions being the most dependent. Peru obtains water from glaciers for nearly half of the year (Juen et al. 2007; Benn and Evans 2010) while the Pacific Northwest and other similar low latitude temperate areas obtain glacier runoff primarily during the summer months. Regions separated by a mountain range may exhibit a higher dependency on glacier runoff in one region compared to the other even though they share similar boundaries. For example, the Karakoram region of China is more dependent on glacier runoff from the Himalayas than Nepal (Rees and Collins 2006), thus changes in discharge will have more adverse effects on the water management of the Karakoram region (Benn and Evans 2010).

The Wind River Range glaciers in West-Central Wyoming, U.S.A., like many of the glaciers across the globe are in recession. Naftz et al. (2002) found that the average temperature on Upper Fremont Glacier has increased by 3.5°C between 1960 and the early 1990s while Wyoming's average temperature has increased ~1.1°C since 1900 (EPA 2017). This illustrates that temperatures in alpine areas of Wyoming are increasing faster than the average rate of the state (Chang and Hansen 2014). Numerous authors have shown evidence of area and volume loss across the range, supporting the measurement of higher temperatures on the glaciers (Marston et al. 1991; Naftz and Smith 1993; Wolken 2000; Cheesbrough 2007; VanLooy et al. 2013; VanLooy et al. 2014; DeVisser and Fountain 2015; Marks et al. 2015). The Wind River Range glaciers contribute between 4% – 10% of annual streamflow (Cheesbrough et al. 2009) to downstream communities and reductions in water supply can stress resources of the region. The current area recession rates are increasing across the range and this may contribute a larger amount of water initially (Bradley et al. 2006), however, losses in volume will begin to have a direct effect on discharge as reduction of discharge becomes a function of volume rather than melt rates (Cheesbrough 2007). Glaciers that are healthy and in balance can be counted on for supplying water into the future, however, unhealthy glaciers will have a limited period to supply water downstream. Therefore, detecting changes in glacial activity is of paramount importance to provide watershed managers with information about the contribution of the Wind River Glaciers as changes to glacial discharge rates will affect agriculture, industry, fisheries and recreation (Daddow 1996).

Site of research

The Wind River Range is a mountain range located in West-Central Wyoming (Figure 1). The range is nearly 200 km long and 50 km wide covering 900,000 ha. The crest of the mountain range is the dividing line between Sublet and Fremont Counties and forms the Continental Divide with peaks topping 4,500 m. The crest of the range delineates the three national watersheds the range contributes melt water to in the summer months. The watersheds include the Missouri-Mississippi to the East (of which the Wind River is a part) and the Green-Colorado and the Snake-Columbia (not-labeled) to the West (Meier 1951). As melt water in the range contributes to these three watersheds the Wind River Range is often noted as being the headwaters of the nation. Portions of the range also fall into the Wind River Reservation (Shaded Dark Gray), Fitzpatrick (Shoshone National Forest) (USDA 2017) and Bridger (Bridger-Teton National Forest) Wilderness (Shaded Light Gray) (USDA 2017)

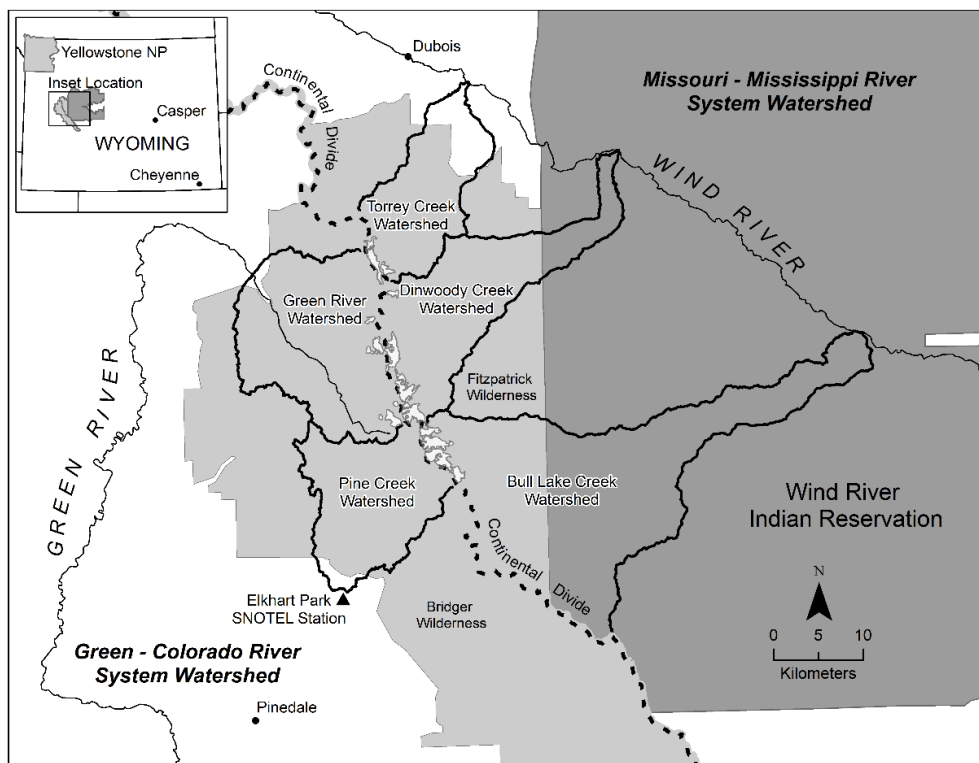


Figure 1. Wind River Range Study Area.

which limits the use of mechanized equipment in the Wilderness area. A recent study by DeVisser and Fountain (2015) indicates the range contains 269 glaciers and perennial snowfields (G&PS) with a total area of $34.34 \pm 0.14 \text{ km}^2$. Of the 269 G&PS, there may be as many as 63 active glaciers. The vast majority of these glaciers exist within five basins in the range; Bull Lake Creek, Dinwoody Creek, and Torrey Creek to the east of the Continental Divide, and the Green River and Pine Creek to the west of the Continental Divide (Figure 1).

The problem

Climate change has caused significant glacial mass decline in the Wind River Range. Documentation of Little Ice Age (LIA) (ca. 1400-1900) terminal moraines has allowed observation of glacial retreat in the range since approximately 1930 (Delo and Wentworth 1931). Nearly all glaciers in the range have been in retreat since the end of the LIA. We can attribute this to an increase in greenhouse gas (GHG) emissions since the beginning of the Industrial Revolution (IPCC 2014). Temperatures across the U.S. Great Plains have increased between $0.56 \text{ }^\circ\text{C}$ and $1.11 \text{ }^\circ\text{F}$ since 1900 (NCA 2014). According to the EPA (2017) Wyoming has increased in temperature between $0.56 \text{ }^\circ\text{C}$ and $1.67 \text{ }^\circ\text{C}$ producing a larger range of change within the state as compared to the Great Plains average. Further, Naftz, et al. (2002) found the air temperatures around Upper Fremont Glacier increased $3.5 \text{ }^\circ\text{C}$ from the 1960s to the 1990s. This suggests alpine areas are responding faster to climate change than the average rate in the state of Wyoming (Chang and Hansen 2014).

As glacial mass continues to decline in the Wind River Range, downstream communities will begin to experience reduced water availability. Although the Wind River Range supplies meltwater to three national watersheds, the primary water user is the Wind River Indian

Reservation. In 1988, the Wind River Indian Reservation was awarded water rights by the Wyoming Supreme Court (Daddow 1996). The water rights total nearly 616,740 km³ per year and supply water for many of the needs of the Wind River Reservation including agriculture, industry, fisheries and recreation (Daddow 1996). The agriculture sector uses water for irrigation to support crop and various livestock production (Daddow 1996). The industrial sector, which is primarily composed of the oil and gas industry, uses this water to produce fluids for hydraulic fracking (Daddow 1996). Fisheries use this water to maintain trout production as the cool runoff from snowmelt and glaciers is ideal to support cold-water species. Lastly, recreation is abundant in the area as the water supplies allow fishing, swimming and boating among many other water related activities.

Streamflow in the range can be both ephemeral and perennial. The flow of the stream is typically dependent on the source of the water (Daddow 1996). Streams originating in the foothills of the Wind River Range typically are ephemeral due to snowmelt being the primary contributor. However, streams originating from glaciers are typically perennial due to contribution from both snowmelt and glacier melt. The streamflow from the Wind River Range is highly important to the Wind River Reservation as the annual precipitation varies from 25.4 – 50.8 cm in the foothills to between 15.2 – 20.3 cm inches in the central portion of the reservation (Daddow 1996). Therefore, the perennial streams are extremely important to all water use in the area, particularly when the ephemeral streams stop contributing to streamflow in the late summer months. Reductions in glacial mass will lead to significant changes in late summer streamflow when the snowpack has melted for the year. Without glacier melt to supplement snowmelt, these perennial streams may tend toward ephemeral and cause significant water restrictions in the Wind River Range.

Complicating loss of glacial mass is the continuation of climate change in the Wind River Range. Not only have average temperatures increased, but the rate and frequency of precipitation events are beginning to show signs of alteration in cycle (NCA 2009). Rain events are becoming more sporadic in that the frequency between storms has increased and the amount of precipitation is higher per storm. The NCA (2009) estimates that there has been a 13% increase in higher intensity rainfall events in the Great Plains. This is largely a function of the warmer climate, as Hegerl et al. (2007) noted, "For every 0.56°C rise in temperature, the water holding capacity of the atmosphere increases by about 4%." Adding to the complexity of the altered precipitation is the regions persistence to tend toward increasing drought from 1958 to 2007 (Guttman and Quayle 1996).

Herein lies the complication of a changing climate. While glaciers begin to reduce contribution to summer and late summer streamflow, the climate continues to warm and experience alterations in precipitation cycles. The enhanced energy flux due to rising temperatures will continue to maintain high annual ablation rates, while the summers in downstream communities will be significantly warmer and drier. By the end of the century, models indicate that the Wind River region will experience drier summers (CMIP3-A 2005). This will increase water demand in the Wind River Indian Reservation to sustain irrigation for agriculture and livestock. All the while increased evapotranspiration, changes in foraging conditions under elevated CO₂ levels and increased water demand from cattle all create significant strains on an ever-decreasing water supply (NCA 2009). Understanding these climate changes are essential to regional planning in the Wind River Region to minimize vulnerability in adapting to changes to streamflow in the future (Wilbanks et al. 2007; Adger et al. 2007; and Hartmann 2008).

The Purpose and Significance of the Study

Given the concerns of potential future depletion of streamflow due to reductions in glacier mass, the purpose of the study is to investigate how the color (i.e. reflectance) of glacially fed lakes could act as a proxy for analyzing changes in glacial activity (i.e. changes in glacier area and factors affecting glacial ablation) which in turn influences streamflow. The significance of this study is that it will provide a novel method of assessing long-term streamflow changes due to changes in glacial mass. The study uses a time series of annual glacial lake reflectance and glacier area change to identify the state of glacier contribution to streamflow which builds upon the lake reflectance work of Wessels et al. (2002), Gallegos et al. (2008), Giardino et al. (2010), and Matta et al. (2017) in the Himalayas. The results provide watershed managers with information to help develop long-term plans to mitigate the effects of reduced glacial runoff in the three main watersheds and multiple basins in the Wind River Region.

Study Objectives

The major objective of the study is to determine if glacial lake reflectance can be used as a proxy for changing glacial conditions, and in turn be used to analyze impacts of the changing glacial conditions on streamflow. To obtain this objective, several sub-objectives were conducted. These sub-objectives include:

- I. Analyze changes in glacier lake reflectance over time between 1984 and 2017.
- II. Calculate glacier area throughout the study period and analyze how glacier area has changed over time in relation to lake reflectance changes.
- III. Conduct statistical analysis of the impact of variables influencing glacio-hydrological conditions as they relate to lake reflectance.

CHAPTER II

LITERATURE REVIEW

Glaciers are made from the collection of annual snow that does not melt in the summer months over a period of many years (NSIDC 2017). Snow that does not melt for a season or two is transformed into a denser state known as firn (NSIDC 2017). As snow continues to accumulate over this firn layer, the pressure exerted densifies the firn and begins to close air pores creating ice (NSIDC 2017). Once a significant amount of ice mass is accumulated, the glacier begins to move downhill due to the force of gravity (NSIDC 2017). Through the years glaciers may wax and wane based on the annual accumulation on the glacier. Glaciers in steady-state may experience variations in years with more ablation and years with more accumulation, but tend to balance out over decades. Advancing glaciers have periods of prolonged growth with most years having more accumulation than ablation. Retreating glaciers have periods of prolonged recession with most years having more ablation than accumulation. Many techniques exist to determine the health of a glacier, of which the majority involve some form of measuring the accumulation and ablation areas.

Studying Glacial Changes

Area change is the most fundamental measurement of a glacier and is the area lost or gained on a glacier over a period (Fountain et al. 1997). As most mountain glaciers have been in decline over the past few decades, the area has changed significantly due to loss in several tens to

hundreds of meters of ice at their termini. Area change can indicate climatic variations as the glaciers respond relatively rapidly to changes in climate. The first study of Wind River Range glaciers by Wentworth and Delo (1931) noted little recession of Dinwoody Glacier from its Little Ice Age (LIA; circa 1900) moraine in 1930. Largely since this study, a trend of terminus recession from the LIA moraine continues (Wentworth and Delo 1931; Meier 1951; Marston 1991; Cheesbrough 2005; VanLooy et al 2013). The change in position can be tracked over a period to indicate the amount of recession from initial terminus position to the final terminus position.

The glacier itself is composed of the ablation area and the accumulation area. The Equilibrium Line Altitude (ELA) is the line that delineates the accumulation area and the ablation area which throughout the melt season may be referred to as the transient snow line (TSL) due to the fluctuating elevation based on seasonal melting at the glacier surface. The ablation area is the area of maximum melt where only bare glacial ice exists. The ablation of the ice can occur by two methods. The first is ice retreat from the terminus of the glacier at the maximum extent of the previous water year. The second is the thinning of ice in the ablation area when the snow has melted from the surface. The accumulation area of a glacier is the area that maintains snow cover at the end of the melt season. The accumulation area can vary from year to year and indicate the overall health of the glacier over a given period as the snow remaining at the end of the melt season will eventually turn into glacial ice. The net mass gain in the accumulation area plus the net mass loss in the ablation area determines mass balance for the glacier (Benn and Evens 2010).

Long-term mass balance measurements can allow general trends to emerge in the growth or recession of a glacier. Several studies focusing on mass balance have been conducted in the

Wind River Range by Marston et al. (1991); Wolken, (2000); Cheesbrough (2005); VanLooy et al. (2013); VanLooy et al. (2014); Marks et al. (2015) and DeVisser and Fountain (2015).

Regardless of methods used, all of these studies indicate that the Wind River Range has been in a state of recession since the end of the LIA.

Measurement of Mass Balance

There are several techniques for measuring the accumulation and ablation areas to calculate mass balance. These techniques involve both field and/or remote sensing derived data and result in determining the net volume change of the glacier over either a single season or on a decadal scale. The two most common mass balance methods in glaciology are the glaciological (*in-situ* based) and geodetic (based on elevation data from either remote sensing or field measurements) methods. Both of these methods have the disadvantage of limited data due to data collection techniques. However, another less comprehensive method known as the Accumulation Area Ratio (AAR) allows for a basic understanding of mass balance through the use of satellite imagery collected with regular frequency.

Glaciological Method

The glaciological method is based on seasonal *in-situ* measurements to determine the amount of snow and ice melt on the glacier, from year to year (Tagborn et al. 1975; Ostrem and Brugman 1991; Fountain et al. 1997; Hagg et al. 2004). This is traditionally accomplished using ice stakes, snow pits, and snow and ice density measurements. The glaciological method is the most difficult method as it requires multiple field campaigns in one season. Although the difficulty is a limitation, the data produced from the studies offer the most insight into glacier

processes and is the recommended method of observation when considering regions with significant glacier mass. Within the Wind River Range several studies have used this method to determine annual snow accumulation and snow and ice densities to produce volume estimates of the remaining ice (Meier 1951; Marston et al. 1991; Naftz and Smith 1993).

Ablation stakes are often placed along the center line of the glacier from the terminus into the accumulation area as well as several cross transects to produce vertical and horizontal profiles of the surface. Results of the seasonal melt are then extrapolated across the glacier (generally following along elevational zones) to calculate the yearly net gain or loss in glacial mass. The ablation stake method is often difficult as it requires repositioning of ablation stakes and significant coordination of resources to create an effective observation network. Ostrem and Brugman (1991) described methods of observing the glaciers using this method including what analysis should be run to determine various characteristics of the glacier. Given the remoteness of many mountain glaciers, this method would be very difficult to employ on many glaciers. Therefore, these studies should be limited to benchmark or index glaciers and secondary glaciers within a region to gain a full understanding of mass change on the glaciers.

Snow pits and ice cores are critical to understanding the mass change of a glacier. Snow pits can be used to determine the amount of accumulation in the accumulation area of the glacier. This snow depth coupled with measurements of ice ablation can allow for the determination of mass change for the year. Further, they can indicate how dense the snow layer and firn layer is for estimates of discharge in future studies. Ice cores can help determine the density of ice. Naftz and Smith (1993) indicated that ice density increased rapidly between the surface and 15 m on Upper Fremont Glacier. Further, Marston estimated the ice, firn and snow to be an average of 800 g/m^3 on Dinwoody glacier in 1991. Understanding the density of the glacier is critical to

understanding the mass remaining within glacierized regions as this will allow better estimates of glacier volume.

Geodetic Method

The geodetic method is used to measure mass balance on glaciers between two study periods and has been used extensively in the Wind River Range (Marston et al. 1991; Wolken 2000; Cheesbrough 2007; VanLooy et al. 2013; VanLooy et al. 2014) as well as many other locations globally. The geodetic method uses elevation data obtained from topographic maps, airborne and spaceborne derived data and aerial and ground photographs. The geodetic method uses the elevation data from two study dates, often separated by many years to several decades. The elevations from the first study date are differenced with the second study date to determine a surface elevation change of the glacier. The study relies on determining the area and surface elevation change of the glacier to produce a volume change often expressed in meters of water equivalence (w.e.). The result is paired with the density of the snow/firn/ice as it can be estimated in multiple locations to determine a mass change in w.e.

Digital Elevation Models (DEMs) from topographic surveys allow researchers to compare previous known estimates of glacier surface elevation and area. Although this is useful to estimate change in mass balance from earlier dates to later study dates, the practice can be rife with error and introduce significant uncertainty into measurements (Benn and Evans 2010). Airborne and spaceborne derived DEMs offer a significant improvement on older topographic maps as they can reduce the grid size to between 1 - 30 m. Airborne sensors such as LIDAR can be used to produce high resolution DEMs, but these data sets are often unavailable in glacierized regions. Therefore, satellite derived DEMs are the preferred choice of many researchers. Two

primary DEMs are the Advanced Spaceborne Thermal Emission and Reflection Radiometer (ASTER) Global Digital Elevation Model (GDEM) and the Shuttle Radar Topographic Mission (SRTM) 30 m void-filled DEM. The ASTER GDEM is developed from passive Nadir and rear facing sensors to produce a stereoscopic image to develop a DEM. The SRTM used an active microwave sensor that emits a single pulse which bounces off the Earth and returns to receivers placed on the space shuttle and on a 60-m boom extended from the shuttle. The dual returns produces an interferometric effect from which a three dimensional model of the terrain can be created. The SRTM DEM is often found to be less precise than the ASTER DEM in many studies. However, these studies are in many locations that only have the SRTM 90 m void-filled DEM. The improvement of horizontal resolution and coastal correction on the 30 m SRTM DEM produced a better vertical accuracy than the ASTER GDEM. As well, since the ASTER GDEM is produced through stereoscopic methods it is subject to the same potential sources of errors as DEMs created from aerial photographs, including elevation errors due to low contrast in locations such as on icefields and glaciers.

Within the Wind River Range, VanLooy et al. (2014) found that ASTER DEMs had significant errors due to these low contrast issues on Continental Glacier. Aerial and ground photographs can also be used to derive DEMs. Aerial platforms produce overlapping stereoscopic images that can be orthorectified to produce DEMs. However, the temporal scale of these imagery tends to be on the order of several years or may only be available from single events. Ground photography holds promise to produce DEMs that can be used in research and has been used extensively in the past (Marston et al. 1991; Wolken 2000; Cheesbrough 2007). The introduction of structure from motion allows researchers to collect imagery of the glacier from tied GPS points (Ryan et al 2015). The imagery can be used to orthorectify the glacier

surface and produce a DEM highlighting the hypsography of the glacier surface. More precise DEMs will allow more accurate assessments of mass balance over extended periods using the geodetic method.

The glaciological method is a great method to use when resources are available. It can often support or confirm the findings of the geodetic method. When used in conjunction with the geodetic method, the glaciological method can become a powerful method of observation and analysis as the range can be studied both locally and globally. This is particularly important given that climate change is altering many of the glaciers on Earth as is evident across many of the Benchmark Glaciers across the globe. The verification of field studies is always necessary when analyzing the effects of climate change on the world's glaciers. Thus, a need for direct glacier measurements will always be required.

Accumulation Area Ratio Method

The Accumulation Area Ratio (AAR) was described by Meier and Post (1962). While this method does not specifically produce a mass balance calculation of the glaciers, it does evaluate the health of a glacier which provides an understanding of the general mass balance. This measure is the ratio between the total area of the accumulation area and the total area of the glacier. Glaciers with an AAR between 0.5 – 0.8 are found to be in steady-state while glaciers below this level are found to lose mass (Meier and Post 1962). More precisely, Paterson (1994) lists alpine glaciers as having a steady-state of 0.67. In contrast, Racoviteanu et al. (2008) found the AAR in the Himalayas to be 0.44, suggesting a need to develop independent AARs for mountain ranges in various regions of the world. While this varies by region, we can generally expect that glaciers below the 0.5 AAR level are in decline, with those closest to 0 in rapid

decline. Glaciers with an AAR more than 0.8 are found to be in a state of advance or mass gain. In the Wind River Range, glaciers have likely been in a state of decline where the AAR has been < 0.5 , with the exceptions of 1945 – 1950 where a steady-state or slight mass gain may have occurred (Meier, 1951). These years likely reside between an AAR of 0.5 – 0.8 as significant changes were not measured (Meier and Post 1962). Additionally, recent research indicates the rate of glacier change is variable between time periods indicating a fluctuating transient snow line (TSL) and AAR due to variable annual melt rates (VanLooy, personal communication). Further, variable melt rates between the glaciers adds to the complexity of determining an AAR for the range. Therefore, all the glaciers must be observed collectively to determine a steady state AAR for the range.

The AAR can be classified three ways including the template method, ELA method and the ELA/AAR method (Racoviteanu et al. 2008). The template method described in (Racoviteanu et al. 2008) and developed by (Khalsa et al. 2004), can be used to determine the AAR for a single glacier or set of glaciers within a region. The method attempts to characterize the glaciers hypsography and makes assumptions based on a linear relationship between the accumulation area ratio and mass balance. Essentially the assumption is that within the same climate region, the variations in mass balance are due to elevation effects (Racoviteanu et al. 2008). This method was used to create a steady-state ratio for two glaciers in the Himalayas (Kulkarni et al 2004; Racoviteanu et al. 2008). The ELA method uses satellite imagery to determine the ELA at the end of the snow water year. This method makes assumptions about the linear relationship with mass balance and elevation. In the Alps, a linear relationship was found with ELA and mass balance to produce a mass change of 0.78 m per 100m. In Western Himalaya this has been estimated to be 0.69 m per 100m. However, debris cover on glaciers

strongly affects the mass balance rate per 100 m due to effects of energy absorption and insolation of the ice surface. The ELA/AAR method uses the relationship between AAR and mass balance to determine the steady-state AAR within a climate region. This method can be applied to a large region or individual glaciers. When observing over the region, the AAR and mass balance is plotted with a single regression line to find the optimal or steady-state AAR for the range. This can be satisfied when mass balance equals zero change.

Imagery for Glacial Analysis

Imagery is one of the most critical components of a remote sensing study to determine glacier attributes (e.g. accumulation area, ablation area, total glacier area, etc.). Imagery ranges from high resolution (< 10 m) to medium resolution (> 10 m) to low resolution (> 50m), however, many studies tend to use medium resolution sensors (Khalsa et al. 2004) such as Landsat (Cheesbrough 2007) and co-register with higher resolution imagery such as IKONOS (Mark and Seltzer 2003; Silverio and Jaquet 2005). Often sensors are co-registered between medium resolution sensors and high-resolution sensors to reduce uncertainty in manually delineated glacier measurements.

Landsat has been monitoring the globe for over 40 years and continues to deliver some of the best medium-resolution satellite imagery available. The spatial resolution of the sensor is adequate to monitor glacier processes including area, ablation area, and accumulation area as even conservative estimates of error are only on the order of $\pm 30\text{m}$. The spectral resolution of the sensor delivers 11 different bands ranging from Visible to the Thermal Infrared wavelengths providing band combinations that can be used in a threshold or differential index. The temporal resolution of the sensor allows a re-imaging time of 16 days providing adequate coverage in the

ablation season. The radiometric resolution offers contrast between snow and ice brightness as the pixel depths range from 8 – 12 bits.

In the United States, the National Agricultural Imaging Program (NAIP) imagery is very popular for glaciological studies as the images have a high spatial resolution (~1 m) which is excellent for delineating glacier surface and area characteristics. More recent NAIP imagery (approximately over the last 20 years) have four different spectral bands ranging from the Visible to NIR wavelengths. As well, the radiometric resolution of NAIP imagery offers contrast between snow and ice as the pixel depth is 8 bits. While the imagery provides significant advantages in spatial resolution, the temporal resolution of the sensor limits the use of this imagery for glacial research as the imagery is taken approximately once every three years.

Delineation of Glacier Characteristics using Remote Sensing

Manual digitization of glacier area and facies has typically been conducted by hand as the method produces accurate results of glacier areas (Albert 2002). However, the use of manual digitization techniques can be very time consuming, especially when considering an entire mountain range or large section of the mountain range. Automated classification of glaciers can save considerable time and improve on human error in manual digitization of glaciers (Racoviteanu et al. 2008; Paul et al. 2015). Casassa et al. (2014), and Burns and Nolin (2013) note that automated delineation of glaciers works well with limited debris cover, although this often requires manual correction after processing (Ambinakudige and Joshi 2010). The methods of delineating glaciers includes unsupervised and supervised classifications, band ratios and Normalized Difference Snow Index (NDSI) among others (Wang et al. 2017). Supervised and unsupervised classifications often fail to identify shadow areas (Wang et al. 2017) and take

considerable post processing time. Therefore, the primary two methods (NDSI and band ratios) have been the subject of many papers (Paul et al. 2013; Burns and Nolin 2013; Paul et al. 2015; Wang et al. 2017).

NDSI can produce estimates of snow and ice cover in a region by selecting a threshold for glacier delineation. Burns and Nolin (2013) used a threshold of 0.42 to delineate glacier boundaries and found them to agree with manually digitized glacier boundaries. However, threshold selection can influence the area of glacier boundaries if not correctly calculated (Paul et al. 2015). Further, the NDSI method requires more preprocessing than the band ratio method as it involves the development of a histogram and subsequent calculations (Paul et al. 2015). Wang et al. (2017) found that the NDSI fails to properly delineate glaciers and lakes. The NDSI formula is:

$$\frac{GREEN - SWIR}{GREEN + SWIR}$$

This band combination is due to high reflectance of snow and ice in the green band versus the extremely low reflectance of the SWIR band (Burns & Nolin 2013). Krishna (2005) found that the NDSI performed the best in delineating glaciers facies compared to rock and forest cover. However, Paul et al. (2002) and Paul et al. (2015) found that NDSI was less accurate than band ratio methods.

The band ratio method was found to be superior for automated glacier area delineation due to the sharp contrast in reflectance between the visible bands and the NIR and SWIR bands (Paul et al. 2013; Wang et al. 2017). Paul et al. (2013) tested several band ratio methods on non-atmospherically corrected imagery including Landsat TM (NIR/SWIR) and TM (RED/SWIR)

with an additional threshold of TM 1 (BLUE) to assist with mapping shadow areas. Both methods were found to work better in various scenarios, however TM (NIR/SWIR) performed better in areas with significant quantities of water (Paul et al. 2013). Wang et al. (2017) used atmospherically corrected imagery on Landsat 8 (RED/SWIR) and (NIR/SWIR). The (NIR/SWIR) band ratio combination was found to be superior in delineating area, however, the method failed to remove lakes on the surface of the glacier (Wang et al. 2017). While the studies include atmospherically and non-atmospherically corrected imagery, both found that the band ratio method was a more suitable option with less processing.

Manual correction using pan sharpened images can improve results of delineating glacier areas (Ambinakudige and Joshi 2010) and reduce uncertainty from the GIS buffer method. Further, Burns and Nolin (2013) note that the best method of digitizing area of debris covered glaciers is manual digitization as classification algorithms may be confused by the spectral signature of the debris areas. Therefore, many studies include both the band ratio and manual digitization techniques to classify debris-free and debris-covered glaciers.

Both classifications utilize Landsat atmospherically corrected surface reflectance imagery. Atmospherically corrected Landsat imagery was used by Burns and Nolin (2013) in the Peruvian Cordillera Blanca and compared to non-atmospherically corrected imagery. They found that atmospherically corrected imagery produced 5% more area on debris-free glaciers compared to the non-atmospherically corrected imagery. This suggests that the atmospheric correction removes distortion from the atmosphere and produces a clearer spectral signature in mixed pixels that assist the band ratio and NDWI classifications.

Hydraulically and Non-Hydraulically Connected Lakes

One of the primary characteristics of active glaciers is that they emit glacial flour (Wentworth and Delo 1931; Meier 1951). Glacial flour is a fine-grained material and is the result of erosion from grinding of plucked boulders along the bedrock of the mountain. This glacial flour suspends very easily, due to fine particle size, producing the characteristic blue, turquoise, and gray color of glacial runoff (Wessels et al. 2002; Gallegos et al. 2008; Giardino, et al. 2010; Matta et al. 2017). Lakes that are hydraulically connected to the glacier have a higher load of suspended material, thus producing a greater reflectance (Giardino et al. 2010; Matta et al. 2017). The higher loads typically are indicative of increased activity in the glacier. This occurs because increased glacier wastage is likely adding more water to the bed where more glacial flour can be emitted (Matta et al. 2017; Benn and Evans 2010), although Pearce et al. (2003) found that discharge of suspended solids is limited by sediment availability. Studies in the Himalayas have determined that most glacial lakes are changing in reflectance and color (Giardino et al. 2010; Matta et al. 2017), likely due to enhanced runoff. More precisely, Matta et al. (2017) found 71% of lakes displayed a change in water color with 38% becoming clearer and 62% more turbid during their study period.

The emission of glacial flour is non-linear as discharge rates increase (Gurnell 1982). Pearce et al. (2003) and Swift et al. (2002) found that emissions are highest in the spring and decrease toward fall likely due to the availability of sediments at the glacier bed (Benn and Evans 2010). As glaciers continue to evolve due to climate change, we can expect to see varying amounts of suspended solids in the water (Benn and Evans 2010). Initially this may lead to an increase in reflectance or change in color due to higher emission of water from the glacier (Giardino et al. 2010; Matta et al. 2017). However, as Rees and Collins (2006) noted, the

emission of water is expected to decline for Himalayan glaciers beginning between 2050 and 2080. Coupled with a decrease in available sediments, the reflectance will likely decrease beginning on the 2050 – 2080 period. In addition, the peak emission of glacier water may have already occurred in the Peruvian Cordillera Blanca (Burns and Nolin 2013). This would likely lead to a shift toward a decrease in reflectance during this period.

We can study the water to infer different properties or characteristics and compare them to changes in the glacier conditions. For example, enhanced melting may increase the number of suspended solids for a period, due to enhanced surface runoff and increase of water at the bed of the glacier. However, as volume of the glacier decreases along with availability of suspended solids, a long-term change in color or reflectance is expected. Glaciers with an AAR < 0.5 are not gaining sufficient mass, thus the area decreases, and velocity slows. This can influence the discharge of suspended solids into the glacial lakes as it reduces the availability of the material. Therefore, we may be able to analyze glacier lake reflectance as an indicator of enhanced glacial discharge through increased melting (Matta et al. 2017). However, at this point there are no known published studies linking glacial lake reflectance and changes in glacial conditions due to climate change.

Glacier Lake Classification and Measurements

There are several different attributes of glacial runoff that indicate whether the water source is hydraulically connected or is an independent water body. These unique identifiers include reflectance (color) and change in area (Pelto et al. 2013). The reflectance of water will indicate the hydraulic connectivity of the lake. An improved method of observing glacier lakes was demonstrated by Giardino et al. (2010) and Matta et al. (2017) as they used lake color as a

proxy for measuring reflectance in ranges of 10. Change in area of glacial lakes also indicates change on a glacier (Quincey et al. 2007; Pelto et al. 2013; Matta et al. 2017). As the glaciers melt further, you will likely see a change in lake area. This is due to thinning or terminus retreat combined with changes to snowfall.

The area of glacial lakes may need to be isolated for analysis of area change over time as well as for lake reflectance value extraction. Lakes can be identified and isolated with a Normalized Difference Water Index (NDWI). The NDWI formula is:

$$\frac{GREEN - NIR}{GREEN + NIR}$$

The NDWI method classifies water features in the Landsat scene with values ranging from (-1) – (+1) with water features being > 0. Gao (1996) devised this index based on the high reflectance of water in the green band and the low reflectance of water in the NIR band. This contrast is unique to water and can be used to create a mask to extract water features. The NDWI method is preferred as it requires the least post-processing to extract lake features in the study area.

The normalized water leaving reflectance (R_w) of glacier lakes is determined with the following formula (Ocean Optics Web Book, 2017):

$$R_w(\lambda) = Rrs(\lambda) * \pi$$

The Rrs is the ratio between upwelling radiance (L_u) and downwelling irradiance (E_d) and is obtained after atmospherically correcting imagery. The Rrs value is multiplied by π which produces a unitless measure of water leaving reflectance (R_w) [0,1].

After the reflectance values have been calculated, the bands in the VISNIR can be integrated to produce a total reflectance for the lakes. The index is:

$$R_w(VIS-NIR) = R_w(BLUE) + R_w(GREEN) + R_w(RED) + R_w(NIR)$$

Matta et al. (2017) has produced the most recent work on the reflectance of glacier lakes building on studies from (Giardino et al. 2010). The study grouped the summed lake reflectance into ranges of 10 to qualitatively describe color as blue $R_w(0-10)$, turquoise $R_w (>10-20)$ and gray $R_w (>20)$ (Figure 2). Using the R_w values from two images, Matta et al. (2017) determined water reflectance has changed in the Himalayas, possibly because of climate change influencing melt rates on glaciers.

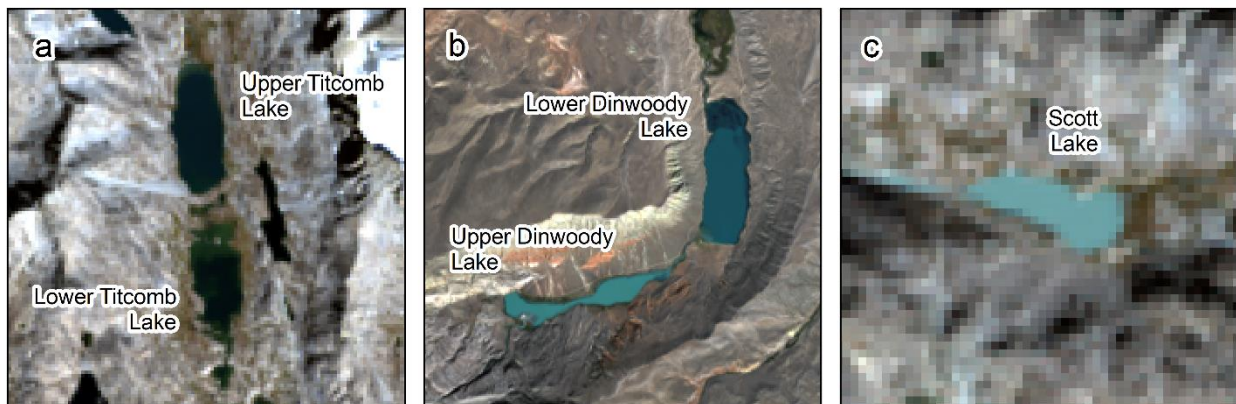


Figure 2. Landsat 8 image (9-12-2015) representing the three lake color classes of glacially fed lakes in the Wind River Range, Wyoming; (a) Upper and Lower Titcomb Lakes (blue), (b) Upper and Lower Dinwoody Lakes (turquoise), and (c) Scott Lake (gray).

Studies in the Wind River Range

The Wind River Range Glaciers are distributed across five major basins of the Missouri-Mississippi and Green-Colorado River Systems. The Wind River, which is located on the east

side of the Continental Divide and is part of the Missouri Mississippi River System, receives glacial melt water contributions from three of the basins: Torrey Creek, Dinwoody Creek, and Bull Lake Creek. Torrey Creek basin is approximately 172 km² and contains 2.87 km² of glacial ice, with two major glaciers: Continental Glacier and an unnamed glacier (Figure 3). Dinwoody Creek basin is approximately 259 km² with 7.07 km² of glacial ice, and contains the largest glaciers in the range, including Dinwoody, Gannett, and

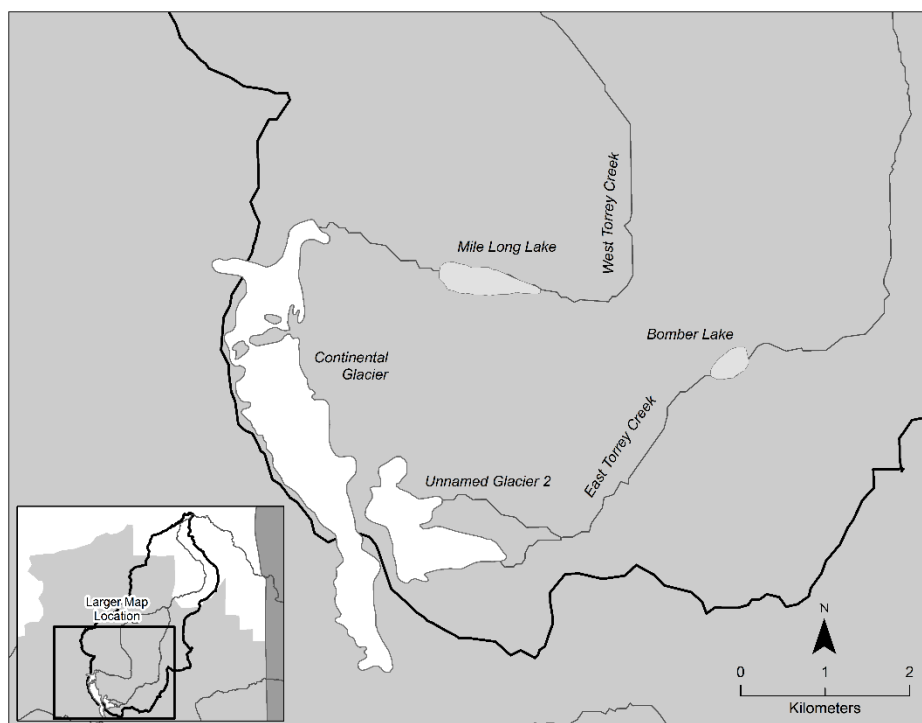


Figure 3. Torrey Creek watershed to the east of the Continental Divide. See Figure 1 for location in the greater Wind River Range area.

Grasshopper Glaciers (Figure 4). Bull Lake Creek basin is the largest in the range at approximately 554 km², and contains the second most amount of glacial ice with 4.94 km². Five large glaciers exist in the basin, which are Knife Point, Bull Lake, Upper Fremont, Sacagawea, and Helen (Figure 5). On the west side of the Continental Divide, two basins contain glacial

mass which contribute to the Green-Colorado River System. The first is actually the headwaters of the Green River itself. For the purposes of this study the basin was delineated as all contributing area above the output of Green River Lakes (Figure 6). The delineated Green River delineated basin is approximately 205 km² and contains the least amount of glacial ice with only basin encompasses approximately 204 km² and contains 3.79 km² of glacial ice, including Mammoth, Baby, and Sourdough Glaciers. Finally, Pine Creek basin, which also flows into the Green River, had to be delineated as all contributing area above Fremont Lake and includes 0.22 km² of glacial ice. Despite this small amount of ice, there are still several named glaciers, including Twins and Sphinx Glaciers (Figure 7).

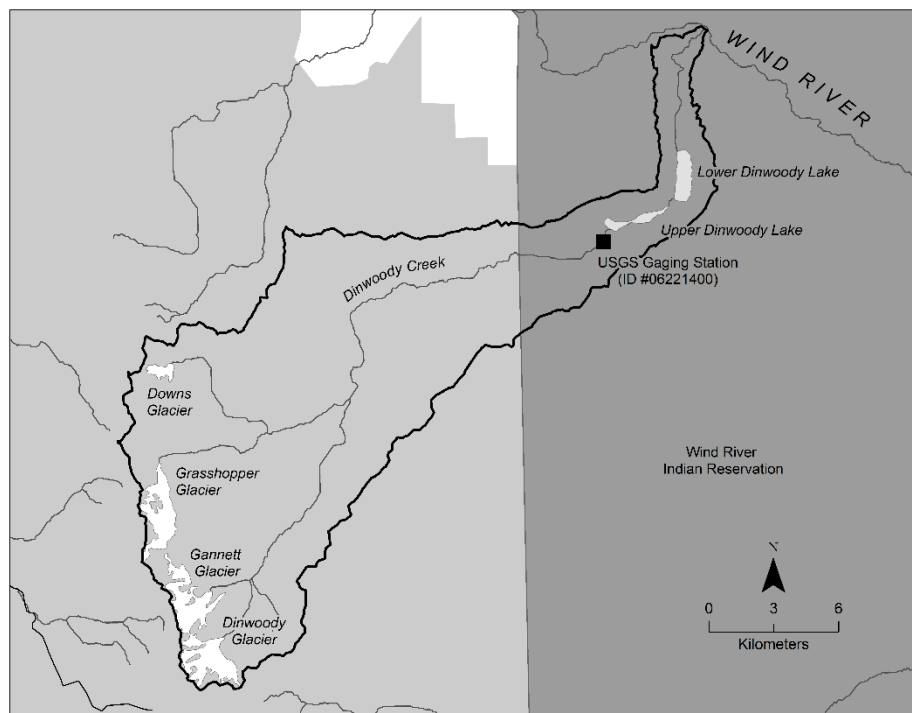


Figure 4. Dinwoody Creek watershed to the east of the Continental Divide. See Figure 1 for location in the greater Wind River Range area.

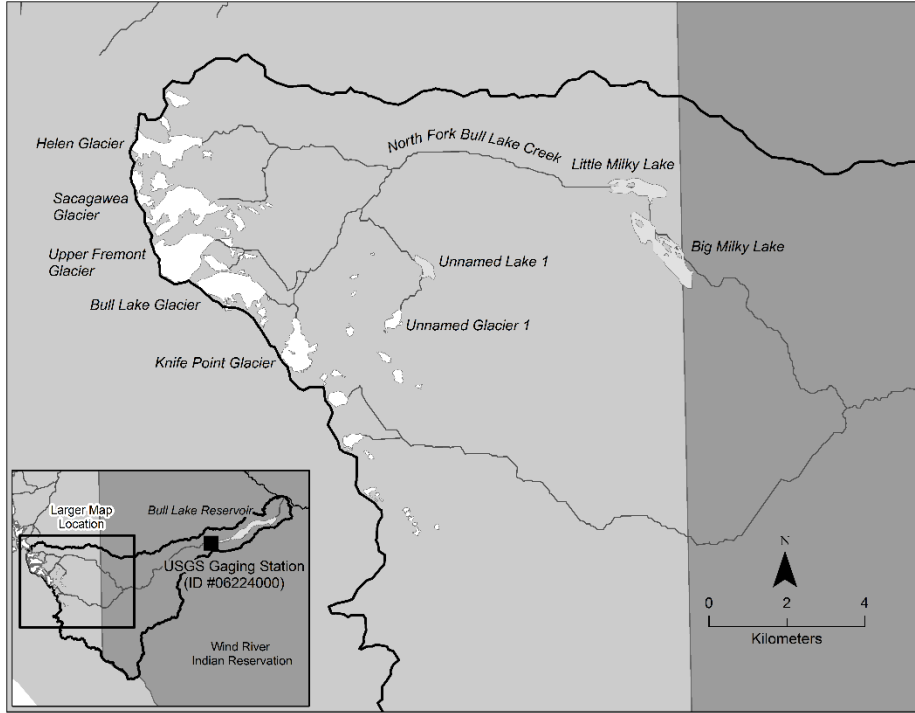


Figure 5. Bull Lake Creek watershed to the east of the Continental Divide. See Figure 1 for location in the greater Wind River Range area.

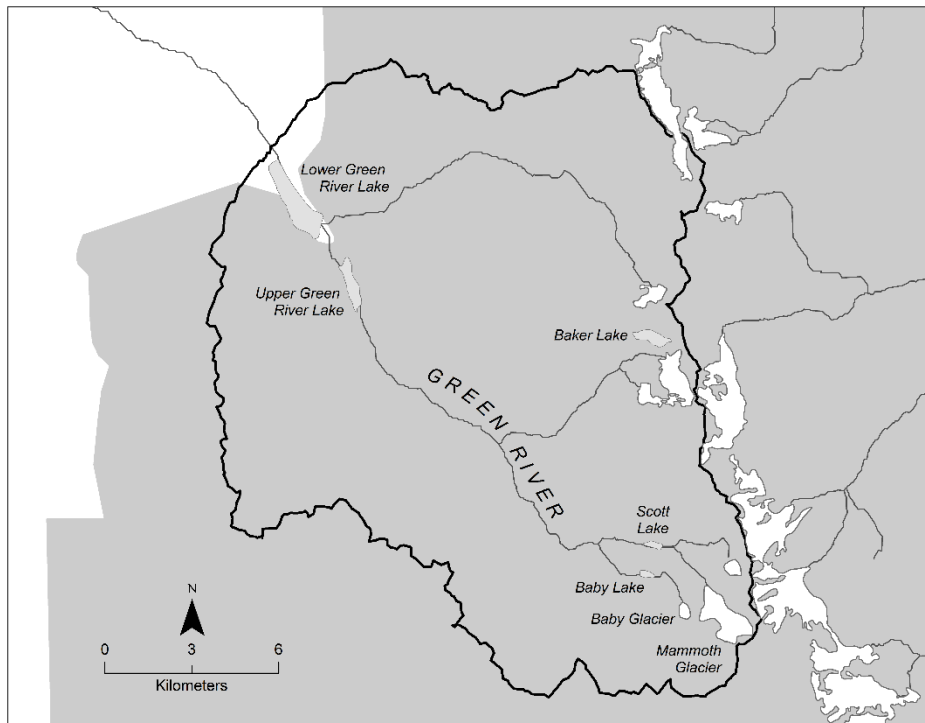


Figure 6. Green River watershed to the west of the Continental Divide. See Figure 1 for location in the greater Wind River Range area.

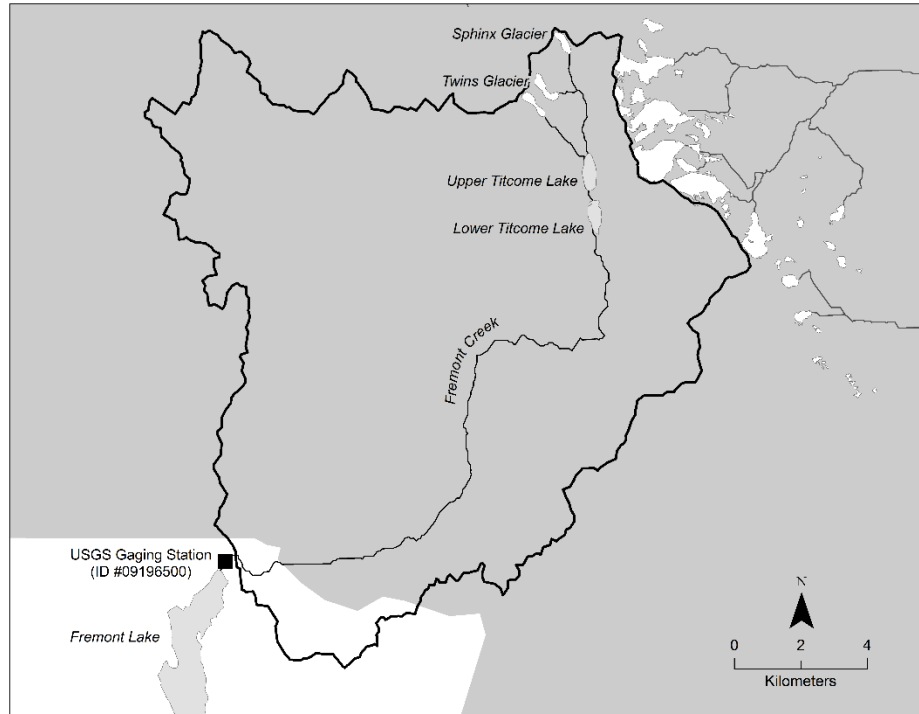


Figure 7. Pine Creek watershed to the west of the Continental Divide. See Figure 1 for location in the greater Wind River Range area.

Glaciers of the Wind River Range were first documented by the Hayden Survey in 1878 (Hayden 1878). While known locally, the glaciers were not well known outside of the Wind River region. This was evident in the Wentworth and Delo (1931) assessment of the Wind River Range in which they attempted to name many of the Dinwoody Glaciers after Doctor Gannett. However, only the glacier off Gannett Peak retained this name as the USGS devised a naming scheme that uses the mountain peak as the name of the glacier. The Wentworth and Delo (1931) study was important as this offered some of the first full observations of the glaciers including details about surface water flow, debris cover and bergschrunds among others. The significant findings of the paper include the recession of the glaciers from the published topographic maps and finding supporting evidence to classify the Wind River Glaciers as active. According to the survey, “North Gannett (Gannett Glacier) glacier’s terminus is between 0.4 - 0.8 km short of mapped position and although not as clear, East Gannett (Dinwoody Glacier) glacier appears to

have shortened at the terminus as well, although close to the LIA moraine (Wentworth and Delo 1931).” Wentworth and Delo (1931) also went on to describe active glaciers by their milky discharge and inactive glaciers and snowfields by the lack of turbidity in discharge. Dinwoody Creek was of interest due to the high amount of glacial flour in downstream lakes nearly 20 miles from the terminus of the Dinwoody Glaciers. The discharge indicates a significant amount of glacial erosion at the bed of the Dinwoody Glaciers (Wentworth and Delo 1931).

Meier (1951) studied the Wind River Range in 1951 and completed the most extensive assessment of the Wind River glaciers as he documented many of the range’s glacier characteristics. This study was imperative as it confirmed that the Wind River Range contains the largest amount of glacier ice in the continental United States outside of Washington and Alaska. Given the limited resources of the study, Meier (1951) chose to focus on “real glaciers”. The real glaciers were selected based on emission of glacial flour from melt-water. Glaciers that did not emit turbid melt water were found to be stagnant ice masses and were excluded from the study.

Meier (1951) conducted research on 14 named glaciers in the Wind River Range including Gannett, Dinwoody, Mammoth, Helen and Knife Point Glaciers. Gannett glacier is considered a system of valley glaciers (Meier 1951) as the area-altitude distribution indicated significant mass distribution toward the upper portions of the glacier. The glacier was approximately 4 km wide and 2.4 km long with an area of 4.58 km² and maximum slopes ranging from 35 - 60°. The ablation area ratio was approximately 0.30, with an accumulation area ratio of approximately 0.70. Gannett glacier was estimated to be 5.6 km² at the LIA maximum extent.

Dinwoody glacier is considered a palmate cirque due to the many “fingers” of ice feeding the glacier. The area-altitude distribution graph indicates that most of the mass is in the middle of the glacier which is indicative of cirque glaciers. The glacier was approximately 3.2 km wide and 2.4 km miles long with an area of 3.5 km² and an average slope of 10° on the middle portion. The glacier was estimated to be 3.8 km² at the LIA maximum extent. This figure includes the area of Gooseneck glacier which was a tributary to Dinwoody until 1936. Meier conducted extensive studies using the glaciological method to determine the ablation characteristics of Dinwoody glacier. Ablation was found to be highest around 3,660 m and range from 25.4 cm in the upper portions of the glacier to nearly 177.8 cm near the firn limit. However, the AAR was a sizable portion of the glacier as the average accumulation for the year averaged to be approximately 220 cm. In total, Dinwoody discharged 16.6×10^6 m³ of water while accumulating 27.2×10^6 m³ of water to produce a net gain of 10.6×10^6 m³ of water. Meier (1951) noted this was rather unusual and deviated from the trend of net loss since the LIA.

The area-altitude distribution of Mammoth glacier shows that it is a valley glacier type with most of the area in the upper portion of the glacier. Mammoth glacier was approximately 3.4 km long and 1.2 km wide with an area of 4 km². In 1945, the AAR was approximately 0.68 with an ablation area ratio of 0.32. The glacier receded approximately 12% from the Gannett Peak Quadrangle produced in the 1930s. Given the ease of travel and relatively benign surface features of Mammoth, Meier (1951) recommended this glacier be used for further glaciological study.

Helen glacier is a normal valley glacier with a cirque at the upper portion. The area-altitude distribution shows most of the area in the middle of the glacier. This is likely due to the convergence of three tongues of the glacier at this location. Accumulation in this region was

likely due to avalanching from higher peaks. Helen was 2.4 km long and approximately 0.55 km wide with an area of 1.6 km² and an average slope of 7% not to exceed 18% at the terminus. The accumulation area covered nearly the entire glacier with little bare ice showing. The glacier lost approximately 25% of the LIA area (Meier 1951). Given the remoteness of this glacier, little repeat photography could be found limiting the comparison of recession in the past.

Knife point glacier is considered a combination of a cirque glacier and valley glacier. The area-altitude diagram shows that the north and south lobes of the glacier have different area distributions. The south lobe favors area in the lower altitudes whereas the north lobe favors area in the upper altitudes. Knife point was 4 km long and has an area of 3 km² and an average slope of 6 – 10 % not to exceed 15% at the terminus. The AAR was approximately 0.52 with an ablation area ratio of 0.48. In 1950, approximately 30% of the glacier area was below the firm line. This indicates a significant increase of ablation when compared to the previous ablation period in 1949. The glacier has lost approximately 16.5% of the LIA area (Meier 1951).

The glaciers in the Meier (1951) study have all receded from the LIA moraine with rates varying between 7% on Upper Fremont Glacier and 25% on Helen Glacier and averaging 13% across the studied areas of the range. Although the rates vary, it does highlight the fact that climate changes have affected the glaciers at different rates. This is evident in the variable amounts of ablation on different glaciers. Dinwoody glacier had an AAR of nearly 1.0 during the study period while Knife Point glacier had an AAR of 0.52. Traveling a few miles down range from Dinwoody to Knife Point, the ablation was significantly different. This shows that incredible variability is possible in some years where glaciers in different regions of the range are responding at different rates. While the glaciers have been in recession, there are still many active glaciers in the range. This was well documented in the Meier (1951) study as he noted the

“milky” stream discharge from rock flour on Sacagawea, Heap Steep, Twins and Sphinx glaciers among many others.

In 2005, Cheesbrough conducted his Master’s thesis in the Wind River Range. The study was primarily a remote sensing study with a glaciological study to provide a volume for Dinwoody Glacier. The study used Landsat imagery to collect characteristics for “42 glacial complexes” from 1985 – 2005 and further estimated the terminus position and surface area for nine other glaciers from 1966-2001 using aerial photography. The Landsat and aerial images were processed with an unsupervised classification to classify the various glacier facies. The aerial images were further processed to extract a DEM from stereo pair imagery. The images were corrected with GPS points taken on the glacier. The glaciological study used an ice-penetrating radar transect that calculated surface to bedrock depth. Both remote sensing, the geodetic and glaciological methods used in conjunction with each other provided an understanding of mass-change in the range and the streamflow from annual ablation.

The 42 glacial complexes considered in the study can be split into two groups. The first group is composed of large glaciers ($>0.5 \text{ km}^2$) and contains 17 of the glacial complexes. The second group is composed of small glaciers ($<0.5 \text{ km}^2$) and contains 25 of the glacial complexes. The distinction between the two groups is important as the smaller group appears to be losing area at a faster rate (Meier 1951; Cheesbrough 2007) and are more susceptible to climate change (Grenshaw & Fountain 2006). The small glacier group experienced a 43% loss in area whereas the large glaciers decreased approximately 28% for an average of 37% leaving a remaining 30.48 km^2 of ice in the range. The decline also varied by region with the central portion of the main glacier field receding at the lowest rate, although this was likely the result of larger glacial masses in the central portion of the range.

When comparing volume loss, the larger glaciers are contributing a larger percentage of discharge. The estimated total volume loss between 1985 – 2005 was $410 \text{ m}^3 \times 10^6$ or $370 \text{ m}^3 \times 10^6$ w.e. This large volume of water was estimated to contribute between 4.7% - 9.8% of flow at nearly $0.4 - 0.67 \text{ m}^3 \text{ s}^{-1}$ in three different gage stations in the Wind River Area. Dinwoody, the most scrutinized of the glaciers, corresponded to a $66 \text{ m}^3 \times 10^6$ loss of ice volume or $60 \text{ m}^3 \times 10^6$ w.e. from 1983 – 2001. This 18-year period corresponded to the same loss as a previous 25-year period studied by Marston et al. (1991). When applying volume-area scaling techniques proposed by Bahr et al. (1997), the technique was found to underestimate Dinwoody's volume by 40%. Given that the discharge rates to creeks are dependent on volume, the estimated rates may significantly underestimate the true late summer contribution to streamflow.

VanLooy et al. (2013) used the geodetic method to determine mass loss on Continental Glacier from 1966-2011. The study used a topographic map from 1966, an ASTER DEM from 2006, and elevations obtained from high precision GPS points in 2011. The study determined that Continental Glacier was composed of an upper section and lower section. The upper section is 1.76 km^2 while the lower section is 0.74 km^2 . It is important to note the two sections separately as they appear to be responding differently to climate change. Between 1966 – 2006 the upper section of Continental Glacier was melting at $-0.51 \pm 0.19 \text{ m}^2 \text{ y}^{-1}$ with a volume loss of $0.033 \pm 0.02 \text{ km}^3 \text{ y}^{-1}$. Between 1966 – 2006 the lower section of Continental Glacier is melting at $0.06 \pm 0.19 \text{ m}^2 \text{ y}^{-1}$ with a volume loss of $0.02 \pm 0.02 \text{ km}^3 \text{ y}^{-1}$. The upper section had limited coverage from the high accuracy GPS and the estimation of mass loss is only representative of the area sampled. The upper section is likely ablating faster due to several factors including high energy flux relative to surrounding areas (VanLooy et al. 2013; Wolken 2000) and phenomena such as windblown snow (VanLooy et al. 2013).

CHAPTER III

METHODOLOGY

To achieve the objectives of this research, glacier area and glacial lake area were delineated, and glacial lake reflectance was calculated for the study period. First preprocessing was conducted on Landsat medium resolution imagery using the remote sensing software ENVI 5.3. The Landsat preprocessing involved two ENVI 5.3 preprocessing techniques including radiometric correction and atmospheric correction. Once preprocessing was completed, three different band math calculations were run on the images. These three calculations were conducted for the extraction of glacier and glacial lake areas, as well as glacial lake reflectance values. Extracted glacier areas were used to determine the total glacier area for each observation date, which allowed for area change comparisons over time. The extracted lake areas allowed for extraction of lake reflectance values which were used to determine the change in reflectance over time. A regression analysis was conducted on glacier lake reflectance values over time to identify long-term change trends. Additionally, a multi-linear regression was conducted on Upper Dinwoody Lake to determine the relationship between lake reflectance and three variables critical to explaining the measured variability. This analysis was conducted in an attempt to establish a relationship between changes in glacier mass balance and observed changes in glacier lake reflectance. Finally, a comparison between glacier area and long-term streamflow was conducted to identify the relationship between glacier area, declines in streamflow, and their

relationship with changing glacial lake reflectance across the range. The analytical flow process for this study is detailed in a flow diagram in Figure 8.

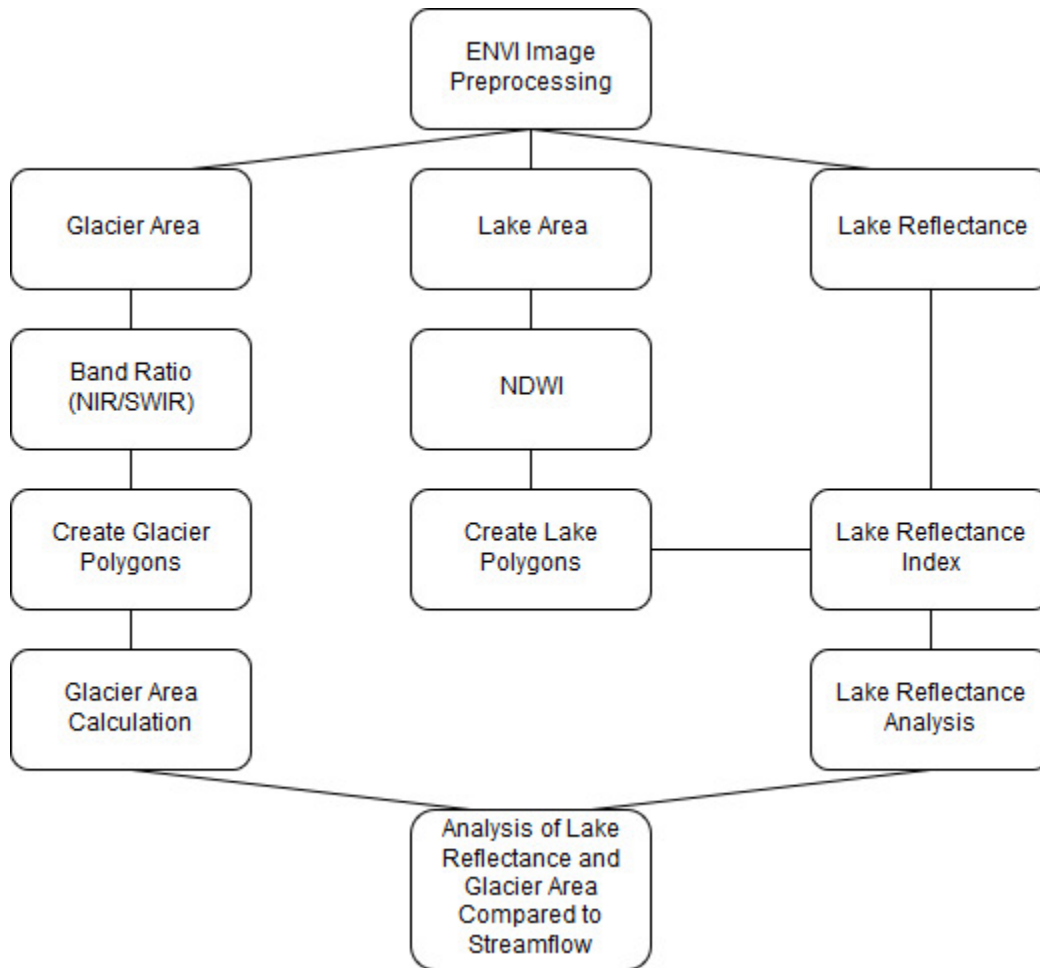


Figure 8. Flow diagram of analytical process.

Data Sets

The Landsat platform is ideal for monitoring glaciers for this study. The 40 years of imagery plus 30-meter spatial resolution and 16-day temporal resolution are essential for conducting seasonal and long-term observations of glaciated regions. Further, the scene size is

185 km x 180 km which encompasses the entire Wind River Range in one scene (USGS, 2016). This is a significant advantage over many high-resolution sensors that must sacrifice scene size with resolution (Table 1). Most important is the multi-spectral data the Landsat series collects. This study uses the Blue, Green, Red, NIR and SWIR bands on the Landsat 5, 7, and 8 sensors for the delineation of glacier area as well as for calculating glacial lake reflectance. Landsat 7 was only used from 1999 – 2003 as the satellite had a scan line correction issue after May 2003.

The Shuttle Radar Topographic Mission (SRTM) Digital Elevation Model (DEM) dataset was used to calculate slope of the study area terrain for differentiating lakes from shadow areas. Spatial resolution of the SRTM DEM is 30 m with a vertical accuracy of 16m. The 30 m pixel size does not require re-sampling when pairing with the 30m Landsat image resolution. Although the dataset was collected in February, 2000, it can be used during the length of the study period as the watershed areas have not changed (Table 2).

The Parameter-elevation Regressions on Independent Slopes Model (PRISM) climate data is ideal for temperature analysis as the data is developed from multiple weather stations (PRISM, 2018). The PRISM data set is an analytical model that can produce daily, seasonal and average temperature for a given location. The primary use of the PRISM dataset is to produce interpolated daily temperature and precipitation data in areas without weather stations. The data can be obtained for 0.8 x 0.8 km² or 4 x 4 km² grid cells which provides enough resolution to select a grid cell over a specific area of a glacier. Although this dataset is interpolated, it provides a reasonable means of temperature comparison over time. The study uses daily temperature data converted to a mean summer temperature for (June, July, August, and September) between 1984 – 2017.

Table 1. Landsat sensor characteristics.

Landsat Series¹	Bands²	Wavelength² (mm)	Middle Wavelength	Spatial Resolution²	Temporal Resolution²	Radiometric Resolution²	Dates²
5	Blue	0.45 – 0.52	0.49	30	16 days	8-bit	3/1984 – 1/2013
	Green	0.52 – 0.60	0.56	30			
	Red	0.63 – 0.69	0.66	30			
	NIR	0.76 – 0.90	0.83	30			
	SWIR	1.55 – 1.75	1.65	30			
7	Blue	0.45 – 0.52	0.49	30	16 days	8-bit	4/1999 - present
	Green	0.52 – 0.60	0.56	30			
	Red	0.63 – 0.69	0.66	30			
	NIR	0.76 – 0.90	0.83	30			
	SWIR	1.55 – 1.75	1.65	30			
8	Blue	0.45 – 0.51	0.48	30	16 days	12-bit	2/2013 - present
	Green	0.53 – 0.59	0.56	30			
	Red	0.64 – 0.67	0.66	30			
	NIR	0.85 – 0.88	0.87	30			
	SWIR	1.57 – 1.65	1.61	30			

1. Imagery source, USGS (2017). Earth Explorer. Retrieved August 28, 2017, from <https://earthexplorer.usgs.gov/>

2. Data acquired from scene metadata

Table 2. SRTM Characteristics¹.

Mission	Type	Band	Horizontal Resolution (m)	Vertical Resolution (m)	Shuttle (Altitude km)	Dates
SRTM	DEM	C, X	30	16	Endeavor (233)	February 11 – 22, 2000

1. SRTM characteristics acquired from, NASA JPL. Retrieved September 14, 2017, from <https://www2.jpl.nasa.gov/srtm/statistics.html>

The Snowpack Telemetry (SNOTEL) climate data is ideal for Snow Water Equivalence (SWE) analysis as SNOTEL sites are located throughout the Wind River Range, with some sites at elevations > 3,000 m (NRCS 2018). The SNOTEL program is a network of nearly 730 stations and provides data on high elevation temperature, precipitation and SWE with some stations having more than 30 years of data. The primary use of the SNOTEL dataset is to analyze the snowpack in the Western United States over time. Although the stations are > 1,000 m below the highest peaks of the Wind River Range, the data provides a quantitative measure to determine whether the season received high or low snowfall throughout the range. The study uses the Elkhart Park (Site # 468) SNOTEL station (Figure 1) maximum annual SWE data between 1987 – 2017.

The USGS gage station data is ideal for analyzing long-term streamflow changes in the range. The USGS gage station collection program covers all 50 states including Puerto Rico with 10,283 active sites (USGS 2018). Three unimpaired gage stations were used in the study to identify change in three basins. The Dinwoody Creek basin was analyzed using the Dinwoody Creek gage station (#06221400) directly above Upper Dinwoody Lake (Figure 4). The Bull Lake Creek basin was analyzed using the Bull Lake Creek gage station (#06224000) directly

above Bull Lake Reservoir (Figure 5). The Pine Creek basin was analyzed using the Pine Creek gage station (#09196500) directly above Fremont Lake (Figure 7). The primary use of this dataset is to analyze summer streamflow changes in the range as they relate to changes in reflectance and glacier area. The study uses these station data for (June, July, August, and September) between ~ 1950 – 2017.

Image Correction

Images from Landsat are corrected for surface reflectance to obtain the actual ground value of the pixel reflectance. This assists with the delineation of reflectance signatures from various sources as it removes the atmospheric distortion that can impair non-atmospherically corrected images. The image correction process requires two steps. The first is radiometric calibration and the second is atmospheric correction.

Radiometric correction is essential as it accounts for differences in the sensor to calibrate the image. The image is loaded into the ENVI 5.3 Landsat radiometric calibration function to convert the raw image pixel values to at-sensor radiance values from the gain and offset values contained in the image metadata. The result is a band interleaved by line (.BIL) format that is input into the Fast Line-of-sight Atmospheric Analysis of Hypercubes (FLAASH) atmospheric correction program (Harris Geospatial Solutions 2017). The FLAASH atmospheric correction corrects the image for atmospheric distortion by using several user defined inputs including the atmospheric model, sensor data and water retrieval band. The output of the atmospheric correction is a surface reflectance corrected image. The surface corrected image pixel values ($R_{rs}(\lambda)$) were then multiplied by π to produce a unitless measure of reflectance (R_w). These images are used for the study to ensure consistent results throughout the data collection process.

Ratios and Indices for Analysis

The study requires using remote sensing ratios to automatically classify glacier area and surface characteristics. While many different methods were identified in the literature review section, the study uses the NIR and SWIR bands on the Landsat series. The NIR band has a higher reflectance on snow and ice than in the SWIR band and therefore a ratio of the two bands is used to delineate snow and ice in the image (Paul et al. 2013; Wang et al. 2017). The equation for this ratio is:

$$Eq\ 1: \frac{NIR}{SWIR}$$

This automatic classification is the best ratio to use when considering glaciers with significant amounts of water in the scene (Paul et al. 2013). The images were processed using equation 1 using ArcGIS 10.4 band math tools.

To extract water features (i.e. lakes) in the imagery, the Normalized Differential Water Index (NDWI) was used. This index classifies various water features in the scene while minimizing influence from water on the surface of glaciers, as values are typically very close to zero and can be differentiated from lakes in the scene. The NDWI ratio uses the Green band and the NIR band. For water, the Green band has a higher reflectance than the NIR band and this is used to create a differential index between the two bands (Gao 1996). The equation for this is:

$$Eq\ 2: NDWI = \frac{GREEN - NIR}{GREEN + NIR}$$

This produces a gradient of values that range from (-1) – (+1) with values above 0 having some water influence.

To extract water reflectance values for the analysis of lake color, the VIS bands (Blue, Green and Red) and NIR band were used. These bands are critical to studying glacier lake change as the lakes range from blue to gray. Gray lakes typically display a stronger reflectance due to a greater amount of glacial sediment while blue lakes have a lower reflectance due to little or no glacial sediment. This calculation accounts for both glacial and non-glacial lake types to be classified over time and allows for an analysis of variability in lake reflectance in relation to changing glacial conditions. The index for this is:

$$Eq\ 3: R_{w(VIS-NIR)} = R_w(BLUE) + R_w(GREEN) + R_w(RED) + R_w(NIR)$$

This unit-less index classifies water from 0 – 0.20 reflectance (R_w) based on the color of the water at the time of scene collection.

Analytical Process

Defining Glacial Areas

The Eq. 1 ratio, conducted in ArcGIS 10.4, produces a raster with reflectance values from 0 - >30. These values were classified into a single ice category to obtain glacier and snow area as one polygon which produces a total area. This produces a simple method of obtaining total glacier area as each glacier is subject to a different snow and ice delineation value due to varying topography on the glacier surface. The glacial areas extracted for each year were calculated in ArcGIS 10.4 for comparison of change over time. For further analysis of total glacier area, the

SRTM DEM was used to delineate the glaciers by watershed for comparison of area changes to streamflow.

Defining Lake Area and Extracting Reflectance Values

After processing the NDWI calculation, a polygon is created for each lake and clips the results of the NDWI. The lake polygon is used to extract the lake in all four Landsat bands.

These extracted lake bands are stacked and used in the lake reflectance calculation.

The lake turbidity index (Eq. 3) produces a raster with lake reflectance (R_w) values of 0 – 0.20. The reflectance values from each pixel across the individual lakes were extracted in ArcGIS 10.4 and averaged for individual lake reflectance values in an individual image. The annual mean summer glacial lake reflectance was calculated for each individual lake (using between one and four images) during the summer melt season (July, August, September) of each year. These mean annual summer lake reflectance values are classified into three turbidity categories roughly representing a range of colors including blue (0 – 0.05), turquoise (0.05 – 0.10) and gray (>0.10) (Figure 9). These color ranges differ from Matta et al. (2017) as different gain and offset values were used for radiometric calibration. These ranges were delineated by comparing the summed R_w values with visual observation of the lake color.

Statistical and Descriptive Analysis

Determining the trends in annual mean summer lake reflectance over time is one of the primary goals of this study. To accomplish this, a linear regression is conducted in Microsoft EXCEL to produce an R^2 and p value to show if the change trend is explained by the

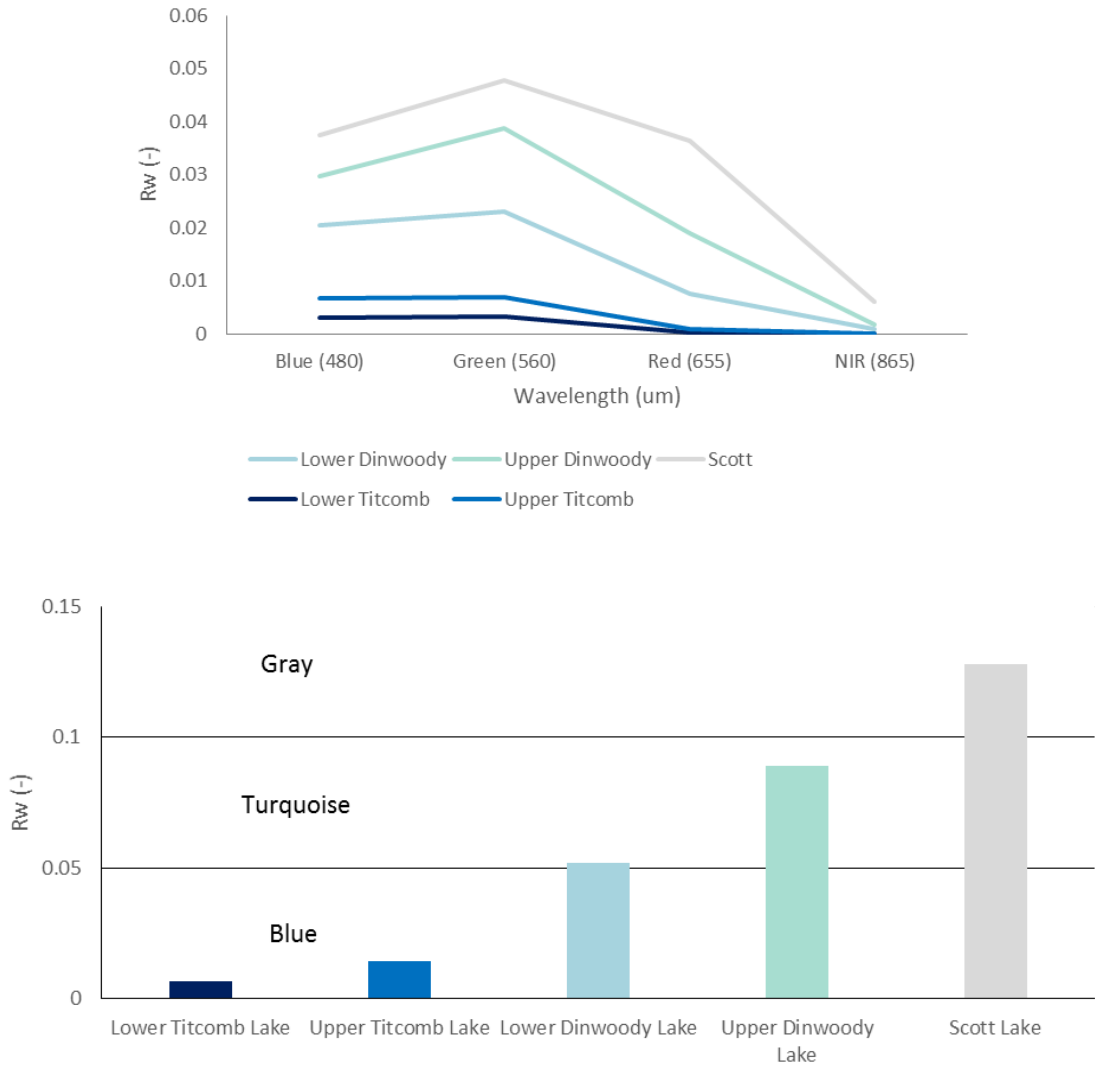


Figure 9. Glacial lake reflectance values (R_w) for the Blue, Green, Red, and NIR wavelengths (top), and summed glacial lake reflectance values ($R_{w(VIS-NIR)}$) indicating color classes (bottom) for Lower Titcomb, Upper Titcomb, Lower Dinwoody, Upper Dinwoody, and Scott Lakes in the Wind River Range, Wyoming.

regression equation. An additional multilinear regression analysis is run on Upper Dinwoody Lake in Microsoft EXCEL which compares changes in lake reflectance and three variables which influence glacial mass balance and the discharge of glacial sediments into the lakes. These variables include mean temperature, snow water equivalence (SWE), and lake area.

A final analysis is conducted in Microsoft EXCEL to understand how changes in glacier area and glacial lake reflectance relate to changes in streamflow over time for individual selected

basins of the Wind River Range. The long-term streamflow is compared to glacier area to identify how glacier contributions are changing due to decreasing mass. This provides insight into how streamflow is changing, which may be indicative of glaciers supplying melt water to lakes and streams in the range. The glacier area and streamflow data are also compared to lake reflectance to discuss how variations in lake reflectance may indicate changes in the activity of the glaciers.

Uncertainty

Uncertainty is one of the main limitations of a remote sensing study and is based on the radiometric uncertainty of each Landsat sensor as well as area uncertainties at the edge of the glaciers. The maximum radiometric uncertainty for Landsat 5 is $\pm 5\%$, Landsat 7 is $\pm 4\%$ and Landsat 8 is $\pm 3\%$ (USGS 2018). This uncertainty may produce minor variations in the post atmospherically corrected surface reflectance values, although this effect is limited by radiometrically calibrating the images in ENVI 5.3. Further, the USGS also cross-calibrated the sensors on each of the Landsat platforms to ensure long-term data continuity which limits variability between the sensors.

Due to the resolution of the imagery there is also an uncertainty of 30 m in the pixel size of the Landsat imagery. Due to lack of additional variables, this uncertainty calculation essentially equates to a 30-meter buffer of uncertainty around the boundary of the glacier.

CHAPTER IV

RESULTS

Individual lakes may be hydrologically connected to individual glaciers or to a collection of glaciers. Lakes with glacially fed streams were identified and selected for analysis, however only lakes with >80 pixels were included as too few pixels led to problems in analysis as the lakes were not large enough for a significant number of lake-only pixels. In total, 14 glacial lakes were analyzed between 1984 - 2017 in which regression analyses were conducted to determine if the regression equation can explain the change in summer mean monthly reflectance over time. The reflectance and subsequent water color of the glacially fed lakes are changing over time across the range. The lakes show a mixture of change scenarios which can be categorized into three groups: 1. Lakes with increased reflectance, 2. Lakes with no change in reflectance, and 3. Lakes with decreased reflectance.

Glacial lakes with increased reflectance

Scott Lake is hydraulically connected to Mammoth Glacier (~1.63 km²) on the west side of the Continental Divide in the range (Figure 6). The meltwater from Mammoth Glacier flows directly into Scott Lake approximately 2 km downstream from the terminus of the glacier. Minor Glacier (~0.24 km²) also appears to contribute meltwater, but overall meltwater contributions to Scott Lake appear to be dominated by Mammoth Glacier. Results of monthly

annual glacial lake reflectance over time for Scott Lake shows a significant increase in reflectance over the study period with a p value of < 0.01 and an R^2 value of 0.34 (Figure 10). Reflectance over the study period fluctuates with an overall increasing trend and a peak reflectance occurring in 2001. Results of glacial lake reflectance shows clustering of high values between 1989-1991 and 2000-2004. The lake ranges from turquoise in 1992, to gray in 2003 and 2015.

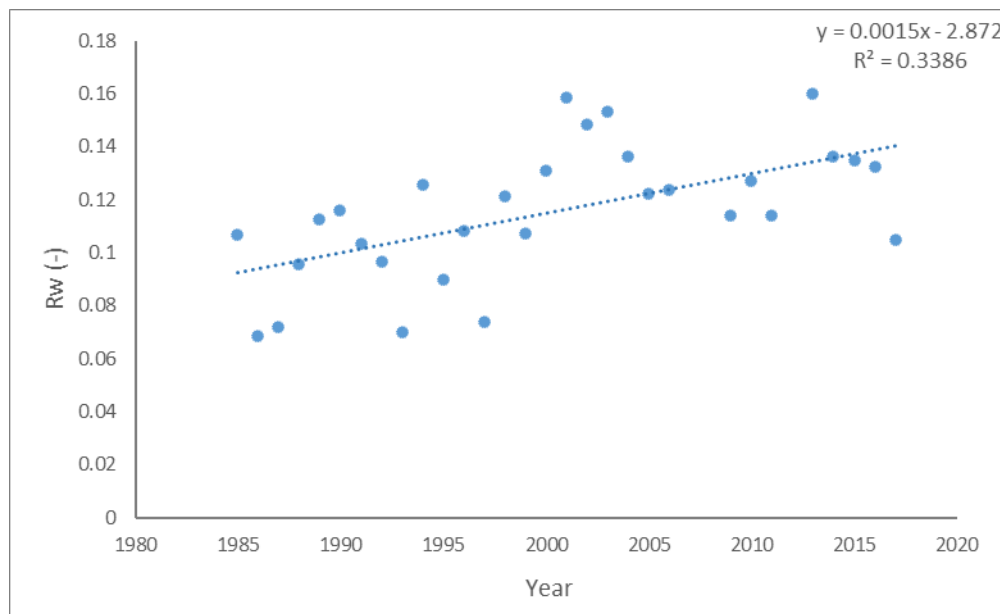


Figure 10. Scatter plot of mean late summer glacial lake reflectance (R_w) for Scott Lake. Blue dotted line indicates trend line with equation and R^2 value.

Upper Green River Lake (UGRL) and Lower Green River Lake (LGRL) are hydraulically connected to several small and large glaciers including Mammoth and Baby glaciers in Green River basin ($\sim 3.79 \text{ km}^2$) on the west side of the Continental Divide in the range (Figure 6). The meltwater from these glaciers first flows into UGRL and then LGRL. UGRL is approximately 17.5 km downstream from the terminus of Mammoth Glacier which has the largest area of glaciers in the Green River basin. Results of glacial lake reflectance over time for

UGRL shows a significant increase in reflectance over the study period with a p value of < 0.01 and an R^2 value of 0.36 (Figure 11). An example of glacial lake reflectance variability over time is presented for true color images of Upper Green River Lake with R_w values for the corresponding dates in Figure 12.

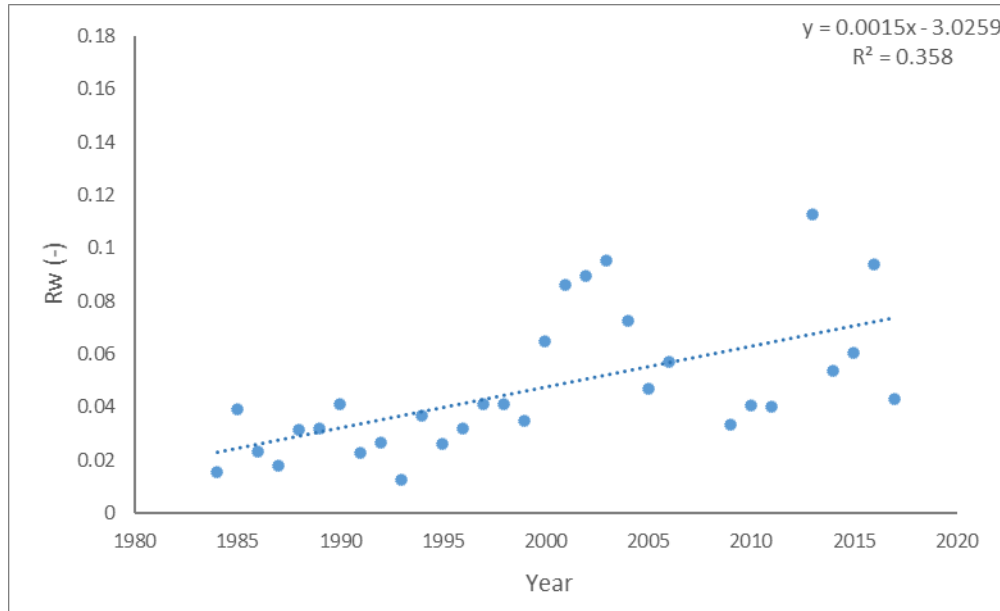


Figure 11. Scatter plot of mean late summer glacial lake reflectance (R_w) for Upper Green River Lake. Blue dotted line indicates trend line with equation and R^2 value.

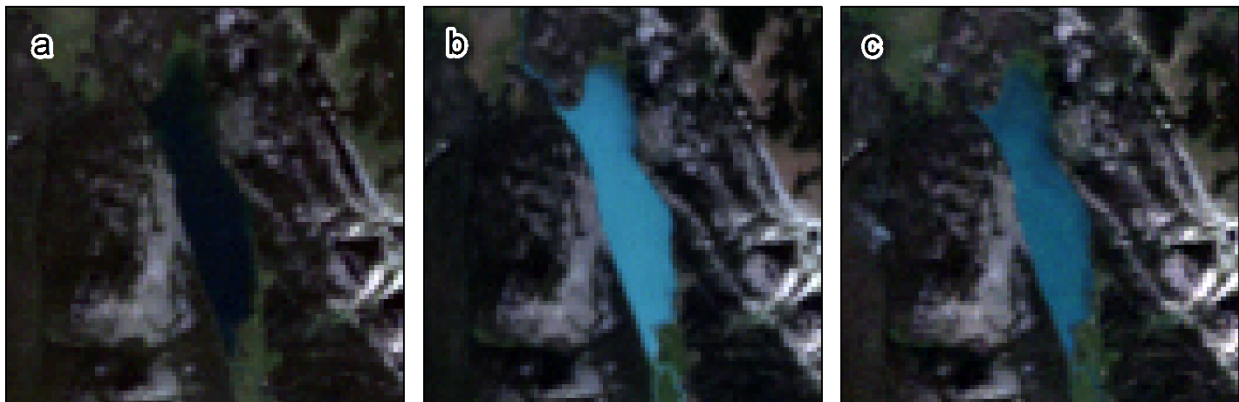


Figure 12. True color images showing Upper Green River Lake color variation with corresponding R_w values for August (a) 1993 (R_w value of 0.01), (b) 2002 (R_w value of 0.09) and (c) 2010 (R_w value of 0.05).

Results of glacial lake reflectance over time for LGRL shows a significant increase in reflectance over the study period with a p value of < 0.01 and an R^2 value of 0.28 (Figure 13). The peak for UGRL is in 2003 while the peak for LGRL is in 2001. UGRL has a clustering of high values between 2000-2004 while LGRL has clustering between 2001-2003. UGRL ranges from blue in 1992 to turquoise in 2003 and 2015 while LGRL is blue during these three periods. There are similarities in the pattern of reflectance between the lakes as UGRL feeds into LGRL. However, the measured reflectance for LGRL is lower than UGRL likely due to settling of glacial sediments within UGRL and a larger volume of water in LGRL. This same pattern occurs in all lakes in the study area consisting of upper and lower lakes.

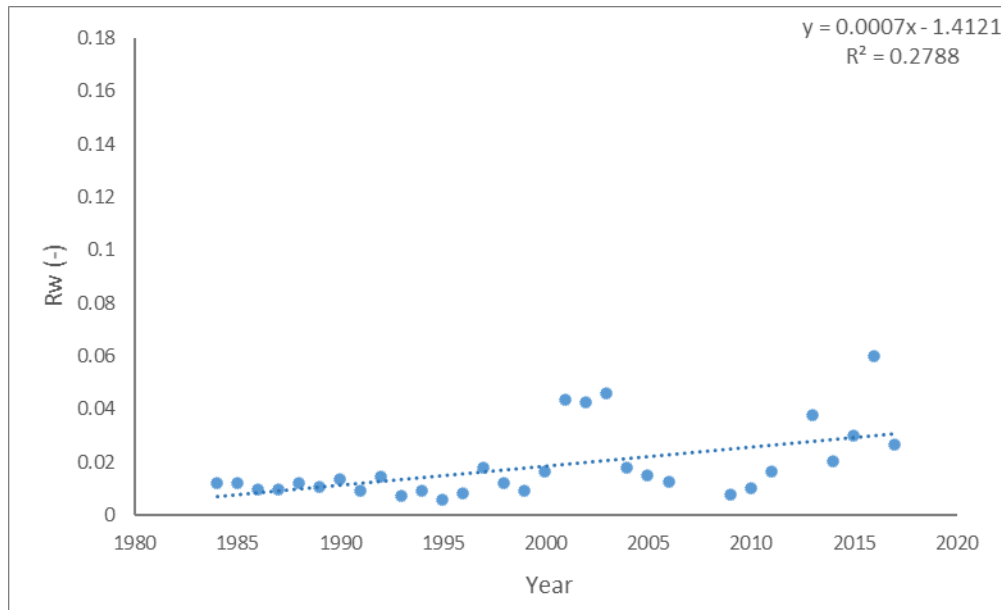


Figure 13. Scatter plot of mean late summer glacial lake reflectance (Rw) for Lower Green River Lake. Blue dotted line indicates trend line with equation and R^2 value.

Upper Dinwoody Lake (UDL) and Lower Dinwoody Lake (LDL) are hydraulically connected to several small and large glaciers including Dinwoody, Gannett and Grasshopper (~7.07 km²) in Dinwoody basin on the east side of the Continental Divide in the range (Figure 4). The meltwater from these glaciers flow first into UDL and then LDL. UDL is approximately 32.5 km downstream from the terminus of Dinwoody Glacier which is one of the largest glaciers by area in the Dinwoody Creek watershed. Results of glacial lake reflectance over time for UDL shows a significant increase in reflectance over the study period with a p value of < 0.01 and an R² value of 0.21 (Figure 14). LDL shows a significant increase in reflectance over the study period with a p value of 0.05 and an R² value of 0.09 (Figure 15).

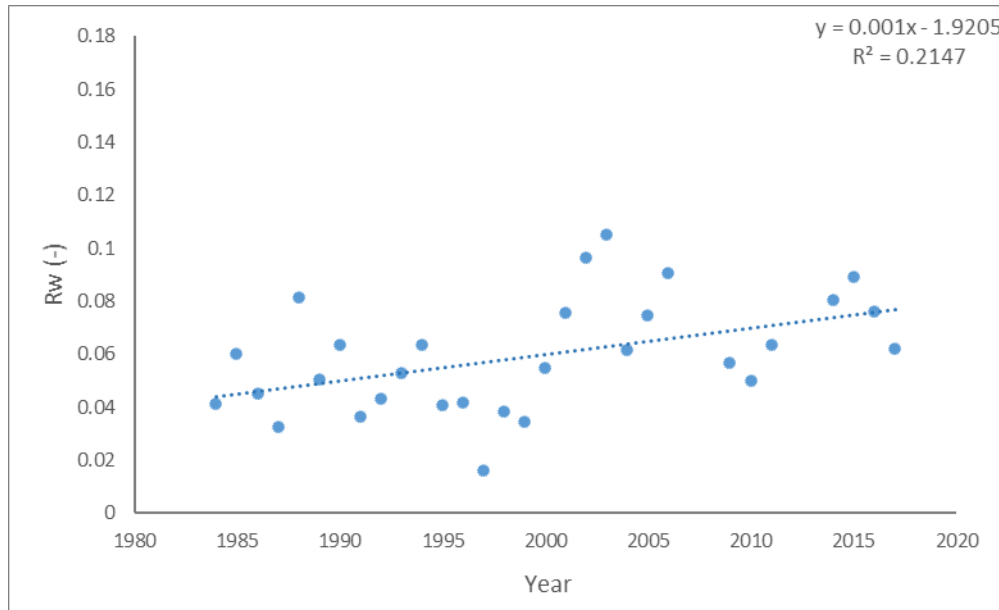


Figure 14. Scatter plot of mean late summer glacial lake reflectance (Rw) for Upper Dinwoody Lake. Blue dotted line indicates trend line with equation and R² value.

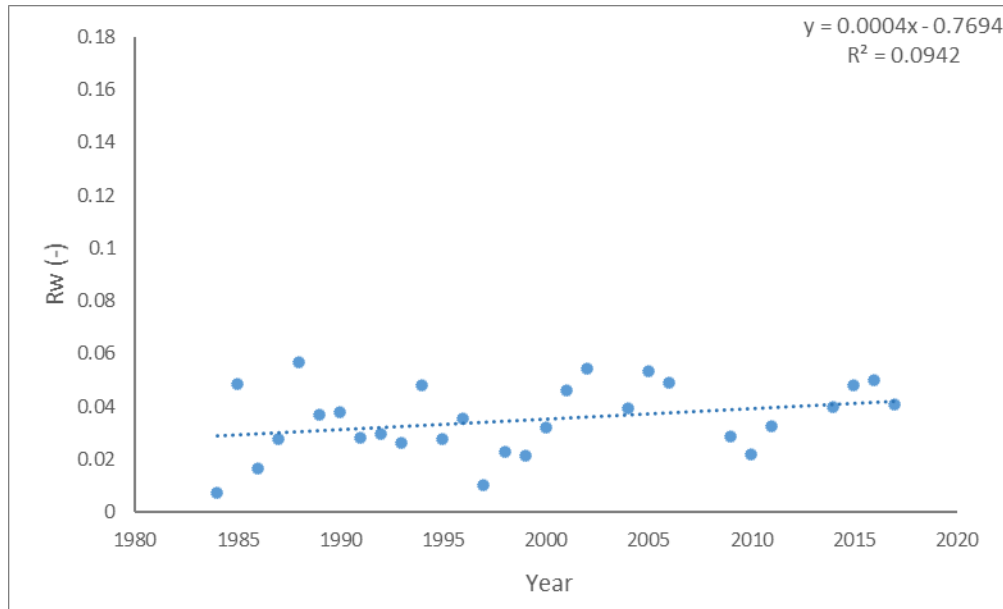


Figure 15. Scatter plot of mean late summer glacial lake reflectance (Rw) for Lower Dinwoody Lake. Blue dotted line indicates trend line with equation and R² value.

The peak reflectance for UDL was in 2003 while the peak for LDL was 1988. UDL has a clustering of high values between 1988-1990, 2001-2006 and 2014-2016 while LDL has clustering between 1988-1990, 2001-2006 and 2015-2016. UDL ranges from blue in 1992 to gray in 2003 and turquoise in 2015 while LDL ranges from blue in 1992 to turquoise in 2002 and blue in 2015.

Mile Long Lake (MLL) is hydraulically connected to Continental Glacier (~2.10 km²) on the East Side of the Continental Divide (Figure 3). The meltwater from Continental Glacier flows directly into Mile Long Lake approximately 1.5 km downstream from the terminus of the glacier. Results of glacial lake reflectance over time for MLL shows a significant increase in reflectance over the study period with a p value of 0.06 and an R² value of 0.09 (Figure 16). Reflectance over the study period fluctuates with an overall increasing trend and a peak reflectance occurring in 2016. MLL has a clustering of high values between 1988-1992 and 2001-2004. The lake ranges from blue in 1992, turquoise in 2003 and blue in 2015.

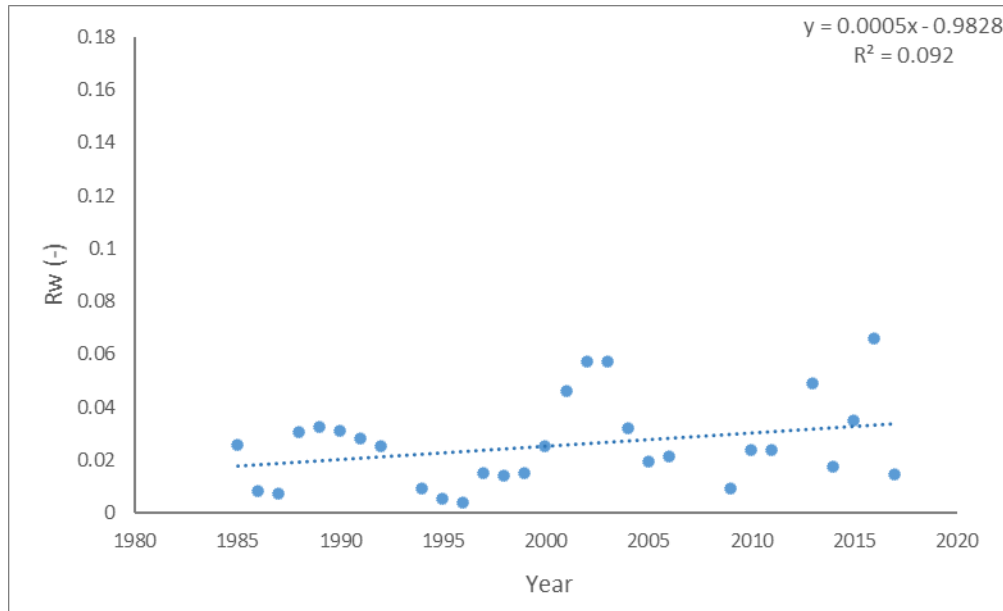


Figure 16. Scatter plot of mean late summer glacial lake reflectance (Rw) for Mile Long Lake. Blue dotted line indicates trend line with equation and R² value.

Unnamed Lake 1 (UL1) is hydraulically connected to an unnamed glacier (<0.1 km²) on the east side of the Continental Divide in the range (Figure 5). The meltwater from Unnamed Glacier 1 (UG1) flows directly into UL1 approximately 1 km downstream from the terminus of the glacier. Results of glacial lake reflectance over time for UL1 shows a significant increase in reflectance over the study period with a p value 0.01 and an R² of 0.10 (Figure 17). Reflectance over the study period fluctuates with an overall increasing trend for the lake. The peak reflectance for UL1 was in 2001 UL1 has a clustering of values between 1985-1988, 2000-2002 and 2013-2016. The lake is blue in 1992, 2003 and 2015. The reflectance in this lake is increasing, however, this is on a very small glacier (<0.10 km²) and no change in color is observed.

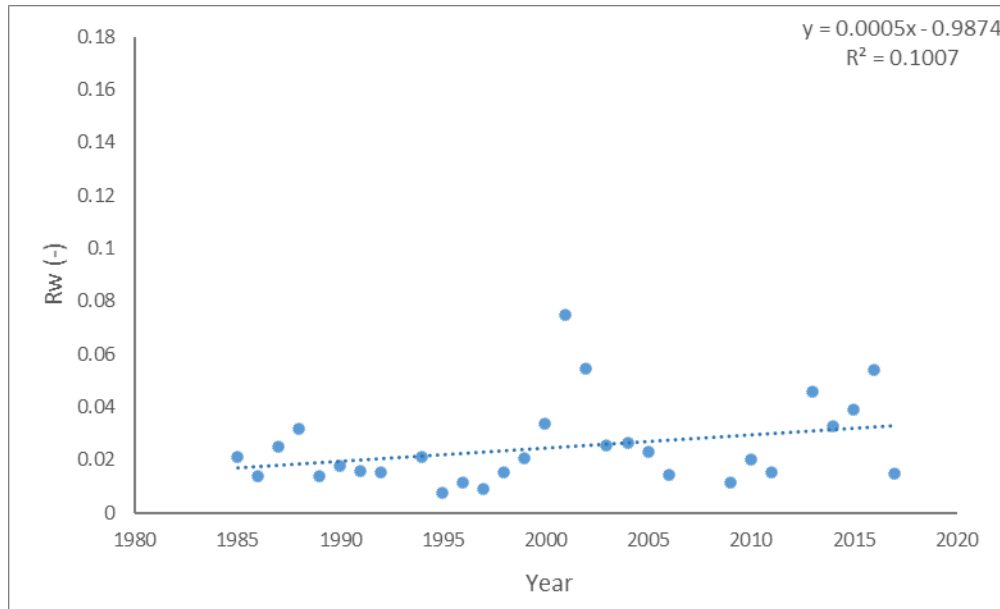


Figure 17. Scatter plot of mean late summer glacial lake reflectance (Rw) for Unnamed Lake 1. Blue dotted line indicates trend line with equation and R² value.

Glacial lakes with no change in reflectance

Little Milky Lake (LML) and Big Milky Lake (BML) are hydraulically connected to several small and large glaciers (~4.94 km²) including Upper Fremont, Sacagawea and Knife Point in Bull Lake Creek basin on the east side of the Continental Divide in the range (Figure 5). The meltwater from these glaciers first flows into LML and then BML. LML is approximately 11.5 km downstream from the terminus of Upper Fremont Glacier which is one of the largest glaciers in the Bull Lake Creek watershed. Results of glacial lake reflectance over time for LML show no change in reflectance over the study period with a p value of 0.47 and an R² value of 0.02 (Figure 18). Results of glacial lake reflectance over time for BML show no change in reflectance over the study period with a p value of 0.34 and an R² value of 0.03 (Figure 19). The peak for LML and BML is in 2001. LML has a clustering of high values between 1988-1995, 2000-2002 and 2013-2016 while BML has clustering between 1988-1995, 2000-2003 and

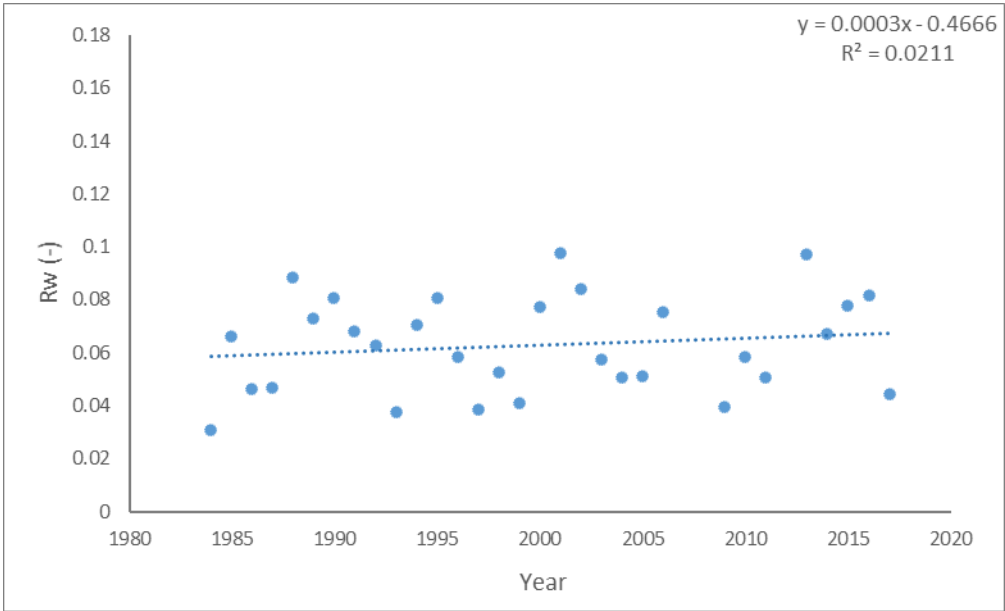


Figure 18. Scatter plot of mean late summer glacial lake reflectance (R_w) for Little Milky Lake. Blue dotted line indicates trend line with equation and R² value.

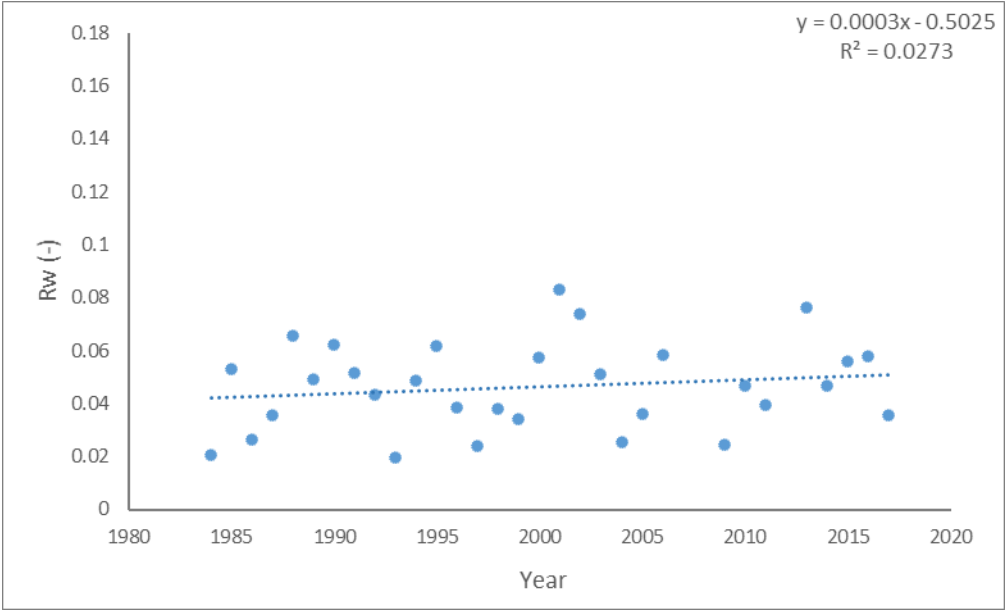


Figure 19. Scatter plot of mean late summer glacial lake reflectance (R_w) for Big Milky Lake. Blue dotted line indicates trend line with equation and R² value.

2013-2017. LML is turquoise in 1992, 2003 and 2015 while BML is blue in 1992 and turquoise in 2003 and 2015.

Upper Titcomb Lake (UTL) and Lower Titcomb Lake (LTL) are hydraulically connected to a few small glaciers (~0.12 km²) in Pine Creek basin on the west side of the Continental Divide in the range (Figure 7). The meltwater from these glaciers first flows into UTL and then LTL. UTL is approximately 3 km downstream from the terminus of Sphinx Glacier which is one of the largest glaciers in the Pine Creek watershed. Results of glacial lake reflectance over time for UTL shows no change in reflectance over the study period with a p value of 0.29 and an R² value of 0.07 (Figure 20). Results of glacial lake reflectance over time for LTL shows no change in reflectance over the study period with a p value of 0.88 and an R² value of < 0.01 (Figure 21). These lakes are generally clear, however in years with ideal glacial melt conditions, the lakes can appear gray. UTL has a clustering of high values between 1985-1990, 2001-2003 and 2013-2016 while LTL has clustering between 1985-1990, 2001-2002 and 2013-2016. The peak reflectance for UTL and LTL is in 2001. UTL and LTL are blue in 1992, 2003 and 2015.

Bomber Lake (BL) is hydrologically connected to Unnamed Glacier 2 (UG2) (~0.53 km²) on the east side of the Continental Divide in the range (Figure 3). The meltwater from UG2 flows directly into BL approximately 4 km downstream from the terminus of the glacier. Results of glacial lake reflectance over time for BL shows no change in reflectance over the study period with a p value of 0.69 and an R² value of < 0.01 (Figure 22). Reflectance over the study period fluctuates with a peak reflectance occurring in 1985. BL has a clustering of high values between 1985-1988, 2000-2002 and 2013-2017. The lake ranges from blue in 1992 and 2003 to turquoise in 2015.

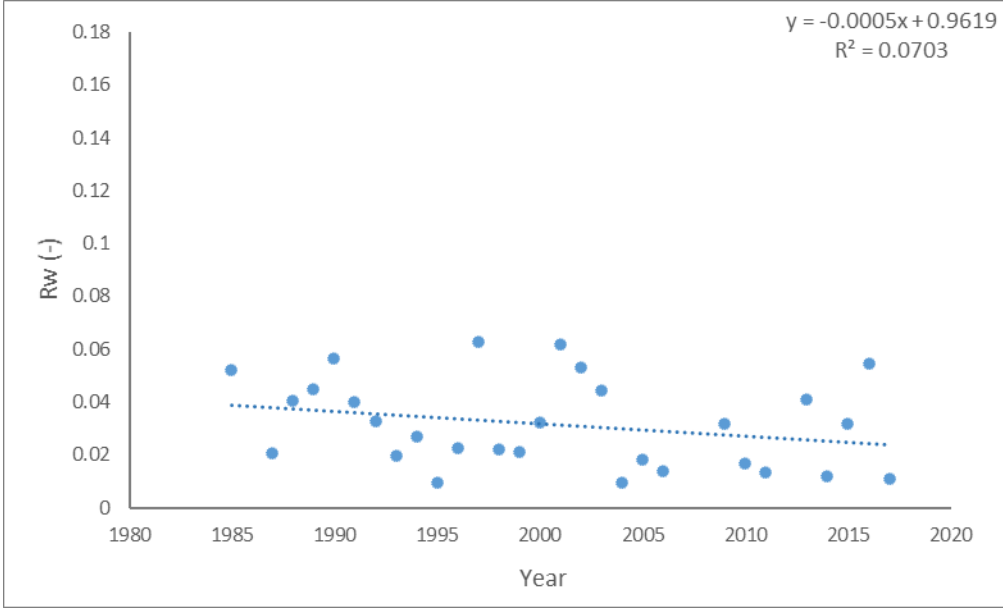


Figure 20. Scatter plot of mean late summer glacial lake reflectance (Rw) for Upper Titcomb Lake. Blue dotted line indicates trend line with equation and R^2 value.

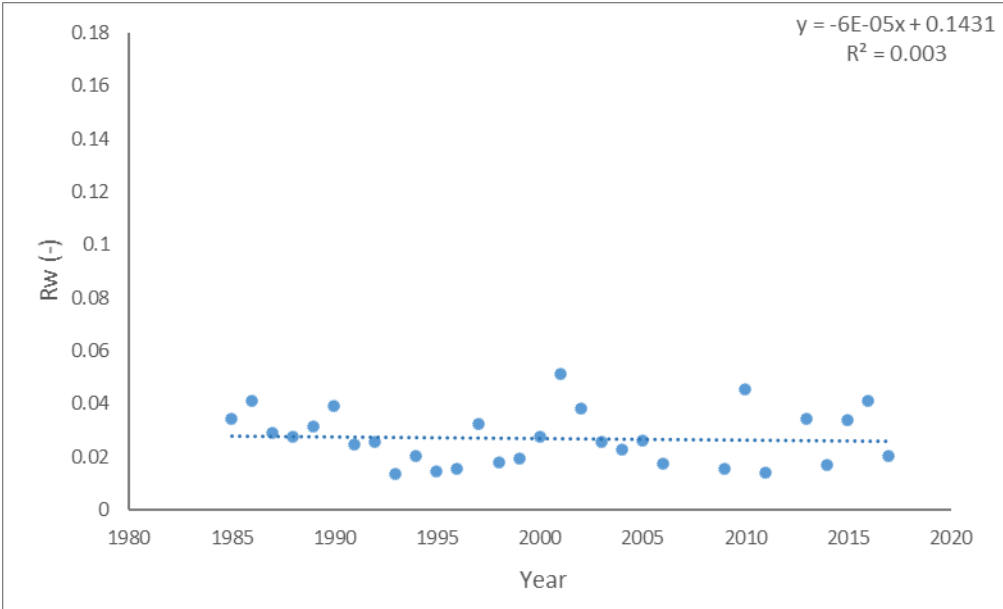


Figure 21. Scatter plot of mean late summer glacial lake reflectance (Rw) for Lower Titcomb Lake. Blue dotted line indicates trend line with equation and R^2 value.

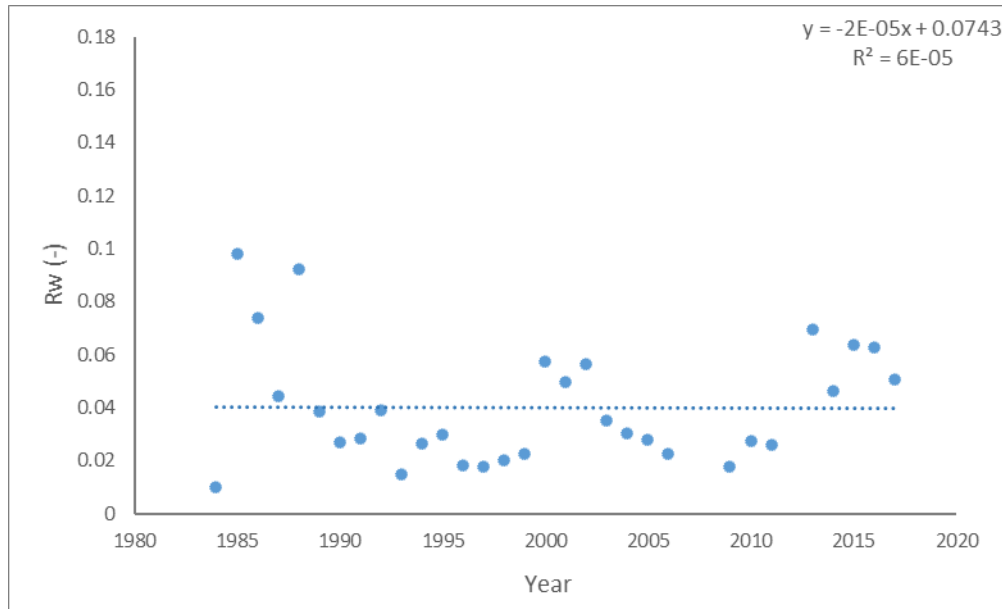


Figure 22. Scatter plot of mean late summer glacial lake reflectance (Rw) for Bomber Lake. Blue dotted line indicates trend line with equation and R² value.

Glacial lakes with a decrease in reflectance

Baby Lake (BbL) is hydrologically connected to Baby Glacier (BG) (~0.15 km²) on the west side of the Continental Divide in the range (Figure 6). The meltwater from BG flows directly into BbL approximately 1.5 km downstream from the terminus of the glacier. Results of glacial lake reflectance over time for BbL show a decrease in reflectance over the study period with a p value of < 0.01 and an R² value of 0.43 (Figure 23). Reflectance over the study period fluctuates with an overall decreasing trend and a peak reflectance occurring in 1987. BbL has a clustering of high values between 1988-1997, 2001-2002 and 2013-2017. The lake ranges from gray in 1992 to turquoise in 2003 and 2015.

Baker Lake (BkL) does not appear hydrologically connected to any surface glaciers on the west side of the Continental Divide in the range (Figure 6), yet the lake appears to have



Figure 23. Scatter plot of mean late summer glacial lake reflectance (Rw) for Baby Lake. Blue dotted line indicates trend line with equation and R² value.

hydraulic connectivity to a subsurface ice source north of the lake. The meltwater likely flows from the ice source directly into BkL. Results of glacial lake reflectance over time for BkL shows a decrease in reflectance over the study period with a p value of < 0.01 and an R² value of 0.66 (Figure 24). Reflectance over the study period fluctuates with an overall decreasing trend and a peak reflectance occurring in 1986. BkL has a clustering of high values between 1990-1992, 1996-2001 and 2013-2015. Although this lake does not appear to have a surface glacier, the lake might be hydraulically connected to a subsurface ice source. In ideal glacial melt condition years, the lake becomes active and varies in color. However, over the study period this reflectance continues to decrease and the lake does not appear as turbid as in the past. The lake ranges from turquoise in 1992 and 2003 to blue in 2015.

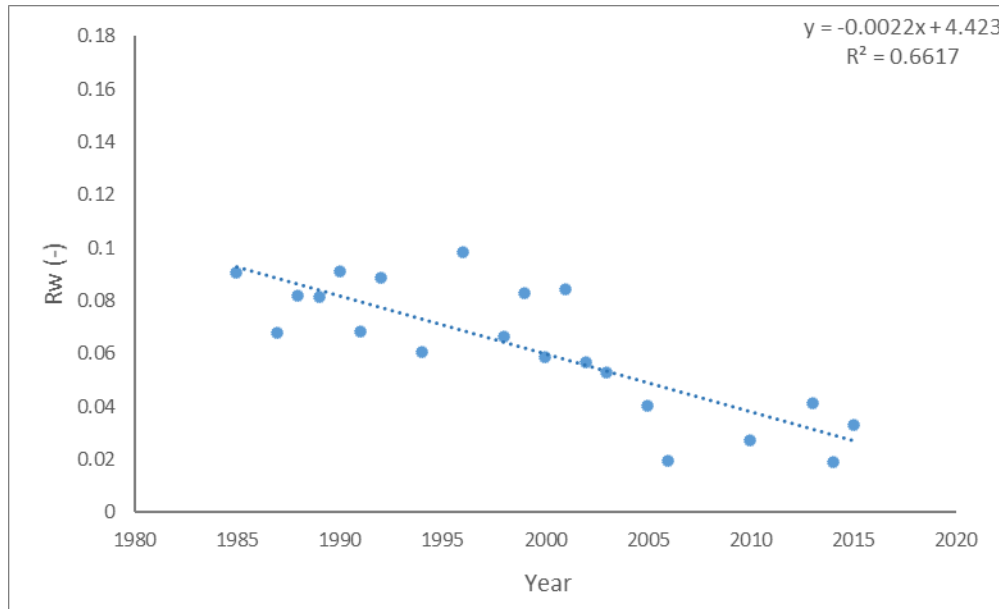


Figure 24. Scatter plot of mean late summer glacial lake reflectance (Rw) for Baker Lake. Blue dotted line indicates trend line with equation and R² value.

Mean reflectance of all glacial lakes over time

In total, 14 lakes were analyzed for their change in reflectance (Table 3). The lakes encompass the east and west sides of the Continental divide and represent change from basins with varying glacier meltwater contribution. When comparing all lakes in the range, the mean reflectance shows an increase in reflectance over the study period with a p value of 0.10 and an R² of 0.09 (Figure 25). Reflectance over the study period fluctuates with an overall increasing trend and a peak reflectance occurring in 2001. The significance (p) value is likely influenced by the amount of lakes increasing in reflectance compared to those with no change or decreasing reflectance.

Table 3. Change in glacial lake reflectance for the 14 analyzed lakes between 1984 and 2017(R^2 , significance (p) values, and trend of reflectance change for each lake over the study period).

Lake Name	R^2	p	Trend of Change
Baby	0.43	≤ 0.01	Decrease
Baker	0.66	≤ 0.01	Decrease
Big Milky	0.03	0.34	No Change
Bomber	≤ 0.01	0.69	No Change
Unnamed	0.10	≤ 0.01	Increase
Little Milky	0.02	0.47	No Change
Lower Dinwoody	0.09	≤ 0.05	Increase
Lower GRL	0.28	≤ 0.01	Increase
Lower Titcomb	≤ 0.01	0.884	No Change
Mile Long	0.09	≤ 0.10	Increase
Scott	0.34	≤ 0.01	Increase
Upper Dinwoody	0.21	≤ 0.01	Increase
Upper GRL	0.36	≤ 0.01	Increase
Upper Titcomb	0.07	0.287	No Change
Mean of WRR Lakes	0.09	≤ 0.10	Increase

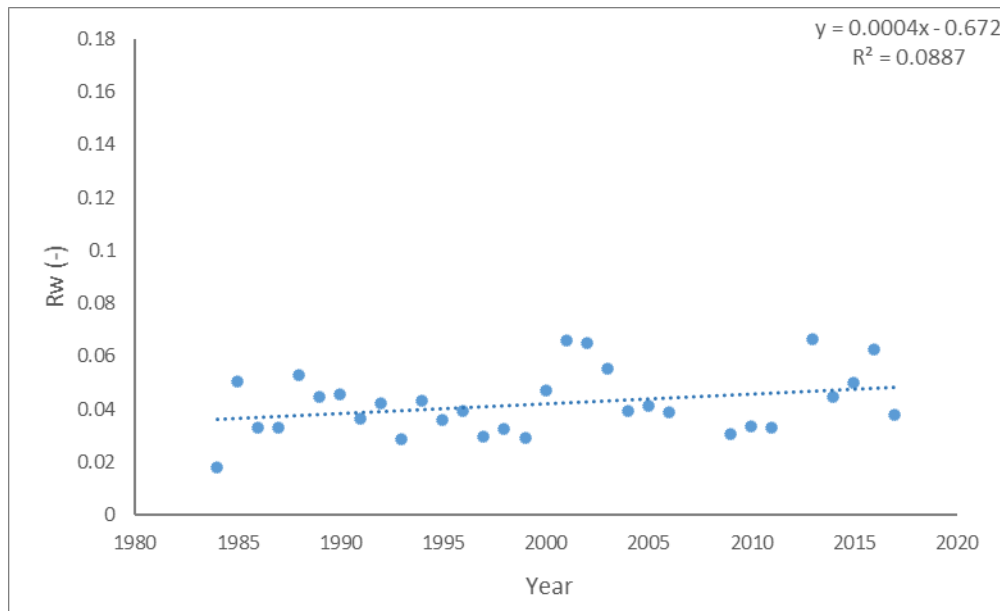


Figure 25. Scatter plot of mean late summer glacial lake reflectance (Rw) for all lakes in the Wind River Range. Blue dotted line indicates trend line with equation and R² value.

Area Change Analysis

An area change analysis was conducted to compare with the reflectance changes observed in glacial lakes. As glaciers decline in area they begin to lose their ability to supplement streamflow. Glaciers should be tracked over time to identify areas that have experienced significant change and what these impacts are on streamflow. The changes were identified for upper and lower sections with a delineation point at ~ 3,600 m, which is the mean elevation of all Wind River Range glaciers. In addition to the basin wide change, the breakdown of the upper and lower sections can further isolate where the change is occurring. Due to limitations in the Landsat imagery, specifically excessive cloud and snow cover for many of the dates, only three years had sufficient imagery for glacier area analysis.

The results for the first year selected (1992) indicate that the total area was 29.8 km² with an uncertainty of ± 0.894 km² (Table 4). The lower area was 13.73 km² and the upper area was 16.07 km². The second year selected (2003) for area change analysis indicated that the total area was 23.05 km² with an uncertainty of ± 0.692 km². The lower area was 11.23 km² and the upper area was 11.82 km². In the third year (2015) results indicated that the total area was 19.02 km² with an uncertainty of ± 0.57 km². The lower area was 8.33 km² and the upper area was 10.41 km².

Table 4. Total glacial area (km²) and the percent change between observation dates for the Wind River Range glaciers.

Year	Total Area (loss km²) (% change)	Upper Area (loss km²) (% change)	Lower Area (loss km²) (% change)
1992	29.8	16.07	13.73
2003	23.05 (-6.75)(-22.7%)	11.82 (-4.25)(-26.3%)	11.23 (-2.5) (-18.2%)
2015	19.02 (-4.3) (-17.5%)	10.41 (-1.41)(-12.1%)	8.61 (-2.62) (-25.6%)

Each basin in the range responds differently as local conditions such as temperature, snowfall and shading vary across the range. Bull Lake basin had an area of 7.8 km² in 1992 and 4.94 km² in 2015 for a total loss of 2.86 km² (Table 5). Dinwoody Creek basin had an area of 10.8 km² in 1992 and 7.07 km² in 2015 for a total loss of 3.73 km². Green River Lakes basin had an area of 5.6 km² in 1992 and 3.79 km² in 2015 for a total loss of 1.81 km². Torrey Creek basin had an area of 4.92 km² in 1992 and 2.87 km² in 2015 for a total loss of 2.05 km². These values describe the change in the individual basin and can be compared to other basins to determine how glaciers are melting in different portions of the range.

In total, the Wind River Range lost approximately 10.8 km² between 1992 and 2015. Area loss was highest in the first period as compared to the second period despite the increase in temperatures in the second period. The 2015 area measurement may be slightly influenced by a snow event a few days prior to measurement. Analysis of NAIP imagery collected a day prior to the Landsat image indicates that the snow has melted considerably between the two image dates, yet the upper portions of the glaciers may include additional snow as glacier area.

Table 5. Total glacier area (A) (km²) and change in area (%) from the previous year by basin for the observation dates.

Year	A (BL) (%Change)	A (GR) (%Change)	A (TC) (%Change)	A (DWC) (%Change)	A (PC) (%Change)
1992	7.8	5.6	4.92	10.8	0.51
2003	6.41 (-17.8%)	4.14 (-26.1%)	3.5 (-28.9%)	8.6 (-20.4%)	0.29 (-43.1%)
2015	4.94 (-23%)	3.79 (-8.4%)	2.87 (-18%)	7.07 (-17.8%)	0.12 (58.6%)

BL = Bull Lake

TC = Torrey Creek

GR = Green River Lakes

DWC = Dinwoody Creek

PC = Pine Creek

CHAPTER V

DISCUSSION

Glacier area change analysis through Landsat imagery can provide information on approximate area loss and can provide a linear estimate of rate of change between observations. The area loss can be broken down into the whole range, by basin, by elevation and by glacier to analyze how the glaciers are changing over time. These data are important as at a minimum water resource managers are provided with an updated area estimate and estimated rate of change to try to understand the impacts of glacial melting on streamflow. Limitations in quality imagery for area change analysis often lead to gaps between observation years, which is why only three dates were analyzed in this study (1992, 2003, and 2015). As ablation is not a linear process with the same amount of area loss per year, it is more likely that significant changes in area occur in a short period between area measurements, but this detail was not captured in this analysis.

However, changes in glacier area are an indication of changes in glacial activity, specifically mass balance (Bahr et al. 1997), which influences the amount of sediment discharged in the glacial meltwater represented by variations in meltwater color (i.e. reflectance). This suggests that glacial lake reflectance can be used to identify changes in glacial activity and the “health” of the glacier. With the archive of Landsat imagery, nearly annual analysis of glacial lake reflectance is possible, allowing for the gaps between glacier area measurements to be filled, providing greater detail on the fluctuating glacial conditions over time.

Of the 14 lakes analyzed in this study for the Wind River Range, seven are increasing in lake reflectance, five have no change, and two are decreasing in reflectance. This indicates that several change scenarios are occurring with the glaciers of the Wind River Range. However, these results do not identify the specific factors leading to the lake reflectance changes. To understand this we must identify the controlling factors of reflectance and the driving forces behind these changes. As glacial lake reflectance is related to the discharge of sediment caused by glacial activity, the driving forces behind glacial lake reflectance are related to the mass balance of the glacier. These include the two primary climatic factors of snow cover (which is related to snow water equivalence (SWE)) and temperature (Rothlisberger and Lang 1987; Paterson 1994). Glacial lake reflectance is also influenced by the amount of water discharging (i.e. streamflow) into the lake which can come from both glacial and non-glacial sources, as well as the size of the lake which is related to the concentration of sediments leading to reflectivity. Therefore, the impact of these major factors are discussed along with additional analysis to determine their significance on glacial lake reflectance. Finally, the changing glacial conditions for three of the basins in the Wind River Range based on this analysis is also presented.

Climatic factors controlling glacial lake reflectance

Snow cover (represented by SWE) and increasing mean temperatures (T_{mean}) are the primary controllers to glacier ablation. Snow water equivalence data was obtained from the Elkhart Park SNOTEL station (SNOTEL 2018) which is situated at 2,865 meters above mean sea level and is located on the west side of the continental divide (Figure 1). Analysis of the SWE data involved collecting the maximum annual SWE as this maximum value provides a proxy of the amount of snow cover from the previous winter (Figure 26). The T_{mean} data are the

average summer mean temperatures (Figure 27) from a grid cell over cirque 3 on Dinwoody Glacier on the east side of the Continental Divide (Figure 4) (PRISM 2018). Low snow cover exposes the ice surface which has a lower albedo than snow and in conjunction with high temperatures glacial ablation will increase. The opposite is true with high snow cover and lower temperatures as glacial ablation will be limited. A regression of T_{mean} and SWE produces a p value of < 0.1 and an R^2 of 0.11 (Figure 28). This suggests that high snow years are typically cooler than low snow years and will result in less glacial melting, which in turn will lead to less sediment laden glacial meltwater contributing to the lakes causing them to have a lower reflectance. In years of high temperatures and low snow fall, more glacial ablation will occur leading to greater sediment laden glacial meltwater flowing into the lakes causing them to have a higher reflectance.

Snow cover within Pine Creek Basin in the Wind River Range is melting approximately 16 ± 10 days earlier in the 2000s as compared to 1972 - 1999 (Hall et al. 2015). As well, temperatures have increased by 3.5°C on Upper Fremont glacier from the early 1960s to the 1990s (Naftz et al. 2002). These factors are likely contributing to increased glacial melt which is leading to the overall increase in glacial lake reflectance over time within the Wind River Range (Figure 25). This trend is likely to continue as alpine environments are changing much more rapidly as compared to lower elevations (Bradley et al. 2006).

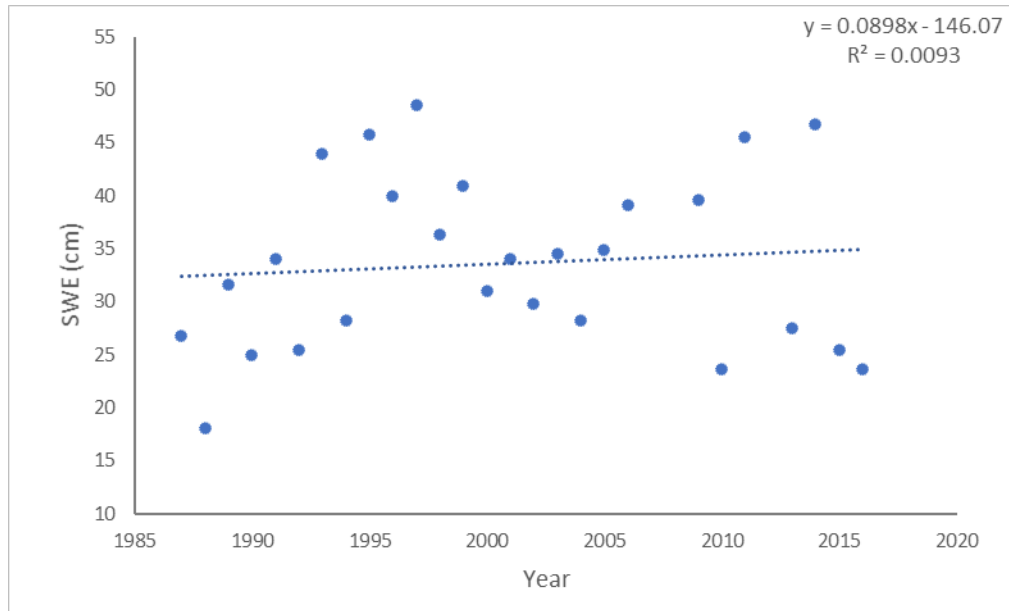


Figure 26. Scatter plot of maximum annual SWE (cm) for the Elkhart Park SNOTEL station over time. Blue dotted line indicates trend line with equation and R^2 value.

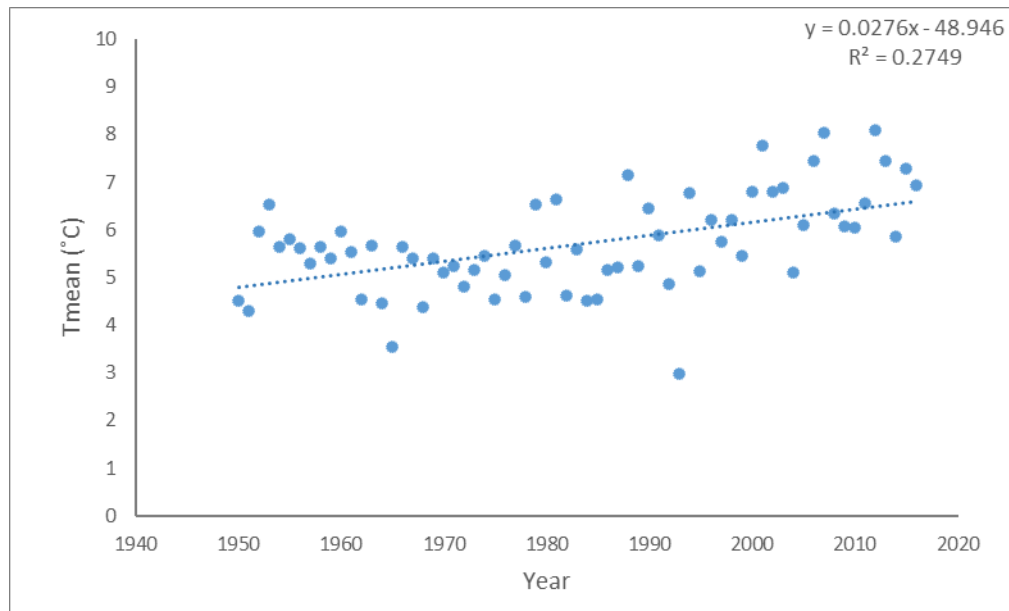


Figure 27. Scatter plot of mean summer maximum temperatures (°C) for Dinwoody Glacier from PRISM data set over time. Blue dotted line indicates trend line with equation and R^2 value.

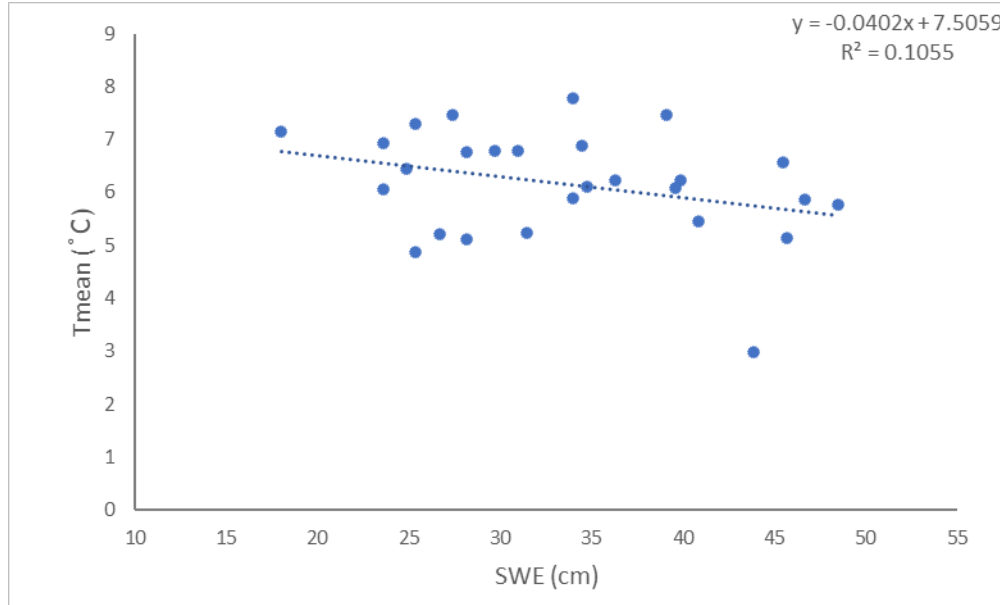


Figure 28. Scatter plot of mean summer temperature (°C) and max annual SWE (cm) for the Elkhart Park SNOTEL station. Blue dotted line indicates trend line with equation and R² value.

Other factors controlling glacial lake reflectance

Glacier area is another controlling factor to changing glacier reflectance, as glacier area and glacier volume are related (Bahr et al. 1997). As glacier volume declines, the amount of rock flour decreases due to decreased surface area available for erosion at the bed of the glacier among other factors such as velocity changes related to reduced mass, loss of ice with entrained materials and water availability to flush the solids (Benn and Evans 2010). Rock flour availability is critical to the change in reflectance. The decline in rock flour leads to a decrease in reflectance over time. As glaciers begin to decline in area they typically experience steady-state conditions in cooler years, possibly due to shading of the glacier surface as they shrink closer to steep mountain headwalls. However, in hot years the snow cover melts and the glacier is subject to ablation. This produces an increase in reflectance despite the small size of the

glacier however, the reflectance is lower than when the glacier was large likely due to the loss of area and its ability to supply rock flour.

Lake area is another important factor to changing glacier reflectance. The reflectance of a small lake is typically higher than a larger lake. This is due to the amount of water within the lake as larger lakes require more rock flour input to increase in reflectance compared to smaller lakes. Typically, the smallest lakes are closest to glaciers and feed into larger lakes further downstream. Within the Wind River Range basins there are several pairs of lakes including the Milky Lakes, Dinwoody Lakes, and Green River Lakes. Each lake pair has a higher reflectance upper lake and a lower reflectance lower lake as the larger lakes require more rock flour input to produce similar reflectance. This same relationship exists between Scott Lake and the Green River Lakes. Scott Lake is highly reflective and feeds water to Upper Green River Lake and the Lower Green River Lake. This process illustrates a decreasing reflectance as lake area increases along with an increasing distance from the glacier.

One final fundamental association exists between glaciers and glacial lake reflectance. This involves the concept of relative water sources. As snow decreases and maximum temperature increases, a larger amount of water will come from the glaciers to supplement streamflow. Therefore, the increase of sediment laden glacial meltwater will lead to an increase in glacial lake reflectance. However, years in which snow pack is high and temperatures are low, the sediment laden glacial melt water will be diluted by the relatively high concentration of snow melt water discharging into the lake. Cable et al. (2011) sampled oxygen/hydrogen isotopes to identify flow in Dinwoody Creek. Vandeberg and VanLooy (2016) conducted a similar study in Torrey Creek. Both studies found similar findings in the sense that hotter years have higher flow from glacier melt water and cooler years have more snow melt influence. As

temperatures continue to increase while snow decreases, more water will come from glaciers until they shrink to the point that flow rates decline during the dry late summer season. The lack of late summer streamflow from the glaciers leads to a decrease in glacial lake reflectance.

Analysis of Upper Dinwoody Lake

A multi-linear regression analysis was conducted to determine if the variables of snow water equivalence (SWE), mean temperature (T_{mean}) and lake area can explain the variation in reflectance of Upper Dinwoody Lake (UDL). The analysis was conducted from 1990 – 2015 and omits 2007 and 2008 as well as 2012 due to missing data. Data for 2003 and 2013 were collected from the median values as Glacier Lake Outburst Flood (GLOF) events occurred in the late season which led to high estimations of mean annual reflectance. Reflectance for Upper Dinwoody Lake was described above and can be referenced in Figure 14.

SWE varies from season to season and over time has not varied much in the Elkhart Park SNOTEL station data since 1987. However, this only shows the change from 1987. Hall et al. (2012) determined snowfall in Fremont Basin has melted 21 days earlier in the season in the early 2000s than in 1970. While this data is from another basin, it does represent a general trend of high and low snowfall years. SWE does not have a significant trend over time with a p value of 0.63 and an R^2 of < 0.01 as the values vary from year to year (Figure 26). Comparing SWE to UDL reflectance, SWE has a p value of 0.39 with an R^2 of 0.03 (Figure 29). This does little to explain the variation of change in SWE and change in reflectance. However, this variable is considered for the multi-linear regression analysis as snowfall is critical to the mass balance of glaciers and in turn glacier melt water production.

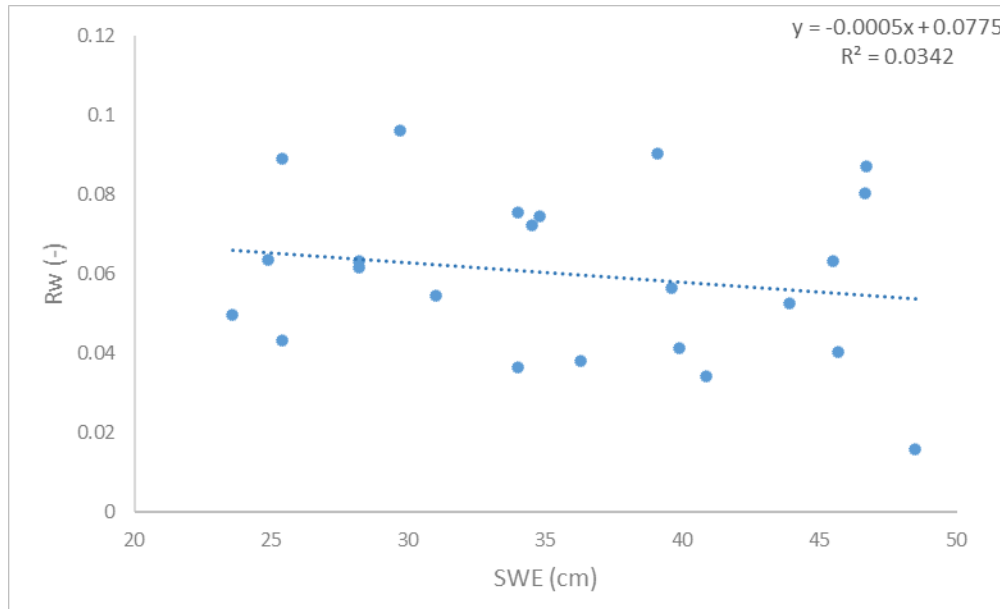


Figure 29. Scatter plot of mean summer lake reflectance (Rw) for Upper Dinwoody Lake compared with SWE (cm) for Elkhart Park SNOTEL station. Blue dotted line indicates trend line with equation and R² value.

T_{mean} is increasing annually over the range between 1950 - 2015. PRISM data (PRISM, 2017) from an upper section of Dinwoody glacier indicates T_{mean} has increased ~ 2 °C. While this is only one location in the range it does show that temperatures are changing over time with a p value of < 0.01 and an R^2 of 0.27 (Figure 27). As a consequence of increased temperatures, glaciers in the range are melting at a higher rate due to increased exposed ice surface from melted snow cover. This in turn affects UDL reflectance due to larger contributions of glacier melt water relative to snow melt water. When comparing temperature to UDL reflectance it shows that T_{mean} has a p value of < 0.01 and an R^2 of 0.30 (Figure 30). This indicates that as T_{mean} increases the reflectance of UDL also increases. This variable is considered for the multi-linear regression analysis as T_{mean} is critical to the mass balance of glaciers and is a significant variable in explaining the variation of reflectance individually.

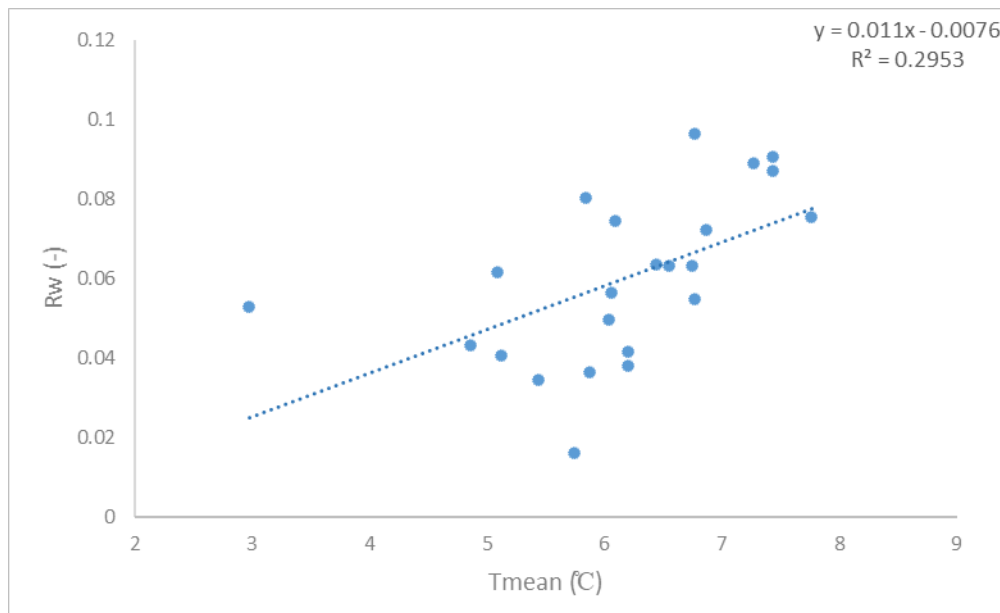


Figure 30. Scatter plot of mean summer lake reflectance (Rw) for Upper Dinwoody Lake compared with mean temperature (°C) for Dinwoody Glacier. Blue dotted line indicates trend line with equation and R² value.

Lake area does not significantly fluctuate over the study period. This is occurring despite the decrease in streamflow over time. Subsequently, the lake area appears to have an optimal range in streamflow where the lake is largest. The area change over the study period for the lake has a p value of 0.60 and an R² of 0.01 (Figure 31). However, the lakes are increasing in reflectance over time and have a relationship with lake area. When comparing reflectance and lake area the p value is < 0.01 and the R² is 0.34 (Figure 32). This indicates that reflectance is highest when lakes are at their largest. This variable is considered for the multi-linear regression as lake area is the result of discharge from snow and ice and is a significant variable in explaining the variation of reflectance individually. Table 6 shows the statistical description of SWE, T_{mean} and lake area.

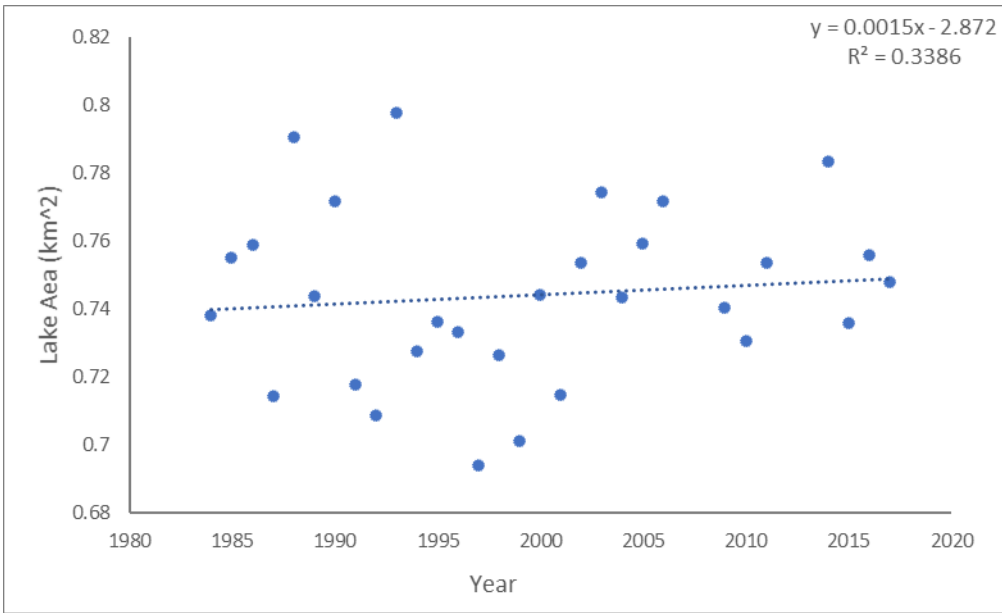


Figure 31. Scatter plot of mean summer lake area (km²) for Upper Dinwoody Lake over time. Blue dotted line indicates trend line with equation and R² value.

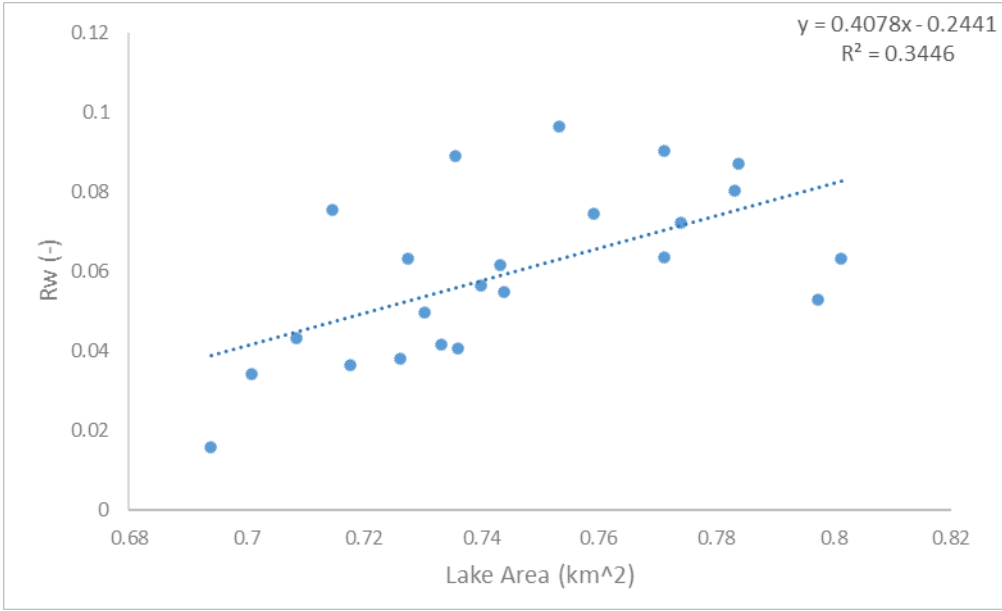


Figure 32. Scatter plot of mean summer lake reflectance (Rw) compared to mean summer lake area (km²) for Upper Dinwoody Lake. Blue dotted line indicates trend line with equation and R² value.

Table 6. Descriptive statistics of the SWE (cm) at the Elkhart Park SNOTL Station, lake area (km²) of Upper Dinwoody Lake, and T_{mean} (°C) from the PRISM data over Dinwoody Glacier.

Variable	Mean	Median	Std Dev	Min	Max	N
SWE	35.93	34.8	7.96	23.6	48.5	23
Lake Area	0.75	0.74	0.03	0.69	0.80	23
Tmean	6.16	6.21	1.04	2.97	7.76	23

A multi-linear regression was conducted to determine the influencing factors on glacial lake reflectance of UDL. Reflectance was plotted against the three variables including lake area, SWE, and T_{mean}. The analysis shows that the combined variables produced an R² value of 0.70 (Figure 33) with lake area and T_{mean} being significant at the 99% confidence level with p values < 0.01, while SWE is significant at the 90% confidence level with a p value of 0.06. This indicates that the selected variables account for 70% of lake reflectance variability. This produces a predictive model equation of:

$$Pred(Rw) = -0.31228 + (0.452047(Lake\ Area)) + (0.00983(T_{Mean})) - (0.00071(SWE))$$

This indicates that as lake area and T_{mean} increase and SWE decreases, the glacial lake reflectance increases. Similarly, as the lake area and T_{mean} decrease and SWE increases, the glacial lake reflectance decreases. Table 7 shows the coefficients and significance (p-values) for the three variables of the predictive model for glacial lake reflectance of Upper Dinwoody Lake.

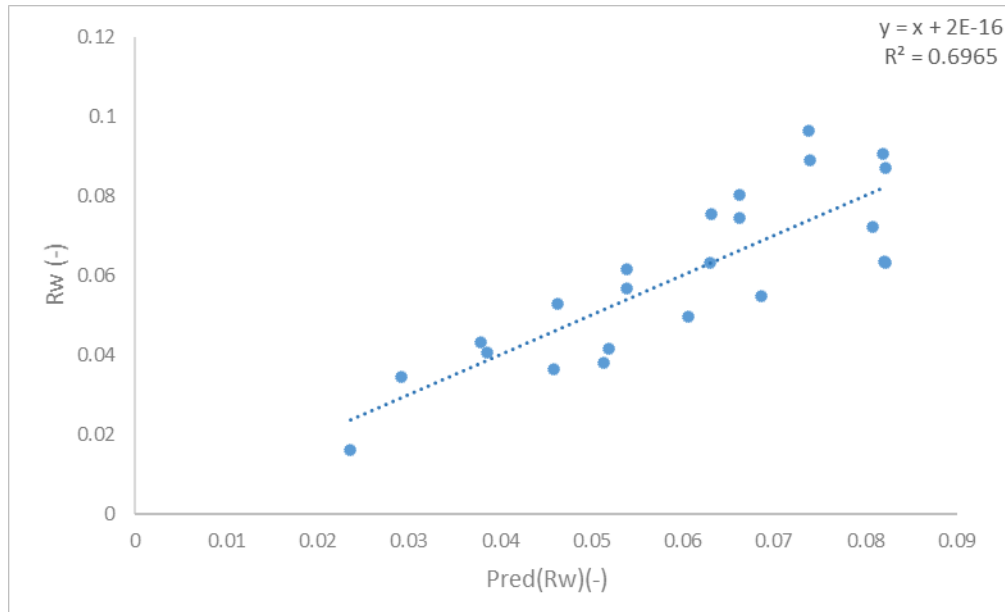


Figure 33. Scatter plot of mean summer lake reflectance (Rw) with predicted mean summer lake reflectance (Pred(Rw)) for Upper Dinwoody Lake. The multi-linear regression compares mean summer lake reflectance to SWE (cm), lake area (km²) and T_{mean} (°C). Blue dotted line indicates trend line with equation and R² value.

Table 7. Coefficients and significance (p-values) of the variables of SWE (cm), T_{mean} (°C) and lake area (km²) in the predictive model for glacial lake reflectance of Upper Dinwoody Lake.

. Variable	Coefficient	P value
SWE	-0.00071	0.06**
Lake Area	0.452047	< 0.01*
Tmean	0.00983	< 0.01*

* - Significant at 99%

** - Significant at 90%

While the R^2 value of 0.70 is a good estimation of UDL reflectance variability, it still does not explain the other 30% of the model variability. This can likely be explained by the SWE data as the data is from the Elkhart Park SNOTEL station on the west side of the Continental Divide and lack of a glacier area variable (SNOTEL, 2018). More representative data from all major glaciers in Dinwoody Creek or a basin wide snow cover analysis may dramatically improve SWE p value and R^2 value in the multi-linear regression. While this was not the only factor leading to a decrease in p value and R^2 value, it is a primary factor and this variable could significantly increase predictability of lake reflectance using the variables. Further, the lack of a glacier area variable likely produces the lower R^2 value. The study only produced three glacier area measurements. Due to the limited data, they could not be included in the analysis.

Lake area is a unique factor that has implications for both streamflow and reflectance and warrants further analysis. Lake area in UDL has remained stable over the study period despite a decrease in streamflow. Subsequently, it appears streamflow and lake area have a unique relationship where maximum lake area and reflectance occurs when streamflow is between $8.5 - 9.5 \text{ m}^3\text{s}^{-1}$ (Figure 34). Values < 8.5 and $> 9.5 \text{ m}^3\text{s}^{-1}$ are associated with smaller lakes, where lake area values far above this tend to be lowest. Values $< 8.5 \text{ m}^3\text{s}^{-1}$ tend to have more reflective lakes than values $> 9.5 \text{ m}^3\text{s}^{-1}$. This is likely due to the Wind River Indian Reservation irrigation canals constructed in 1935 (WRIP, 1995) as the lake reaches a critical point where lake volume is largest before discharging excess volume into the canal. This produces a parabolic distribution and subsequently a 2nd order polynomial regression was performed on lake size and streamflow and results in a p value of < 0.01 and an R^2 of 0.48. So, as the flow in Dinwoody Creek continues to decrease through the optimal flow rate, lake area will increase. However, the flow

will eventually reach a point where the optimal streamflow cannot be reached, and the lake will begin to decline in area.

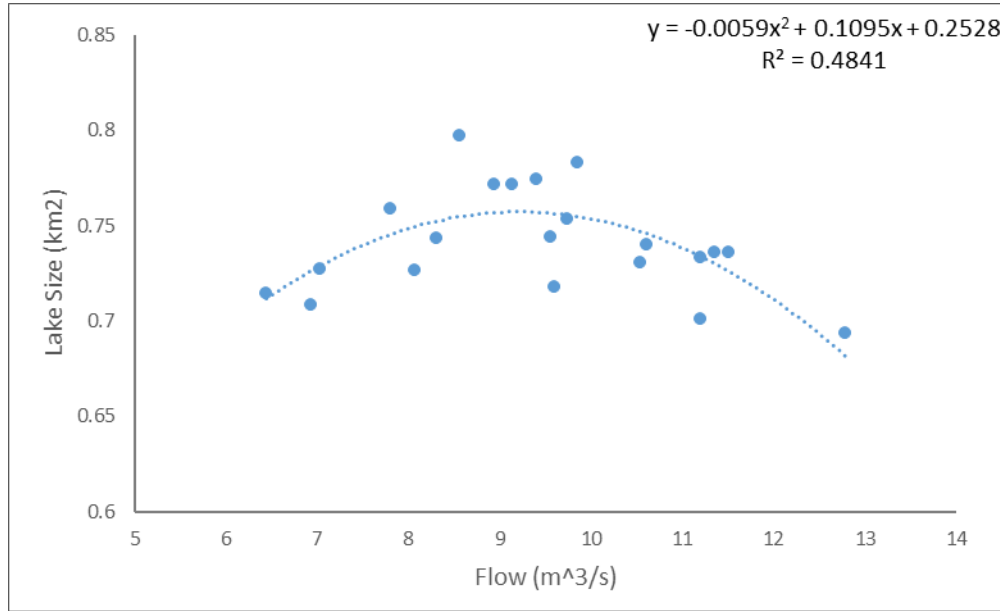


Figure 34. Scatter plot of mean summer lake size (km²) and mean summer streamflow (m³ s⁻¹). Blue dotted line indicates trend line with equation and R² value.

Basin-wide Lake Reflectance Changes Compared to Stream Flow, SWE, and Glacier Area

Glacial lake reflectance has been shown to be related to factors which control glacial activity, and in turn are related to annual climatic conditions. However, glacial activity has an impact on streamflow within the glacial basins. Given these connections, a discussion of the possible use of changing glacial lake reflectance as a proxy for changes in streamflow is presented for three of the glacial basins in the Wind River Range. Pine Creek, Bull Lake Creek and Dinwoody Creek basins have been selected as they have unimpaired streamflow data as well as represent two of the three trends of glacial lake reflectance change (increase and no change).

Pine Creek basin has the lowest glacial mass (0.22 km^2) in the range and has very little influence from glaciers to streamflow. Comparing streamflow to SWE indicates that when SWE is high, streamflow is also high and subsequently lower snow years, have lower flow. The comparison of streamflow to SWE produces a p value of < 0.01 and an R^2 of 0.49 (Figure 35). The streamflow at the USGS Gage Station (#09196500) above Fremont Lake (Figure 7) has declined approximately $4.5 \text{ m}^3 \text{ s}^{-1}$ since 1940 with a p value of 0.03 and an R^2 of 0.07 (Figure 36). This result is likely due to reduced snow cover in Pine Creek basin as detailed by Hall et al. (2015).

When looking at the Titcomb Lakes within Pine Creek Basin we can see that the reflectance of the lakes does not have a significant change trend over time. This lack of change is likely due to the basin having small glacial mass as they cannot supply large volumes of water. The lakes have been primarily blue for the duration of the study period ranging from 0.01 – 0.06 (Figures 20 and 21) indicating very little glacial influence. It is likely that the basin is far beyond the peak of glacial meltwater contributions and this is indicative of a post-decline phase where reflectance only increases when optimal ablation conditions are present. The basin will likely not experience significant decreases in streamflow from the near complete loss of glacial mass, rather the primary influence in streamflow will be the variations in SWE. Any further declines to snowpack in this region will likely have devastating effects on stakeholders who require surface water for production (i.e. industry, agriculture, livestock, etc.).

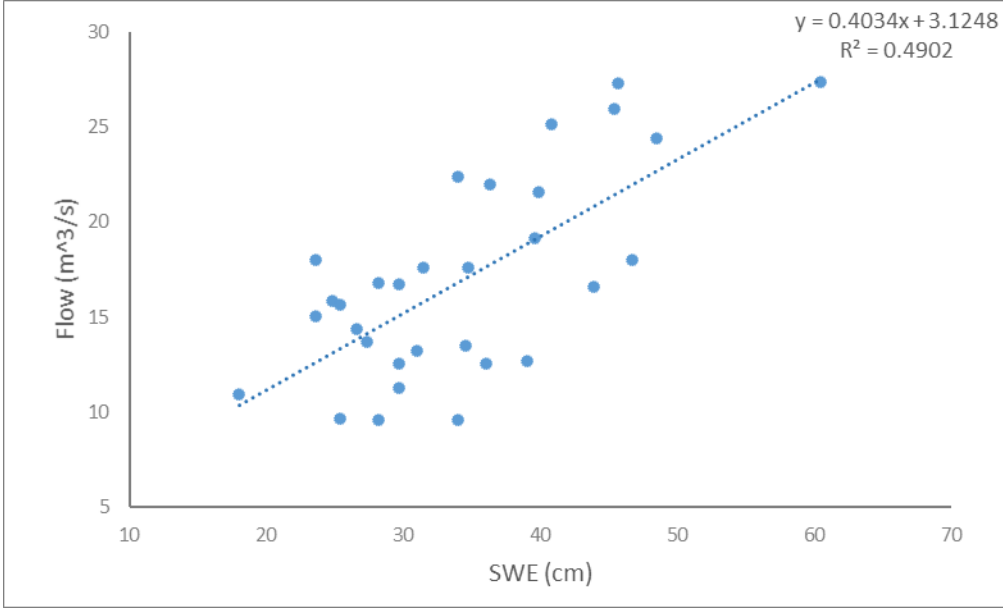


Figure 35. Scatter plot of mean summer streamflow ($\text{m}^3 \text{s}^{-1}$) and max annual SWE (cm) in Pine Creek. Blue dotted line indicates trend line with equation and R^2 value.

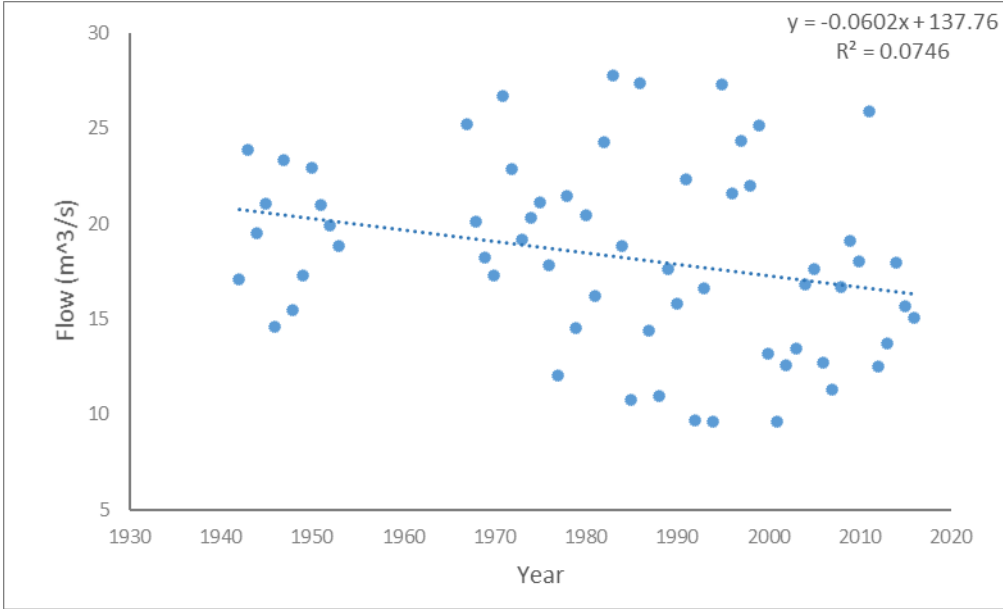


Figure 36. Scatter plot of mean summer streamflow ($\text{m}^3 \text{s}^{-1}$) over time at the Pine Creek USGS Gage Station. Blue dotted line indicates trend line with equation and R^2 value.

Bull Lake Creek basin has the second largest glacial mass (4.94 km²) in the Wind River Range. The basin is rather large and has two sections. The northerly section is glaciated and the southerly is non-glaciated. Comparing streamflow to SWE produces a p value of < 0.01 and an R² of 0.63 (Figure 37), where high SWE correlates with a high streamflow. The streamflow at the USGS Gage Station (#06224000) above Bull Lake Reservoir (Figure 5) has a decreasing trend since 1950 with a p value of 0.12 and an R² of 0.04 resulting in a decrease of < 2.5 m³ s⁻¹ (Figure 38). Glaciers in the basin have likely ameliorated the decline by supplementing additional water in low snow years to streamflow even as glacial mass continues to decrease.

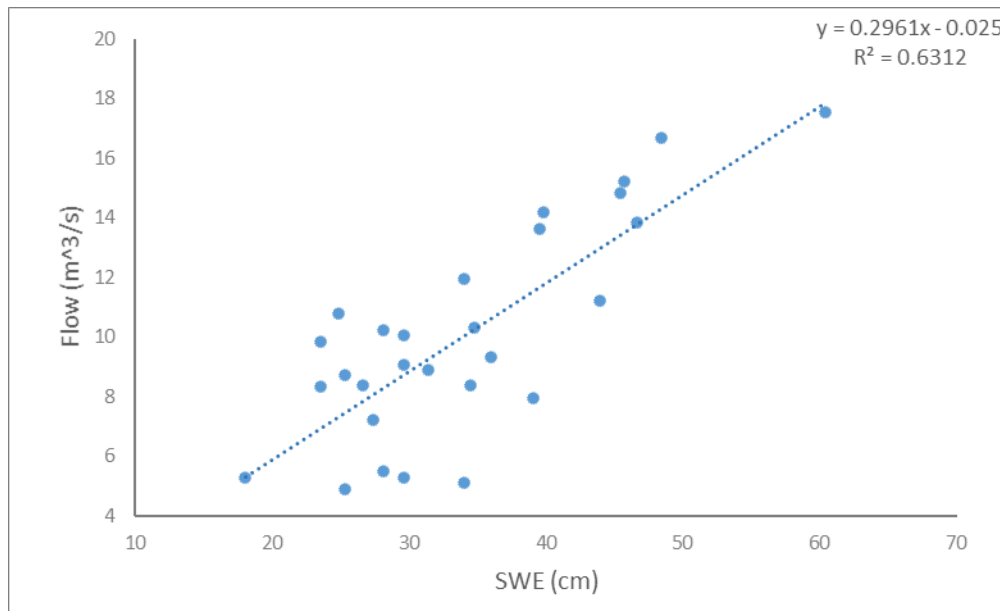


Figure 37. Scatter plot of mean summer streamflow (m³ s⁻¹) and max annual SWE (cm) in Bull Lake Creek. Blue dotted line indicates trend line with equation and R² value.

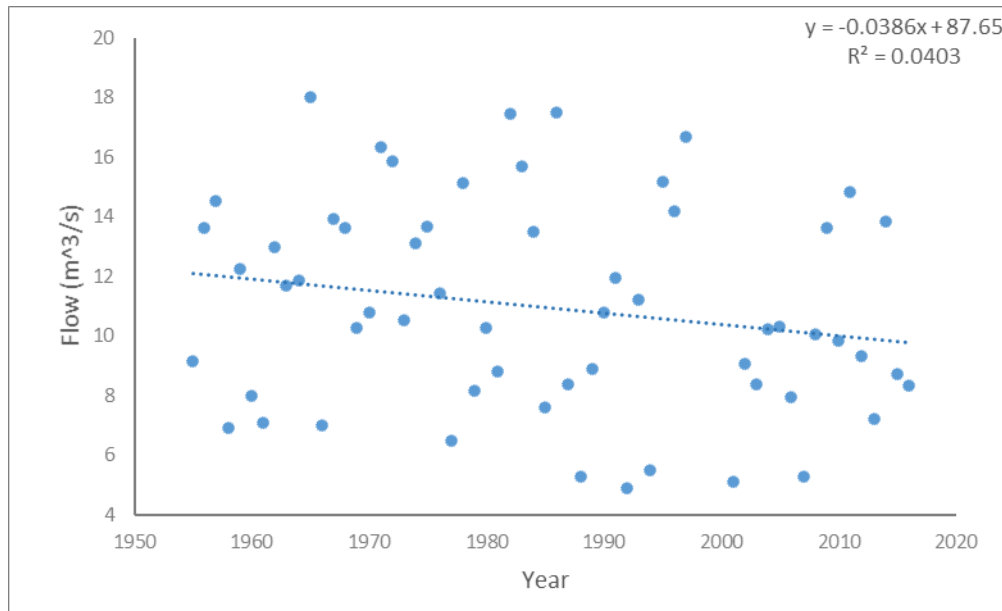


Figure 38. Scatter plot of mean summer streamflow (cms) and time at the Bull Lake Creek USGS Gage Station. Blue dotted line indicates trend line with equation and R² value.

When looking at the Milky Lakes within Bull Lake Creek Basin we can see that the reflectance of the lakes does not have a significant change trend over time. While lake reflectance fluctuates, it has remained relatively consistent with reflectance values between 0.02 and 0.08 (Figures 18 and 19) even while the melt rate has increased as noted by the large percentages of glacial area loss over the study period (Table 5). This plateau is likely indicative of peaking glacier contribution relative to other water sources. As time continues this trend will likely begin decreasing as glacial mass continues to decline and can no longer contribute meltwater output at the same rate. This may lead to significant declines in streamflow as glaciers are unable to support the same flow rate. This will likely lead to the Bull Lake Creek basin being highly dependent on SWE to produce high streamflow relative to the long-term trend.

Dinwoody Creek is the premier basin in this study as it has the largest glacial mass (7.07 km²). Further, streamflow is measured at the USGS Gage Station (#06221400) above Upper

Dinwoody Lake (Figure 4) allowing for a direct comparison of flow and reflectance. Flow and SWE in Dinwoody Basin shows less of a relationship than in Pine Creek or Bull Lake Creek basins. This is likely due to the SNOTEL SWE data as the data is from another location in the range. Comparing streamflow and SWE produces a p value of 0.19 and an R^2 of 0.06 (Figure 39). The streamflow at the lake has been relatively stable since 1950 with a p value of 0.21 and an R^2 of 0.03 resulting in a decrease of $< 1 \text{ m}^3 \text{ s}^{-1}$ as glacial mass is likely sufficient to reduce streamflow losses (Figure 40). The reflectance for the lake has also increased during this period, indicating glacier contributions are increasing and likely stabilizing flow in the basin.

When looking at the Dinwoody Lakes within Dinwoody Creek Basin we can see that the reflectance of the lakes has a significant change trend over time. While lake reflectance fluctuates, it has increased over the study period with reflectance values between 0.02 and 0.12 (Figures 14 and 15) even while the melt rate was similar between the two study periods as noted by similar percentages of glacial area loss over the study period (Table 5). This increase is indicative of increasing glacier contribution relative to other water sources. As time continues this trend should likely begin peaking as glacial mass continues to decline and can no longer increase meltwater output. This may lead to significant declines in streamflow as glaciers are unable to support the same flow rate.

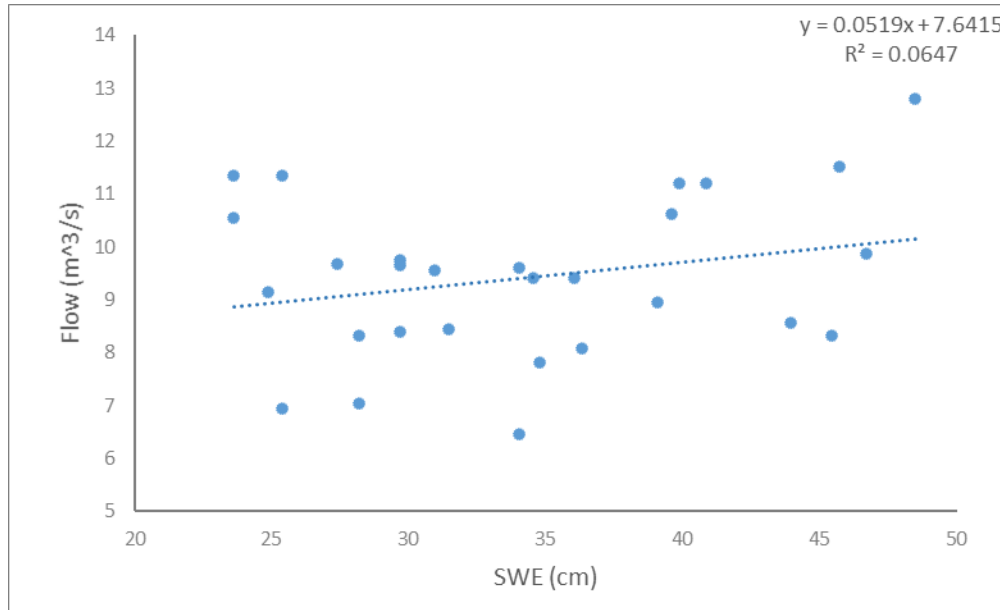


Figure 39. Scatter plot of mean summer streamflow ($\text{m}^3 \text{s}^{-1}$) and max annual SWE (cm) in Dinwoody Creek. Blue dotted line indicates trend line with equation and R^2 value.

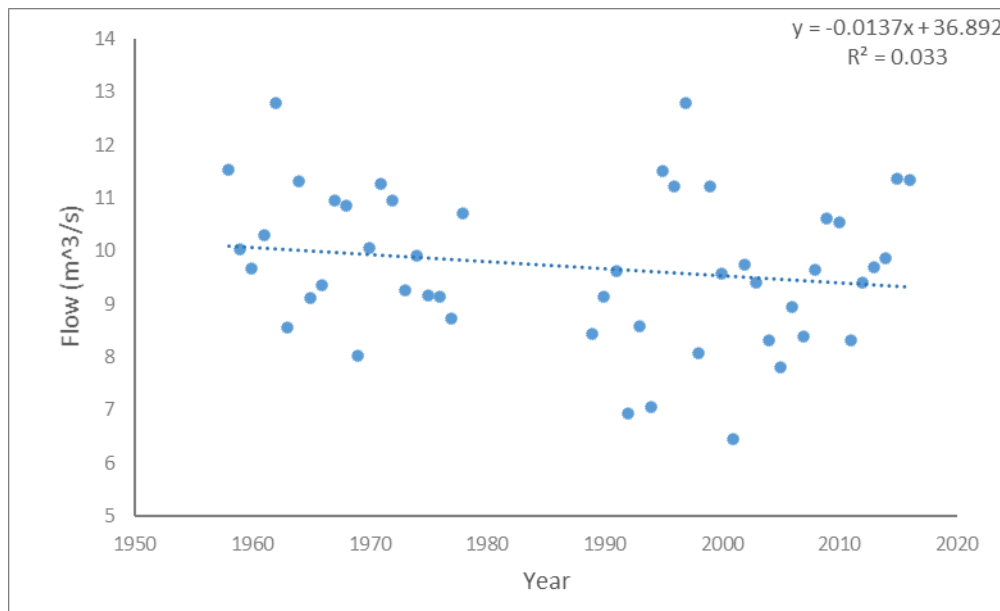


Figure 40. Scatter plot of mean summer streamflow ($\text{m}^3 \text{s}^{-1}$) and over time at the Dinwoody Creek USGS Gage Station. Blue dotted line indicates trend line with equation and R^2 value.

Key Melt Years

Area change provides a linear estimation of glacier mass loss per year in between observation years. However, this fails to identify when glaciers are losing most of their mass. Area change is likely not a linear process, rather the ablation is likely occurring in a single year or period of years between measurements. Using the mean annual lake reflectance converted to a plus-minus anomaly we can identify years of higher glacier contributions and clustered mass loss years for an individual glacier or a collection of glaciers in the range. Regardless of the number of glaciers associated with a lake, primary ablation years will be evident when comparing measured values with the long-term trend.

Monitoring lake reflectance changes over time for an individual lake can identify the years of higher glacier ablation and “key” mass loss, as reflectance has been shown to be related to high maximum temperatures and low SWE, which are the two primary factors influencing glacial ablation. These high reflectance years are relative to the mean over time and indicate the years of higher glacial ablation and sediment laden melt water contribution. The Wind River Range as a whole is losing mass and has clustering of high values between 1988-1990, 2000-2003 and 2013-2016 (Figure 41). In the years where reflectance is a negative anomaly, it can be assumed there is little or no mass lost due to ablation. This concept works on the premise that positive anomaly values indicate ablation whereas negative anomaly values indicate steady-state conditions similar to the AAR ranges proposed by (Meier and Post, 1962). An exception to this may be in 1984 as there is a significant negative anomaly.

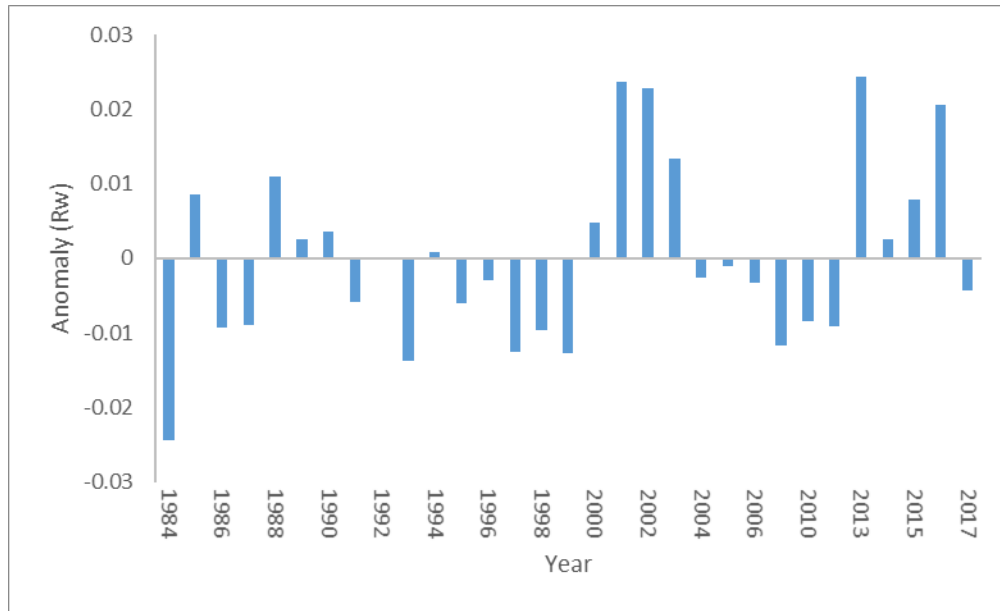


Figure 41. Anomalies of Mean Summer Lake Reflectance (Rw) of the Wind River Range between 1984 – 2017. Blue bars indicate anomaly value.

CHAPTER VI

CONCLUSION

A decrease in glacial mass has occurred in the Wind River Range over the last century due to climate changes. To identify what effect climate change has on the range, we can observe glacier area. While this provides a method to determine basic changes in size over time, it does little to provide detail on the changing glacial conditions, which is often critical for water resource managers. Due to limitations of glacial imagery (e.g. temporal availability and snow cover obscuring glacial extents), current area change estimates can provide only periodic area measurements with often gaps of many years which allows for only a linear area change estimate for a glacier or series of glaciers between two dates. More realistically the ablation occurs in a series of years in which the climatic conditions are ideal for massive ablation. To address this discrepancy by providing more detail of when significant glacial ablation has occurred over time, an analysis of glacial lake reflectance is utilized. This analysis provides a long-term trend for reflectance changes and related glacial mass changes, which influence glacial contributions to streamflow, between 1984 and 2017.

Glacial lake reflectance can serve as a proxy for observing glacier changes related to fluctuating climatic conditions. This analysis includes the primary factors controlling glacier mass changes (i.e. snow cover represented by snow water equivalence, and mean temperature) to understand the relationship between fluctuating climatic conditions and annual changes in glacial lake reflectance. In general, glacial lakes are increasing reflectance over time as a function of the

water discharged by the glaciers “relative” to other water sources. In other words, as snowfall decreases and temperatures increase, more ablation of the glacier occurs. A large ablation area indicates a small snow cover zone. Thus, the snow has a reduced ability to dilute the glacial output. The long-term trend over time can be used to identify changing glacier contributions relative to other water sources.

Glacial lake reflectance can produce insight into three specific processes:

1. Year-to-year changes to glacial mass balance:

The long-term reflectance trends can identify “key” melt years where significant glacial ablation likely occurred. Using the anomalies of glacial lake reflectance against the mean, we can identify anomaly values above the mean that occur in single years or groups of years. These high anomaly reflectance values are likely the years where primary glacial ablation has occurred indicating high glacial melt water contributions relative to other sources of water in streamflow. Anomaly values below the mean likely indicate steady-state conditions of the ice mass where little or no mass change occurs.

2. Long-term trends in glacier activity:

Individual lakes can display three different long-term change scenarios including increase, no change, and decrease. Each trend in reflectance suggests a trend in glacier activity related to climatic conditions. Increases in lake reflectance suggests glaciers are generally increasing in activity by producing and flushing sediments particularly during warm years with low snowpack when glacial ablation is high. These conditions are likely

related to a greater percentage of glacier melt water contributions to streamflow. No change in lake reflectance suggests glacial activity is generally stable with variations in production and flushing of sediments related more to the variability in climatic conditions which control glacial activity. A no change scenario suggests that the percentage of glacial melt water contribution might be peaking particularly if the glaciers are known to be shrinking in area (as in the Wind River Range) and therefore will have less mass to produce or supply sediments to streamflow. A decreasing trend in lake reflectance suggests glacial activity is declining as fewer sediments are being produced and flushed from the glacier. This suggests that a decreasing trend in reflectance may be indicative of glaciers that are becoming inactive or close to disappearing. These conditions also suggest that the percentage of glacial melt water contribution may be decreasing relative to other water sources as the glaciers are not contributing significant amounts of sediment laden glacial melt water to streamflow.

3. How the glacial basins in the Wind River Range are changing in relation to streamflow:

The study uses Dinwoody Creek, Bull Lake Creek and Pine Creek basins to identify long-term streamflow changes in the range. Each basin is likely responding differently based on the remaining glacial mass. Dinwoody Creek has the highest glacial mass and has experienced the smallest decrease in streamflow. This small decrease in streamflow paired with lake reflectance data may indicate that the glaciers in this basin likely have sufficient mass to significantly contribute to streamflow and will continue to supply large

volumes of melt water downstream for the foreseeable future. Bull Lake Creek has the second most glacial mass and has experienced the second most decrease in streamflow. This decrease in streamflow paired with lake reflectance data may indicate that the glaciers in the basin are likely beginning to peak in streamflow contributions as glacial ablation in the basin increased while the reflectance did not show a long-term increase or decrease. Pine Creek has the smallest glacial mass and has experienced the largest decrease in streamflow. The decrease in streamflow paired with lake reflectance data may indicate that the glaciers in the basin are unhealthy and unable to support large volumes of melt water downstream. Therefore, this basin has experienced the greatest decrease to streamflow as it is highly dependent upon snowmelt.

Limitations of the Study

The primary limitations of the research include glacier area calculation and SWE data. The glacier area obtained from Landsat imagery is subject to 30 m spectral resolution. The area of the glaciers for the range decreased 10.78 km^2 with an uncertainty of $\pm 0.32 \text{ km}^2$. The area uncertainty was calculated by accounting for a 30 meter buffer around the glacier polygon resulting in a minimum area loss of 10.46 km^2 and a maximum loss of 11.1 km^2 . While this estimation is likely high, it serves as a good method to identify the possible range of area loss over the study period.

SWE data is from Elkhart Park on the west side of the continental divide. This basin's SWE correlated the best of all basins for Pine Creek, Bull Lake, and Dinwoody Creek Basins. Thus, the analysis comparing streamflow to SWE data used the Elkhart Park data. While the $0.70 R^2$ in the Upper Dinwoody Lake analysis can explain much of the glacier lake reflectance

variability, the 0.30 p value leaves something to be desired in terms of increasing the relationship. Therefore, improved SWE data would likely increase the R^2 for the Dinwoody Lake Reflectance analysis.

Future Work

Future work will include an analysis of AAR for each basin in the range. The current analysis focuses on total area as ice and snow are converted into a single polygon and is clearly delineated between other land covers. However, when attempting to delineate between ice and snow pixels the value is subjective to the glacier topography. In other words, what works for one glacier does not work for another. Therefore, to obtain the values, the analysis will be conducted on a glacier by glacier basis to determine total ice area and total snow area which will allow an AAR to be developed. This study will likely rectify the SWE data limitation from the Upper Dinwoody Lake analysis. The improved data will likely correlate better and increase the p value in the multilinear regression producing a better explanation of the lake reflectance variability.

Additional work will include an analysis of the synoptic scale processes leading to ablation in the range. The range has variation of temperatures and snowfall resulting in variations of lake reflectance. The study shows that higher temperatures and lower snowfall are leading to increases in reflectance among lakes supported by glaciers with sufficient mass. A self-organizing map (SOM) analysis will be used to help identify the patterns that lead to higher temperatures and lower snowfall. This will help support observations of glacial area and glacial lake reflectance change in the range.

Finally, an analysis of Glacier Lake Outburst Floods (GLOF) will be conducted to attempt to determine the factors leading to the Grasshopper Glacier outburst floods in 2003 and

2013. The GLOF on Grasshopper Glacier is the result of a catastrophic release of Grasshopper Lake at the head of the glacier. During these events, a significant increase in streamflow occurs that picks up large loads of debris resulting in peak R_w on Upper Dinwoody Lake of > 0.20 . While uncommon, two of these events have occurred in the last 15 years. An analysis of streamflow prior to Landsat 5 observations indicate this is a new event to occur on Grasshopper Glacier. This indicates changes in climate are likely responsible for the release of Grasshopper Lake. The SOM analysis may provide insight into the conditions necessary for these events to occur.

Application of Results

This analysis provides a novel method of assessing changes in glacial activity over time in relation to changing climatic conditions. The analysis can be performed on any glacier or glacial system that contributes melt water to streamflow, provided the lake reflectance can be extracted in these areas. The Wind River Range provided an excellent study area as the range is at a mid-latitude and is subject to the climate changes experienced in this region. As a result, the range shows a mixture of lake reflectance change scenarios which identify varying conditions in glacial activity by the contributions of sediment laden glacial melt water feeding the lakes.

There are many different mountain ranges across the globe with similar locations and elevations as the Wind River Range. There are also ranges that are at higher latitudes and elevations that may not be experiencing the same change. Whatever the case, this analysis can be used to track long-term changes in glacier contribution. All lakes will display some pattern, whether it be increase, no change, or decrease in reflectivity. Most important, this can be used to provide an understanding of trends glacial activity or “health” of the glacier.

The glacial lake reflectance data can be of use to water resource managers as identifying decreases in glacial activity can be indicative of a declining ability of a glacier to significantly contribute melt water to streamflow, which is imperative to long-term regional planning. Providing analysis on how glaciers are influencing streamflow can assist in implementing water conservation efforts in the region. The Wind River Indian Reservation holds water rights to a majority of annual streamflow. This is highly important as their industries are supported by the annual meltwater from the range. As rainfall in the region continues to decline along with increasing temperatures, implementing water conservation strategies will allow the Wind River Range communities to adapt to climate changes in the region. Therefore, due to the relationships of glacial “health” and glacial lake reflectance, and in turn the importance of glacial meltwater to regional summer streamflow, continued monitoring of the reflectance of glacial lakes is necessary for regional water resource management.

REFERENCES

- Adger, W. N., S. Agrawala, M. M. Q. Mirza, C. Conde, K. O'Brien, J. Pulhin, R. Pulwarty, B. Smit, and K. Takahashi. "Assessment of Adaptation Practices, Options, Constraints and Capacity." In *Climate Change 2007: Impacts, Adaptation and Vulnerability*, 717-743. Vol. Contribution of Working Group II to the Fourth Assessment Report of the Intergovernmental Panel on Climate Change. Cambridge, UK and New York, NY: Cambridge University Press, 2007.
- Albert, T. H. (2002). Evaluation of remote sensing techniques for ice-area classification applied to the tropical Quelccaya Ice Cap, Peru. *Polar Geography*, 26,210–226
- Ambinakudige, S., & Joshi, K. (2010). Remote Sensing of Cryosphere. *Icimod*, 1.
<https://doi.org/10.1002/9781118368909>
- Arendt, A.A.; Echelmeyer, K.A.; Harrison, W.D.; Lingle, C.S.; Valentine, V.B. Rapid wastage of Alaska glaciers and their contribution to rising sea level. *Science* 2002, 297 (5580), 382-386
- Bahr, D., Meier, M., and Peckman, S., (1997). The physical basis of glacier volume area scaling, *Journal of Geophysical Research*, vol. 102, B9, p. 20,355-20,362.
- Benn, D. I., & Evans, D. J. A. (2010). Glacier & Glaciation. *Journal of Chemical Information and Modeling*, 2, 817. <https://doi.org/10.1017/CBO9781107415324.004>

- Berthier, E., Arnaud, Y., Kumar, R., Ahmad, S., Wagnon, P., & Chevallier, P. (2007). Remote sensing estimates of glacier mass balances in the Himachal Pradesh (Western Himalaya, India). *Remote Sensing of Environment*, 108(3), 327–338.
<https://doi.org/10.1016/j.rse.2006.11.017>
- Bindoff, N. L. et al. 2007. Observations: oceanic climate change and sea level. In Solomon, S. et al. (eds), *Climate Change 2007: The Physical Science Basis. Contribution of Working Group I to the Fourth Assessment of the Intergovernmental Panel on Climate Change*. Cambridge University Press.
- Bradley R, Vuille M, Diaz H, Vergara W (2006) Threats to water supplies in the tropical Andes. *Science*. doi:10.1126/science. 1128087
- Burns, P., & Nolin, A. (2013). Using atmospherically-corrected Landsat imagery to measure glacier area change in the Cordillera Blanca, Peru from 1987 to 2010. *Remote Sensing of Environment*, 140, 165–178. <https://doi.org/10.1016/j.rse.2013.08.026>
- Cable, J., Ogle, K., & Williams, D. (2011). Contribution of glacier meltwater to streamflow in the Wind River Range, Wyoming, inferred via a Bayesian mixing model applied to isotopic measurements. *Hydrological Processes*, 25(14), 2228–2236.
<https://doi.org/10.1002/hyp.7982>
- Carturan, L., Baroni, C., Becker, M., Bellin, A., Cainelli, O., Carton, A., ... Seppi, R. (2013). Decay of a long-term monitored glacier: Careser Glacier (Ortles-Cevedale, European Alps). *Cryosphere*, 7(6), 1819–1838. <https://doi.org/10.5194/tc-7-1819-2013>
- Casassa, G., Rodriguez, J., & Loriaux, T. (2014). *Global Land Ice Measurements from Space*. *Global Land Ice Measurements from Space*. [https://doi.org/10.1007/978-3-540-79818-](https://doi.org/10.1007/978-3-540-79818-7)

- Chang, T., & Hansen, A. J. (2014). Greater Yellowstone Ecosystem. *Landscape Climate Change Vulnerability Project*, 1–8.
- Cheesbrough, Kyle S., Glacial Recession in Wyoming's Wind River Range , M.S., Department of Civil and Architectural Engineering, December 2007
- Cheesbrough, K., Edmunds, J., Tootle, G., Kerr, G., & Pochop, L. (2009). Estimated wind river range (Wyoming, USA) glacier melt water contributions to agriculture. *Remote Sensing*, 1(4), 818–828. <https://doi.org/10.3390/rs1040818>
- CMIP3_A: This analysis uses 15 models simulations from the WCRP CMIP3 that were available at resolutions finer than 4 degrees (CCSM 3.0, CSIRO, UKMO-HadCM3, IPSL, ECHAM5/MPI, CGCM3.1(T47), GFDL2.0,UKMO-HadGEM1, MIROC3.2(medres), MRI-CGCM2.3.2a, CNRM, GFDL2.1, INMCM3, ECHO-G, PCM).
- Daddow, B. R. L. (1996). WATER RESOURCES OF THE WIND RIVER INDIAN RESERVATION , WYOMING Water-Resources Investigations Report 95-4223
- datasets. *Global and Planetary Change*, 56(1–2): 137–152. doi: 10.1016/j.gloplacha.2006.07.013
- DeVisser, M. H., & Fountain, A. G. (2015). A century of glacier change in the Wind River Range, WY. *Geomorphology*, 232, 103–116. <https://doi.org/10.1016/j.geomorph.2014.10.017>
- Dyrgerov, M. and Meier, M. F. 2005. Glaciers and the Changing Earth System: A 2004 Snapshot. Institute of Arctic and Alpine Research, Boulder, Colorado, Occasional Paper no. 58.

- EPA (2016). What Climate Change Means for Wyoming. Retrieved June 6, 2017 from, <https://19january2017snapshot.epa.gov/sites/production/files/2016-09/documents/climate-change-wy.pdf>
- Fountain, A.G., Krimmel, R.M., Trabant, D.C. (1997). Strategy for monitoring glaciers. US Geological Survey Circular, 1132, 19
- Furbish, D. J. and Andrews, J. T. 1984. The use of hypsometry to indicate long-term stability and response of valley glaciers to changes in mass transfer. *Journal of Glaciology* 30, 199–211.
- Gallegos, C. L., Davies-Colley, R. J., & Gall, M. (2008). Optical closure in lakes with contrasting extremes of reflectance. *Limnology and Oceanography*, 53(5), 2021–2034. <https://doi.org/10.4319/lo.2008.53.5.2021>
- Gao B C, 1996. NDWI-A normalized difference water index for remote sensing of vegetation liquid water from space. *Remote Sensing of Environment*, 58(3): 257–266. doi: 10.1016/S0034- 4257(96)00067-3
- Giardino, C., Oggioni, A., Bresciani, M., & Yan, H. (2010). Remote sensing of suspended particulate matter in Himalayan Lakes. *Mountain Research and Development*, 30(2), 157–168. <https://doi.org/10.1659/MRD-JOURNAL-D-09-00042.1>
- Granshaw, F. D., and Fountain, A. G. (2006). “Glacier change (1958–1998) in the north cascades national park complex. Washington USA.” *J. Glaciol.*, 52(177), 251–256.
- Gurnell, A. M. 1982. The dynamics of suspended sediment concentration in an Alpine proglacial stream network. *Hydrological Aspects of Alpine and High Mountain Areas*. IASH Publication 138, 319–30

- Guttman, N. B., and R. G. Quayle. "A Historical Perspective of U.S. Climate Divisions." *Bulletin of the American Meteorological Society* 77, no. 2 (1996): 293-303
- Hagg, W.; Braun, L.; Uvarov, V.N.; Makarevich, K.G. A Comparison of three Methods of Mass Balance Determination in the Tuyuksu Glacier Region, Tien Shan. *J Glaciol* 2004, 50 (171), 505-510.
- Hall, D. K., Foster, J. L., DiGirolamo, N. E., & Riggs, G. A. (2012). Snow cover, snowmelt timing and stream power in the Wind River Range, Wyoming. *Geomorphology*, 137(1), 87–93. <https://doi.org/10.1016/j.geomorph.2010.11.011>
- Hall, D. K., Crawford, C. J., DiGirolamo, N. E., Riggs, G. A., & Foster, J. L. (2015). Detection of earlier snowmelt in the wind river range, wyoming, using landsat imagery, 1972-2013. *Remote Sensing of Environment*, 162, 45–54. <https://doi.org/10.1016/j.rse.2015.01.032>
- Harris Geospatial Solutions (2017). ENVI 5.4
- Hartmann, H. C.. "Decision Support for Water Resources Management." In *Uses and Limitations of Observations, Data, Forecasts, and Other Projections in Decision Support for Selected Sectors and Regions*, 45-55. Vol. Synthesis and Assessment Product 5.1. Washington, D.C.: U.S. Climate Change Science Program, 2008.
- Haug, T., Rolstad, C., Elvehøy, H., Jackson M., and Maalen- Johansen, I.: Geodetic mass balance of the western Svartisen ice cap, Norway, in the periods 1968–1985 and 1985–2002, *Ann. Glaciol.*, 50, 119–125, 2009
- Hayden, F.V., 1878. Discovery of recent glaciers in Wyoming. *Am. Nat.* 12, 827–833.

- Hegerl, G. C., F. W. Zwiers, P. Braconnot, N. Gillett, Y. Luo, J. A. Marengo Orsini, N. Nicholls, J. E. Penner, and P. A. Stott. "Understanding and Attributing Climate Change." In *Climate Change 2007: The Physical Science Basis*, 663-745. Vol. Contribution of Working Group I to the Fourth Assessment Report of the Intergovernmental Panel on Climate Change. Cambridge, UK and New York, NY: Cambridge University Press, 2007.
- Juen, I., Kaser, G. and Georges, C. 2007. Modelling observed and future runoff from a glacierized tropical catchment (Cordillera Blanca, Peru). *Global and Planetary Change* 50, 37–48
- Khalsa, S.J.S., Dyrgerov, M.B., Khromova, T., Raup, B. H., & Barry, R.G. (2004). Space-based mapping of glacier changes using aster and gis tools. *IEEE transactions on geosciences and remote sensing*, 42, pp. 2177-2183.
- Krishna, A.P. Snow and glacier cover assessment in the high mountains of Sikkim Himalaya. *Hydrolog Process* 2005, 19 (12), 2375-2383.
- Kulkarni, A.V.; Rathore, B.P.; Alex, S. Monitoring of glacial mass balance in the Baspa basin using accumulation area ratio method. *Curr Sci* 2004, 86 (1), 185-190.
- Mark, B. G., & Seltzer, G. O. (2003). Tropical glacier meltwater contribution to stream discharge: A case study in the Cordillera Blanca, Peru. *Journal of Glaciology*, 49, 271–281
- Marks, J., Piburn, J., Tootle, G., Kerr, G., & Oubeidillah, A. (2015). Estimates of glacier mass loss and contribution to streamflow in the Wind River range in wyoming: Case study. *Journal of Hydrologic Engineering*, 20(8). [https://doi.org/10.1061/\(ASCE\)HE.1943-5584.0001050](https://doi.org/10.1061/(ASCE)HE.1943-5584.0001050)

- Marston RA, Pochop LO, Kerr GL, Varuska ML and Veryzer DI (1991) Recent glacier changes in the Wind River Range, Wyoming. *Phys. Geogr.*, 12(2), 115–123 (doi: 10.1080/ 02723646.1991.10642421)
- Matta, E., Giardino, C., Boggero, A., Bresciani, M., Matta, E., Giardino, C., ... Bresciani, M. (2017). Use of Satellite and In Situ Reflectance Data for Lake Water Color Use of Satellite and In Situ Reflectance Data for Lake Water Color Characterization in the Everest Himalayan Region. *Bio One*, 37(1), 16–23. <https://doi.org/10.1659/MRD-JOURNAL-D-15-00052.1>
- Meier, M. & Post, A. (1962). Recent variations in mass net budgets of glaciers in western North America. *Symposium of Obergurgl*, 63-77
- Meier, M. F. (1951). *Glaciers of the Gannett Peak-Fremont Peak Area , Wyoming.*
- Naftz DL, Smith M (1993) Ice thickness, ablation, and other glaciological measurements on Upper Fremont Glacier, Wyoming. *Phys Geogr* 14:404–414
- Naftz DL, Susong DD, Schuster PF, Cecil LD, Dettinger MD, Michel RL, Kendall C (2002) Ice core evidence of rapid air temperature increases since 1960 in alpine areas of the Wind River Range, Wyoming, United States. *J Geophys Res D Atmos* 107:XV–XVI
- National Climate Assessment (NCA) (2009). *Global Climate Change Impacts in the United States.* Cambridge University Press, 2009)
- National Climate Assessment (NCA) (2014). *Great Plains.* Retrieved June 6, 2017 from, <http://nca2014.globalchange.gov/report/regions/great-plains>
- National Resource Conservation Service (NRCS) (2018). *Snow Telemetry (SNOTEL) and Snow Course Data and Products.* Retrieved June 6, 2017 from, <https://www.wcc.nrcs.usda.gov/snow/>

- National Snow and Ice Data Center (NSIDC) (2017). About Glaciers. Retrieved June 28, 2017 from, <https://nsidc.org/cryosphere/glaciers/information.html>
- Ocean Optics Webbook (2018). Overview of Optical Oceanography. Reflectances. Retrieved December 10, 2017 from, http://www.oceanopticsbook.info/view/overview_of_optical_oceanography/reflectances
- Østrem, G., & Brugman, M. (1991). Mass Balance Measurement Techniques, a Manual for Field and Office Work, National Hydrological Research Institute (NHRI). *Science Report, 4*.
- Paterson, W. S. B., The Physics of Glaciers, 480 pp. 3rd. Ed., Pergmon, Taarrytown, N.Y., 1994
- Paul, F., Barrand, N., Berthier, E., Bolch, T., Casey, K., Frey, H., et al. (2013). On the accuracy of glacier outlines derived from remote sensing data. *Annals of Glaciology*, 54.
- Paul, F., Bolch, T., Kääb, A., Nagler, T., Nuth, C., Scharrer, K., ... Van Niel, T. (2015). The glaciers climate change initiative: Methods for creating glacier area, elevation change and velocity products. *Remote Sensing of Environment*, 162, 408–426. <https://doi.org/10.1016/j.rse.2013.07.043>
- Paul, F., Kääb, A., Maisch, M., Kellenberger, T., & Haeberli, W. (2002). The new remote-sensing derived Swiss glacier inventory. 1. Methods. *Annals of Glaciology*, 34(September 1985), 355–361. <https://doi.org/10.3189/172756402781817941>

- Pearce, J. T., Pazzaglia, F. J., Evenson, E. B., Lawson, D. E., Alley, R. B., Germanoski, D. and Denner, J. D. 2003. Bedload component of glacially discharged sediment: Insights from the Matanuska Glacier, Alaska. *Geology* 31, 7–10
- Pelto, M. (2008). Impact of Climate Change on North Cascade Alpine Glaciers, and Alpine Ruoff. *Northwest Science* 82 (1), 65-75
- Pelto, M., Capps, D., Clague, J. J., & Pelto, B. (2013). Rising ELA and expanding proglacial lakes indicate impending rapid retreat of Brady Glacier, Alaska. *Hydrological Processes*, 27(21), 3075–3082. <https://doi.org/10.1002/hyp.9913>
- PRISM Climate Group (2018). PRISM Climate Data. Retrieved June 6, 2017 from, <http://www.prism.oregonstate.edu/>
- Quincey D J, Richardson S D, Luckman A et al., 2007. Early recognition of glacial lake hazards in the Himalaya using remote sensing
- Racoviteanu, A. E., Williams, M. W., & Barry, R. G. (2008). Optical remote sensing of glacier characteristics: A review with focus on the Himalaya. *Sensors*, 8(5), 3355–3383. <https://doi.org/10.3390/s8053355>
- Rasmussen, L. A. (2009). South Cascade Glacier mass balance , 1935 – 2006, *50*(2001), 215–220.
- Rasmussen, L. A., & Conway, H. (2001). Estimating South Cascade Glacier (Washington, USA) mass balance from a distant radiosonde and comparison with Blue Glacier. *Journal of Glaciology*, 47(159), 579-588.
- Rees, H. G. and Collins, D. N. 2006. Regional differences in response of flow in glacier-fed Himalayan rivers to climatic warming. *Hydrological Processes* 20, 2157–69

- Riedel, J., & Larrabee, M. A. (2011). North Cascades National Park Complex glacier mass balance monitoring annual report, water year 2009: North Coast and Cascades Network. *National Park Service, Fort Collins*.
- Rignot, E. J., Rivera, A. and Casassa, G. 2003. Contribution of the Patagonia Icefields of South America to sea level rise. *Science* 302, 434–7
- Röthlisberger, H. and Lang, H. 1987. Glacial hydrology. In Gurnell, A. M. and Clark, M. J. (eds), *Glacio-fluvial Sediment Transfer*. Wiley, New York, 207–84.
- Ryan, J. C., Hubbard, A. L., Box, J. E., Todd, J., Christoffersen, P., Carr, J. R., ... Snooke, N. (2015). UAV photogrammetry and structure from motion to assess calving dynamics at Store Glacier , a large outlet draining the Greenland ice sheet, 1–11.
<https://doi.org/10.5194/tc-9-1-2015>
- Shea, J. M., Moore, R. D., & Stahl, K. (2009). Derivation of melt factors from glacier mass-balance records in western Canada. *Journal of Glaciology*, 55(189), 123–130.
<https://doi.org/10.3189/002214309788608886>
- Silverio, W., & Jaquet, J. -M. (2005). Glacial cover mapping (1987–1996) of the Cordillera Blanca (Peru) using satellite imagery. *Remote Sensing of Environment*, 95, 342–350
- Soruco, A., Vincent, C., Francou, B., Ribstein, P., Berger, T., Sicart, J. E., ... Lejeune, Y. (2009). Mass balance of Glaciar Zongo, Bolivia, between 1956 and 2006, using glaciological, hydrological and geodetic methods. *Annals of Glaciology*, 50(50), 1–8.
<https://doi.org/10.3189/172756409787769799>

- Swift, D. A., Nienow, P. W., Spedding, N. and Hoey, T. B. 2002. Geomorphic implications of subglacial drainage configuration: rates of basal sediment evacuation controlled by seasonal drainage system evolution. *Sedimentary Geology* 149, 5–19
- Tangborn, W. V., Krimmel, R. M., and Meier, M. F. (1975). “A comparison of glacier mass balance by glaciological, hydrological and mapping methods, south cascade glacier, Washington.” *Proc., Moscow Symp., International Association of Hydrological Sciences*, 104, 185–196
- USDA (2017). Bridger Wilderness. Retrieved June 6, 2017 from, <https://www.fs.usda.gov/recrea/btnf/recrea/?recid=77360>
- USDA (2017). Fitzpatrick Wilderness. Retrieved June 6, 2017 from, <https://www.fs.usda.gov/recrea/shoshone/recrea/?recid=80901>
- USGS (2018). USGS Current Water Data for the Nation. Daily Streamflow Conditions. Retrieved June 6, 2017 from, <https://waterdata.usgs.gov/nwis/rt>
- USGS (2018). Landsat Calibration/Validation Update. Retrieved December May 15, 2018, from https://landsat.usgs.gov/sites/default/files/documents/landsat_science_team/2018-02_Day1_Markham_Landsat%20Calibration%20and%20Validation.pdf
- Vandenberg, G. S., & VanLooy, J. A. (2016). Continental Glacier meltwater contributions to late summer stream flow and water quality in the northern Wind River Range, Wyoming, USA. *Environmental Earth Sciences*, 75(5), 1–14. <https://doi.org/10.1007/s12665-016-5295-0>

- Vanlooy, J. A., Miede, C., Vandenberg, G. S., & Forster, R. R. (2014). Ice volume estimation inferred from ice thickness and surface measurements for Continental Glacier, Wind River Range, Wyoming, USA. *Journal of Glaciology*, *60*(221), 478–488.
<https://doi.org/10.3189/2014JoG13J162>
- VanLooy, J. A., Forster, R. R., Barta, D., & Turrin, J. (2013). Spatially variable surface elevation changes and estimated melt water contribution of Continental Glacier in the Wind River Range, Wyoming, USA: 1966–2011. *Geocarto International*, *28*(2), 98–113. <https://doi.org/10.1080/10106049.2012.665500>
- Wagnon, P.; Kumar, R.; Arnaud, Y.; Linda, A.; Sharma, P.; Vincent, C.; Pottakal, J.; Berthier, E.; Ramanathan, A.; Hassnain, S.I.; Chevalier, P. Four years of mass balance on Chhota Shigri Glacier, Himachal Pradesh, India, a new benchmark glacier in the western Himalaya. *J Glaciol* 2007, *53* (183), 603 - 611
- Wang, H. Yang, R. Li, X, Cao, S. (2017). Glacier parameter extraction using Landsat 8 images in the eastern Karakorum. *IOP Conference Series. Earth and environmental science* [1755-1307] yr:2017 vol:57 iss:1 pg:012004
- Wentworth CK and Delo DM (1931) Dinwoody Glaciers, Wind River Mountains, Wyoming: with a brief summary of existing glaciers in the United States. *Geol. Soc. Am. Bull.*, *42*(3), 605–620
- Wessels, R. L., Kargel, J. S., & Kieffer, H. H. (2002). ASTER measurement of supraglacial lakes in the Mount Everest region of the Himalaya. *Annals of Glaciology*, *34*, 399–408.
<https://doi.org/10.3189/172756402781817545>

Wilbanks, T. J., and al.et. "*Conclusions and Research Priorities.*" In *Effects of Climate Change on Energy Production and Use in the United States*, 98-108. Vol. Synthesis and Assessment Product 4.5. Washington, D.C.: U.S. Climate Change Science Program, 2007.

Wind River Irrigation Project (WRIP) (1995). Historic American Engineering Record. HAER No. WY-95

Wise, E. K. (2010). Spatiotemporal variability of the precipitation dipole transition zone in the western United States. *Geophysical Research Letters*, 37(7), 1–5.

<https://doi.org/10.1029/2009GL042193>

Wolken, G.J., 2000. Energy Balance and Spatial Distribution of Net Radiation on Dinwoody Glacier, Wind River Range, Wyoming, USA (Masters Thesis) University of Wyoming.